Phenotypic and functional characterization of mesenchymal stromal cells generated from human bone marrow CD271+ mononuclear cells

Kuçi, Zyrafete

UNIVERSITY OF ZAGREB
SCHOOL OF MEDICINE

Zyrafete Kuçi

Phenotypic and Functional Characterization of Mesenchymal Stromal Cells Generated from Human Bone Marrow $CD271^+$ Mononuclear Cells

DOCTORAL DISSERTATION

Zagreb, 2011.

This study has been performed in the Laboratory for Stem Cell Research and Cell Therapy of the University Children's Hospital, Department of Hematology/Oncology, Frankfurt am Main, Germany (Director: Prof. Thomas Klingebiel, MD.).

Mentor: Prof. Drago Batinić, MD, PhD.

Co-mentor: Prof. Peter Bader, MD.

The work was kindly supported by Wilhelm Sander Stiftung (Grant-No 2006.067.1) (Peter Bader and Selim Kuçi) and "Hilfe für krebskranke Kinder Frankfurt e.V.

Acknowledgements:

I would like to thank my mentors Prof. Peter Bader, MD. (University Children's Hospital in Frankfurt am Main, Germany) and Prof. Drago Batinić, MD, PhD. (University of Zagreb, School of Medicine, Zagreb, Croatia) for their continuous support of my work and critical suggestions in order to improve the design of the experimental work and writing of this doctoral dissertation.

I am also very greatful to Miriam Stais, Vida Meyer and Ralf Lieberz for their excellent technical assistance and Hermann Kreyenberg (PhD.) for the interpretation of the real-time PCR results. I wish to express my gratitude to my co-worker and husband Dr. Selim Kuçi, who helped me design the experiments and perform this study. At the same time, I would like to thank my children for their patience and continuous moral support to bring this work to the end.

CONTENTS

Publications related to the Ph.D. thesis:

1. Z. Kuçi, S. Kuçi, S. Zircher, S. Koller, R.Schubert, H. Bönig, R.Henschler, R.Lieberz, T. Klingebiel, and P.Bader. Mesenchymal stromal cells derived from $CD271^+$ bone marrow mononuclear cells exert potent allosuppressive properties.
Cytotherapy, 2011, Vol 13, Issue 10, 1193-1204.

2. S. Kuçi*, **Z. Kuçi***, H. Kreyenberg, E. Deak, K.Pütsch, S. Huenecke, C.Amara, S. Koller, E. Rettinger, M. Grez, U. Koehl, H. Latifi-Pupovci, R. Henschler, T. Tonn, D. von Laer, T. Klingebiel, P. Bader. CD271 antigen defines a subset of multipotent stromal cells with immunosuppressive and lymphohematopoietic engraftment-promoting properties. **Haematologica, 2010, Vol 95, Issue 4, 651-659.**
(*contributed equally to the work)

Published abstracts (as first author):

1. Z. Kuçi, S. Zircher, S. Koller, R. Schubert, H. Bönig. R. Lieberz, P. Bader, S. Kuçi. Multipotent mesenchymal stromal cells derived from $CD271^+$ bone mononuclear cells exhibit potent allosuppressive properties. **Cytotherapy, Vol. 13** Annual Meeting Abstracts Supplement ISSN 1465-3249 **Abstract Nr. 72** (ISCT 2011 Annual Meeting Abstracts, Rotterdam, The Netherland)

2. Z. Kuçi, H. Kreyenberg, E. Deak, E. Rettinger, R. Henschler. U. Koehl, T. Tonn, M. Grez, T. Klingebiel, P. Bader and S. Kuçi. Mesenchymal stromal cells derived from $CD271^+$ bone mononuclear cells improve the lymphohematopoietic engraftment of $CD133^+$ hematopoietic stem cells. ***First European Conference on Mesenchymal Stem Cells, Toulouse, France 2010***, **Abstract Nr. 13, p.58 (Selected for oral presentation).**

3. Z. Kuçi, H. Kreyenberg, E. Deak, E. Rettinger, R. Henschler, U. Koehl, T. Tonn, M. Grez, D. von Laer, T. Klingebiel, P. Bader, S. Kuçi. Co-transplantation of mesenchymal stromal cells derived from $CD271^+$ bone marrow mononuclear improves the lymphohaematopoietic engraftment of $CD133^+$ haematopoietic stem cells. **Bone Marrow Transplantation Vol. 45, Supplement 2, page 275** (36th Annual Meeting of the European Group for Blood and Marrow Transplantation- EBMT 2010, Vienna, Austria. **Awarded with the first place for the best scientific poster presentation)**

4. Z. Kuçi, S. Köller, H. Kreyenberg, K. Pütsch, E. Deak, S. Hünecke, E. Rettinger, R. Henschler, U. Köhl, T. Tonn, M. Grez, D. von Laer, T. Klingebiel, P.Bader, S. Kuçi. CD271 Antigen Defines a Subset of Mesenchymal Stromal Cells with Immunosuppressive and Engraftment-Promoting Properties. **Cytotherapy, Vol. 11, No 1, 2009, page 38** (ISCT 2009 Annual Meeting Abstracts, San Diego, USA)

5. Z. Kuçi, S. Köller, C. Amara, H. Kreyenberg, U. Köhl, T. Klingebiel, P. Bader, S. Kuçi. Immunomodulatory Potential of Human Mesenchymal Stromal Cells Derived from $CD271^+$ Bone Marrow Mononuclear Cells. **Cytotherapy, Vol. 10, Supplement 1, 2008, Abstract Nr. 99** (ISCT 2008 Annual Meeting Abstracts, Miami, USA)

Abbreviations

APC	Allophycocyanin
BCIP/NBT	5-bromo-4-chloro-3-indolyl phosphate/nitro blue tetrazolium
BDNF	Brain-Derived Neurotrophic Factor
BM	Bone Marrow
BM-MNCs	Bone marrow mononuclear cells
BrdU	5-bromo-2'-deoxyuridine
BSA	Bovine Serum Albumin
CBA	Cytometric Bead Array
CD	Cluster designation
CFE	Colony-Forming Efficiency
CFU-F	Colony forming units-fibroblast
Con-A	Concanavalin A
DC	Dendritic Cell
DMEM	Dulbecco's Modified Eagle Medium
DMSO	Dimethyl sulphoxide
DNA	Deoxyribonucleic acid
DT	Doubling Time
ELISA	Enzyme Linked Immunosorbent Assay
FACS	Fluorescence Activated Cell Sorter
FBS	Foetal Bovine Serum
FITC	Fluorescein Isothiocyanate
G-CSF	Granulocyte-Colony Stimulating Factor
GD2	Ganglioside D2
GFP	Green Fluorescent Protein
GM-CSF	Granulocyte Monocyte-Coloniy Stimulating Factor
GvHD	Graft versus Host Disease
HGF	Hepathocyte Growth Factor
HRP	Horseradish peroxidase
HSA	Human Serum Albumin
HSCT	Human Stem Cell Transplantation
HUCPVCs	Human Umbilical Cord Perivascular Cells
IDO	Indoleamine 2,3-dioxygenase
IGF	Insulin-like Growth Factor
IL	Interleukin
INF-γ	Interferon- γ
LNGFR	Low Affinity Nerve Growth Factor Receptor
MACS	Magnet Activated Cell Sorter
MHC class II	Major Histocompatibility Complex II
MLR	Mixed lymphocyte reaction
MSCs	Mesenchymal stromal cells
NGF	Nerve Growth Factor
NK cell	Natural Killer cell
NO	Nitric Oxide
NOD/SCID	Non-obese diabetic/Severe Combined Immunodeficiency
NT3	Neurotrophin 3
PB-MNC	Peripheral blood mononuclear cells
PBS	Phosphate Buffered Saline
PCR	Polymerase Chain Reaction
PD	Population Doublings

PE	Phycoerythrin
PerCP	Peridinin Chlorophyl Protein
PGE2	Prostaglandin E2
PHA-P	Phytohemagglutinin
PL	Platelet Lysate
POD	Peroxidase
PWM	Pokeweed mitogen
RLU	Relative Light Units
RPMI	Roswell Park Memorial Institute
SEB	Staphylococcal Enterotoxin B Fragment
sHLA-G	Soluble Human Leukocyte Antigen-G
SSEA	Stage-specific embryonic antigen
T regs	T Regulatory Cells
TGF-β	Transforming growth factor -β
TMB	3,3′,5,5′-tetramethylbenzidine
TNF-α	Tumor Necrosis Factor alpha
Trk	Tyrosine kinase
VEGF	Vascular Endothelial Growth Factor

1. INTRODUCTION

1.1. Mesenchymal stromal cells (MSCs)

Mesenchymal stromal cells (MSCs) are non-hematopoietic multipotent cells capable of differentiating at least along three lineages: osteoblasts, adipocytes and chondrocytes. MSCs belong to the stromal cells that play an important role in supporting hematopoiesis through their adhesion/interaction with the hematopoietic stem cells (HSCs) and secretion of cytokines and growth factors that are necessary for HSC differentiation (1).

1.1.1. The discovery and terminology of mesenchymal stromal cells

Mesenchymal stem cells have been of interest long before the term 'MSC' came into existence. German pathologist Cohnheim in 1867 suggested the presence of nonhematopoietic stem cells in bone marrow. He described that bone marrow may be the source of fibroblasts that deposit collagen fibers as a part of the normal process of wound repair (2).

The pioneering studies of differentiation potential of bone marrow cells transplants in the bone tissue came from Friedenstein (3). He and his coworkers (4;5) described for the first time formation of fibroblast colonies in monolayer cultures of cells from bone marrow and spleen cultures. To obtain MSCs they placed whole bone marrow in plastic culture dishes and after 4 hours they removed nonadherent cells. Adherent cells gave rise to typically elongated fibroblast cells from which on the 3^{rd}-5^{th} day appear fibroblast colonies and on the 10^{th}-14^{th} day they already consisted of hundreds or thousands of cells with considerable differences in the shapes and in the density of individual colonies. Friedenstein demonstrated that each colony is derived from a single fibroblastic colony-forming cell (FCFC) or colony forming unit-fibroblastic (CFU-F) (6). They also showed that these *ex vivo* grown cells termed as "stromal mechanocytes" when transplanted under kidney capsule differentiated in bone tissue in the site of the transplantation (7). These cells were able to differentiate into mesenchymal cells as well as fibroblasts (8) and chondroblasts (9). Friedenstein`s observations were followed by other groups throughout the 1980s.

At the beginning of the eighties, extensive *in vitro* studies allowed a more precise characterization of the MSCs. Castro-Malaspina et al. (10) suggested how progenitor cells for CFU-F could be selectively isolated by density gradient (density "cut") at 1.070/cm^3.

The notion of a "stromal stem cell" was proposed for the first time by Owen (11;12), whereas the term human "mesenchymal stem cells" was first introduced by Caplan in 1991 to describe adherent, marrow-derived homogeneous cells that proliferate *ex vivo* and can be differentiated to produce multiple connective cell types (13).

As the “stem cell” label has scientific implications that may or may not be strictly correct, the Mesenchymal and Tissue Stem Cell Committee of the International Society for Cell Therapy (ISCT) recommended a clarification of the nomenclature for these mesenchymal stem cells to be termed “multipotent mesenchymal stromal cells” (14).

1.1.2. Sources of MSCs

Adult bone marrow (BM) contains hematopoietic stem cells (HSCs) as well as non-hematopoietic, stromal cell population. Within this stromal population reside MSCs, which not only support hematopoiesis but also differentiate into multiple lineages, including fat, bone, and cartilage. According to the CFU-F assay the frequency of progenitor cells for MSCs in BM aspirates is 0.001–0.01% (10;15). In newborn this frequency is 1 out $1x10^4$; at 10 years of age 1 out $1x10^5$, after 30 years of life 1 out $2.5x10^5$, at 40 years of age 1 out $4x10^5$, while at 80 years old people 1 out $2x10^6$ (16).

In addition to the bone marrow as a major source of MSCs (4;10;15;17;18), in the last decade MSCs have been also isolated from many other sources such as adipose tissue (19-21), cord blood (22;23), amniotic fluid (24-26), human placenta (27), fetal BM and lung (28), fetal kidney and liver tissues (29;30), fetal skin, fascia of the abdominal rectus muscle and carotid, saphena vein (31), synovium (32), circulating blood (33;34), periosteum (35), cartilage (36), synovial fluid (37), thymus (38), dermis (39), mouse heart (40), dental pulp (41;42) and spleen (43).

1.1.3. Definition criteria for MSCs

Since MSCs are produced in different laboratories using various tissues, methods of isolation, expansion and characterization, the Mesenchymal and Tissue Stem Cell Committee of the International Society for Cell Therapy (ISCT) in order to clarify the nomenclature and to support the development of comparative studies between laboratories proposed the definition of the MSCs (44).

The MSCs must fulfill these minimal criteria:

1) They must adhere to plastic,

2) They should be negative for CD34, CD45, CD14 or CD11b, CD19 or
CD79a, HLA-DR, and positive for CD73, CD90, CD105, and

3) They should be capable of differentiation along three lineages: chondrocyte, osteoblast and adipocyte.

1.1.4. Standard method for generation of MSCs

The protocols for generating MSCs from different species and different sources vary. Standard method for generation of MSCs is the old method using plastic adherence (4). With difference to earlier studies nowadays instead of whole bone marrow, isolated bone marrow mononuclear cells using ficoll gradient are plated into plastic culture dishes to adhere for 48-72 hours. Nonadherent cells are removed and adherent cells are cultured 10-14 days until they reach 70-80% confluence (45-47). Over time in culture, the non-adherent hematopoietic cells are washed away, resulting in small, adherent fibroblast-like cells. When cultured in medium MSCs display an initial lag phase of about 5 days, followed by a log phase of rapid growth for about 5 days, and then fall into a stationary phase (48;49).

In vitro expansion of MSCs is conventionally achieved in medium containing fetal bovine serum (FBS) and is increased by addition of growth factors. However, for widespread clinical applications, MSCs should be cultured in FBS-free medium because of the risk of xenogenic contamination (50) and immunologic consequenses such as development of anti-FBS antibodies (51). Doucet et al. (52) used for the first time platelet lysates (PL) as an alternative to FBS to expand human MSCs. They demonstrated that PL-containing medium promoted efficient MSC expansion and MSCs cultured in the presence of PL maintained their osteogenic, chondrogenic, and adipogenic differentiation properties and retained their immunosuppressive activity.

1.1.5. Heterogeneity of MSCs

1.1.5.1. Heterogeneity concerning the number of progenitor cell for MSCs and their proliferation potential

MSCs generated through plastic adherence represent a heterogeneous group of cells. The heterogeneity of MSCs concerning their proliferative and differentiation potential were reported from Friedenstein (7), who observed the differences in each culture in the shapes and in the density of individual colonies. Later, Owen (11) confirmed the same by describing CFU-F as heterogeneous stem and progenitor cells where some of them had high ability for self-renewal and multipotentiality whereas the other had more limited potential. The differences between BM donors concerning CFU-F number has been also shown by Castro-Malaspina (10;53).

This heterogeneity is typically exemplified by a broad range of colony sizes, representing varying growth rates, and different cell morphologies, ranging from fibroblast-like spindle

shaped cells to large flat cells colonies (48;54;55). Differences in CFU-Fs as well as in proliferation by the same donors of BM at the same time were observed either (48). A decreased number of CFU-Fs and cell proliferation of BM-MSCs with increasing age is often reported (56-62). Moreover, age-dependent and gender-dependent differences in the CFU-F frequency with a decline in the progenitor frequencies in the bone marrow of adult mice (mMSCs), and a lower MSC frequencies in all female donors have been reported (63). In contrast, other authors did not find any changes in the number of bone marrow-derived CFU-Fs, their average size and cell density per CFU-F in the young and old persons (64). Yet, MSCs from old donors exhibited a decreased maximal life span compared with cells from young donors (24 ± 11 population doublings [PD] vs 41 ± 10 PD, $P < 0.05$). The mean PD rate was lower in old donor cells (0.05 ± 0.02 PD/day) compared with young donor cells (0.09 ± 0.02 PD/day, $P < 0.05$) (65). The MSCs isolated from pediatric donors reached a cumulative PD almost twice as high as MSCs isolated from young adult donors after 112 days, and their cell growth was strictly related to the donor's age (66). Phinney reported that at the first passage hMSCs exhibited growth rates *in vitro* that varied up to 12-fold between donors, but no correlation between growth rate and the age or gender of hBM-MSCs donors was found (67).

Age-related changes in human BM-MSCs include increased oxidative damage, increased ROS levels and p21 and p53, suggesting a loss of MSC fitness with age (60). On contrary, Lund at al. reported that mesenchymal stromal cells from donors varying widely in age (8 months to 58 years) are of equal cellular fitness after *in vitro* expansion under hypoxic conditions (68).

Therefore, studies investigating the influence of age on MSCs are contradictory, probably due to differences in experimental parameters such as donor species, sex, age, cell isolation, and cell culture protocols.

1.1.5.2. Heterogeneity concerning the differentiation potential

Differentiation potential represents one of the criteria that should be fulfilled by the cells in order to be defined as mesenchymal stromal cells. Even though the tissue-specific differentiation media for MSCs are standardized, data reported on this issue are contraversial. According to many authors differentiation potential of MSCs may be dependent on the age of the donor (66;69). Osteogenic differentiation (levels of specific ALP activity) declined progressively (40%) with age compared to “young” and “adult” MSCs, whereas chondrogenic differentiation also declined in ‘‘aged’’ MSCs but this did not reach significance. In addition,

adipogenic differentiation did not change significantly with age (60). According to Moerman et al. (70) aging activates adipogenic and suppresses osteogenic programs in mesenchymal marrow stroma/stem cells. In a review article Sethe *et al.* (71) reported that the osteogenic potential of human MSCs decreased with age but adipogenic properties potential was found either to remain unaltered or to increase with age, in contrast to mouse MSCs in which adipogenic potential tends to decrease (63). Other authors, however, did not observe any differences in mineralization matrix formation in young individuals, old individuals, and patients with osteoporosis (64). In line with this, it has been reported that the number of mesenchymal stem cells declines but neither phenotype nor osteogenic and adipogenic differentiation capacities changes with the age of rats (59). Moreover, there are reports which demonstrated gender differences concerning differentiation potential of MSCs. Katsara et al. (63) demonstrated for the first time that male mouse MSCs exhibit stronger differentiation potential towards both, the osteogenic and the adipogenic lineage.

Previous reports described age-dependent and gender-dependent differences as to differentiation potential of MSCs. There are also reports which demonstrated changes in dhe the differentiation potential of MSCs in the same donor depending on the time of donation e.g. Phinney et al. reported evident differences in both growth rate and ALP activity in human MSC cultures established from multiple aspirates obtained over a six month period from the same donors. Therefore, it appears that cellular heterogeneity produced by the method of harvest is propagated within and among different donor populations during culture expansion in vitro (67)

1.1.5.3. Heterogeneity of immunosupressive potential

Mesenchymal stromal cells have been shown to exert an immunomodulatory potential. However, the reports on this potential and its mediators are controversial. As to in vitro studies it is quite evident that most of reports agree that MSCs show the inhibitory effect on proliferation of lymphocytes induced either by mitogens or allogeneic reaction ((72-76). In these experiments the authors demonstrated an inhibition of lymphocyte proliferation from 10-90%. These great variations depend not only on the MNC and MSC donors but also on different experimental designs. Some of the authors used complete PB-MNC cell fraction, while the others used in their experimental setting isolated T lymphocytes or their subsets and dendritic cells as antigen presenting cells (74;77). There are also controversial data on the clinical immunosuppressive effect of MSCs. Le Blanc et al. (78) in a phase II study treated

successfully the acute graft versus host disease, whereas the others have not been able to observe such an effect (79).

1.1.5.4. Heterogeneity at the clonal level

Single-cell-derived (SCD) parent and doughter clones from a mesenchymal cell source, human umbilical cord perivascular cells (HUCPVCs), has a hierarchical schema for MSC self-renewal and differentiation in which a self-renewing multipotent MSC gives rise to more restricted self-renewing progenitors that gradually lose differentiation potential until a state of complete restriction to the fibroblast is reached (80).

It is reported that about one third of single-cell derived clones differentiated into all three lineages. Most of the clones (60-80%) displayed an osteo-chondrogenic (OC) potential and none of them demonstrated a limited osteo-adipogenic (OA) or chondro-adipogenic (CA) differentiation potential. There were no clones found with pure chondrogenic or adipogenic potential either. Clones progressively lost their adipogenic and chondrogenic differentiation potential at increasing cell doublings (81). Russell et al. (82) investigated the relationship between proliferation potential of MSCs and their potency. They demonstrated that tripotent OAC (osteo-, adipo- and chondrogenic) clones were highly proliferative with colony-forming efficiencies that ranged from 35% to 90%; whereas, O clones formed colonies with an efficiency of 5% or less. In addition, differences in immunosuppressive capacity of MSCs derived from different bone marrow donors has been observed (72;73). Xu et al. (83) were the first to show differences in the immunosuppressive potential of mouse MSCs at the clonal level in vitro and in vivo.

Therefore, to avoid or to minimize these differences and to finally obtain a homogeneous population of MSCs there is a need to search for novel markers which may identify progenitor cells for MSCs. Some of the markers used for such a purpose are described below.

1.1.6. Cell surface antigens used for isolation of MSC-progenitors

Despite extensive research, there is still no single cell surface marker that reliably identifies MSCs within the bone marrow. A series of antibodies to surface epitopes have been employed by several investigators as shown below, but almost none of them came into general use.

STRO-1 represents the first antibody used to partially enrich CFU-Fs from human BM (84-87). STRO-1 is also expressed on erythroblasts (84;85), and it is coexpressed by about 20% of

rat $CD34^+$ BM-MNCs. In addition, its expression was identified in the endothelium of arterioles and capillaries (88).

STRO-3 antibody was generated by immunization of mice with the human MSCs derived from $STRO\text{-}1^+$ BM-MNCs. This antibody reacts with a minor subset of $STRO\text{-}1^+$ cells contained within adult BM aspirates and does not react with $CD34^+$ hematopoietic stem cells. STRO-3 identifies a high proportion of bone marrow stromal stem cells that possess extensive proliferative and multilineage differentiation capacity. Using retroviral expression cloning, it was found that STRO-3 binds to tissue nonspecific alkaline phosphatase, a cell surface glycoprotein usually associated with cells of the osteoblast lineage (89).

STRO-4 antibody was generated by immunization of mice with the CD106 (VCAM-1)-selected ovine MSCs as an immunogen. Cells isolated with STRO-4 exhibited reactivity with markers commonly associated with MSCs isolated by plastic adherence including CD29, CD44, and CD166. Moreover, when placed in inductive culture conditions in vitro, STRO-4(+) MSCs exhibited multilineage differentiation potential and were capable of forming osteoblasts, adipocytes and chondrocytes. Biochemical analysis revealed that STRO-4 identified the beta isoform of heat shock protein-90 (Hsp90beta) (90).

CD105/SH2/endoglin (91;92) is expressed by bone marrow progenitor cells (93) and therefore was used to generate MSCs (94), but this antigen is also expressed on endothelial cells (95) and on pre–B cells (96).

CD73

The SH-3 and SH-4 monoclonal antibodies recognize epitopes present on the surface of human MSCs. By using SH-3 antibody, a protein of molecular weight approximately 67 kDa immunoprecipitated from a solubilized membrane preparation of human MSCs. Analysis of peptides derived from this protein by mass spectrometry and sequencing identified it as CD73 (ecto-5'-nucleotidase). These results indicate that both SH-3 and SH-4 epitopes are present on CD73, but they are distinct. CD73, present in lymphoid tissue, plays a role in the activation of B-lymphocytes, signal transduction in the hematopoietic compartment of bone marrow, in bone marrow stromal interactions and in the differentiation of MSCs (97).

STRO-1, CD105 and CD73 antigens as markers, however, are known to be present on other types of BM cells and therefore are not very selective for MPCs (MSC progenitor cells).

SSEA-1 (Stage-specific embryonic antigen-1) identifies the most primitive mesenchymal progenitor cells in the adult murine bone marrow and the same subset in mesenchymal cell cultures. Characterization of SSEA-1+ mesenchymal cells revealed that upon purification these cells gave rise to SSEA-1- mesenchymal cells. Most importantly, a single-cell-derived population was capable of differentiating abundantly into different mesenchymal cell types in vivo (98).

SSEA-4 (Stage-specific embryonic antigen-4) also identifies an adult mesenchymal stem cell and can be used for the prospective isolation of MSCs from whole human bone marrow aspirates in mice and humans. The MSCs generated from SSEA-4^+ BM-MNCs were able to differentiate along adipocytes, osteoblasts and chondrocytes (99).

D7-FIB antibody recognizes the antigen which is a fibroblast-specific molecule of yet-unknown function. D7-FIB^+, $CD45^{low}$, $LNGFR^+$ cells are defined as progenitor cells for MSCs and represent only 0.01% of BM MNCs (93). In comparison to the above mentioned markers, the D7-FIB molecule showed minimal co-expression on other bone marrow cells. It therefore appears to be superior to STRO-1 or CD105 as a marker of MPCs in bone marrow (93).

GD2 (neural ganglioside GD2) represents a novel surface marker for the identification of progenitor cells for MSCs. Martinez et al. (100) demonstrated that GD2 is not only expressed by MSCs newly isolated from bone marrow but also by expanded MSCs in tissue culture, as evaluated by flow cytometry and immunocytochemistry.

CD146 (MCAM, Melanoma-associated adhesion molecule) is another very useful marker for identification and isolation of perivascular cells (pericytes), which are supposed to be the ancestor cells of mesenchymal stomal cells. The evidence that multipotent mesenchymal stromal cells can be obtained from diverse human tissues and share functional properties and gene-expression profile with $CD146^+$ perivascular cells demonstrates at best this relationship (31).

CD271 antigen which is used for generation of MSCs from bone marrow (17;93;101-105), adipose tissue (106;107), trabecular bone (108) and amnion fluid (26).

1.2. CD271 antigen as a marker for isolation of progenitor cells for MSCs

1.2.1. CD271 antigen

CD271 (synonyms: p75NTR or LNGFR: Low-affinity Nerve Growth Factor Receptor) is the sixteenth member of the tumor necrosis factor receptor (TNFR) superfamily of transmembrane proteins. Members of the TNFR family including CD271, share homology in their extracellular domain which binds neurotrophins (109;110), and have a cytoplasmic death domain, although CD271 has a unique intracellular structure and downstream signaling partners. CD271 differs from other members of the TNFR receptor family in that it binds pro-neurotrophins and mature neurotrophins and affects the growth, differentiation and death of the nervous system (111).

1.2.2. Localization of gene for CD271 antigen

The nerve growth factor receptor gene is located at human chromosome region 17q12-17q22, distal to the chromosome 17 breakpoint in acute leukemias (112).

1.2.3 The role of CD271 antigen in the organism

The interaction between nerve growth factor and nerve growth factor receptor (NGFR) plays an essential role in the survival and maintenance of sympathetic and sensory neurons (113;114). The ligands for CD271 are neurotrophins, which are nerve growth factor (NGF), brain-derived neurotrophic factor (BDNF), neurotrophin 3 (NT3) and neurotrophin 4/5 (NT4/5). Recent studies have provided evidence that CD271 also serves as a receptor for the pro-forms of these neurotrophins (111).

Multiple receptor partners and functions

CD271 has contradictory actions; it functions to promote cell survival or induce cell death. These opposing effects are mediated by the association of CD271 with a number of different receptor partners (111). In the absence of tyrosine kinase (Trk) neurotrophin receptor expression, CD271 can induce apoptosis and cell death. The signaling pathways from the CD271-dependent apoptotic response are incompletely understood but are thought to involve activation of Jun N-terminal kinase (JNK) and further downstream events such as release of cytochrome c and activation of caspases 9, 6 and 3 (109). In contrast to CD271-dependent

apoptosis, while in complex with TrkA receptor, CD271 promotes cell growth by enhancing the TrkA downstream signaling induced upon NGF binding (110;115).
In summary, the outcome of CD271 activation depends on the type of ligand and the ability to crosslink and co-ordinate co-receptors, thereby facilitating the activation of specific signaling pathways (111).

1.2.4. Tissue distribution of CD271 antigen

CD271 antigen is expressed on neural and non-neural tissues.

a) Neural Tissue

Nerve growth factor (NGF) is a protein which promotes the survival and differentiation of sensory and sympathetic neurons in culture and plays an important role in neuronal development. Chesa and al. reported that human NGF-R is expressed in the peripheral nerves (nerve fibres, perineum), autonomic ganglia (ganglion, satellite, Schwann cells and spinal cord (posterior horn) and NGF-R expression changes during normal development (116). CD271 is widely expressed in developing neural tissue (115;117). Subpopulations of peripheral sympathetic and sensory neurons express varying levels of the receptor (117). However, in the adult, CNS expression is limited to a few restricted cell populations including olfactory glia, and cerebellar Purkinje neurons (118)

b) Non-neural Tissue

Outside the nervous system, NGFR (CD271) is expressed in bone marrow stroma of humans *in vivo* and *in vitro* (119;120), bone marrow (17;93;101-105), trabecular bone cavity (108), adipose tissue (106;107) and human placenta (26). p75NTR (NGFR) is expressed in myoblasts and developing tissues of mesenchymal origin (116;121), including hair follicles, limb bud fibroblasts, kidney, lung and testes (121). In mature cells, non-neural expression is found in endothelial cells, perivascular fibroblasts, dental pulp cells, prostate, epithelial cells and immune B cells (116;122). NGFR expression in malignant tumors generally parallels to its normal tissue distribution (116). Some human cell lines of non-neuronal cells of neuroectodermal origin, such as melanomas (123), neuroblastomas, meningeal cells, glial cells and Schwann cells (124) also express NGFR. Although little is known about the effects of NGF on those cells, NGFR was detected in a number of cultured cells of mesenchymal, epithelial, and hematopoietic derivation. lmmunohistochemical analysis showed that NGFR is expressed in several non-neural human tissues, and the cell types in which NGFR was found in derivatives from all three germ layers (116;125).

1.2.5. Localization of LNGFR$^+$ (CD271$^+$) cells in bone marrow, their morphology and relationship to the other cells

The LNGFR stromal cells appear in the fetal bone marrow before the hematopoietic activity begins, originate from the vessel adventitia, and radiate in the bone marrow cavity (119). Using immunochemistry these authors described MSC-like cells isolated from bone marrow by anti-p75LNGFR antibodies that were initially shown to stain the stromal compartment of bone marrow. Two anti-nerve growth factor receptor (LNGFR or $p75^{NGFR}$) antibodies, Me20.4 and Me821 1, label stromal cells with dendritic features in fresh smears and in formalin-fixed, paraffin-embedded human bone marrow. These authors described that LNGFR positive cells have an oval nucleus, a scanty cytoplasm with long dendrites that are in close contact with the hematopoietic cells, line the abluminal side of sinus endothelial cells, and provide the scaffold for the hematopoietic marrow. At the electron microscopy level, the immunogold tag labels the body and the long branching dendrites of fibroblast-like cells with scanty cytoplasm containing mitochondria, endoplasmic reticulum, and dense bodies. The LNGFR$^+$ cells are positive for alkaline phosphatase, reticulin, collagen, vimentin, TE-7, and CD13 but negative for endothelial (vWF, CD34, Pal-E), neural (CD56, neurofilament) and leukocyte markers (CD45, CD68) (119).

Caneva at al. (120) using immune-electron-microscopy described human bone marrow cells NGFR+ cells that were showing either a star-shape, with long and convoluted dendritic projections, and branching with each other to form a complex system of lacunae upon which hematopoietic cells were arranged. Other NGFR+ cells had an elongated spindle-like morphology. NGFR+ dendrites were seen in close contact with each other and with the different hematopoietic cells, although definite junctions were never noticed. NGFR+ dendrites were also observed surrounding mature plasma cells, in close apposition with adipocytes or surrounding bone marrow sinusoids. These findings may give some clues about the function of the bone marrow stromal cells, which are known to be involved in the homing and recirculation of hematopoietic cells. In addition, the presence and distribution of NGFR in the bone marrow stroma may support the recent evidence of a co-stimulatory effect of NGF in early hematopoiesis.

1.2.6. CD271 antigen as a versatile marker for isolation of progenitor cells for MSCs

It was demonstrated that the low-affinity nerve growth factor receptor (LNGFR), now clustered as CD271, was the most selective marker (93) for progenitor cells of MSCs.

Accordingly, high-level expression of CD271 on BM-MNCs was reported by independent studies in which this antigen was successfully used for isolation of precursor cells of MSCs (17;93;101-105). Interestingly, the freshly isolated p75LNGFR-fraction was approximately 50% positive for CD133, which was down regulated to 0–1% after culture (17). In addition, isolation of CD271-expressing cells from the bone marrow (17), adipose tissue (106;107), trabecular bone (108) and human placenta (26) has been shown to yield homogeneous cell populations that are rich in clonogenic precursors and have a high capacity to undergo adipogenic and osteogenic differentiation.

1.3. The role of MSCs and their therapeutic use

1.3.1. MSCs in hematopoietic maintenance and engraftment

The microenvironment of mammalian bone marrow is composed of several different elements, including macrophages, fibroblasts, adipocytes, osteoprogenitors, endothelial cells reticular cells and the multipotent MSCs. All these elements contribute to support hematopoiesis and bone homeostasis through a molecular crosstalk between hematopoietic stem cells (HSCs) and cells that comprise the *niche*, involving a large number of molecules, including cadherins, integrins, chemokines and cytokines (126-128). Bone marrow-derived MSCs play a crucial role in the development and differentiation of the lympho-hematopoietic system by secreting a number of growth factors and regulatory cytokines, and by promoting cell-to-cell interactions. Majumdar et al. (129) examined the MSC role as a stromal cell precursor and demonstrated that traditional marrow-derived stromal cells (MDSCs) from the same marrow sample are capable of supporting hematopoietic differentiation *in vitro*. In that study, RT-PCR analysis of cytokines and growth factor mRNA showed that treatment of MSCs with IL-1α upregulates the expression of IL-1 α, G-CS and GM-CSF compared to untreated MSCs. The expression of these cytokines and growth factors suggests that MSCs may function in hematopoiesis. The authors concluded that MSCs in long-term bone marrow culture (LTBMC), maintained the hematopoietic differentiation of CD34+ hematopoietic progenitor cells. Animal models suggest that the transplantation of healthy stromal elements, including MSCs may enhance the ability of the bone marrow microenvironment to support hematopoiesis after stem cell transplantation (130). Cotransplantation of autologous CD34+ hematopoietic stem cells with MSCs improved the hematopoietic engraftment in monkeys (131). Kim et al. (132) demonstrated that cotransplanted BM-MSCs (MSCs) with HSC ($CD34^+$) in NOD/SCID mice, enhanced their engraftment in a MSC dose- dependent manner.

These experimental data, together with the known physiological role played by MSC in sustaining hematopoiesis, have provided the rationale for testing the capacity of these cells to accelerate hematologic recovery in patients receiving myeloablative therapy with HSC support. The first clinical trial on the use of MSC for accelerating hematologic recovery was conducted in women undergoing autologous transplantation for breast cancer. Twenty-eight breast cancer patients were infused with $1–2\times10^6$ MSC/kg, 1-24 hours after transplantation of CD34 cells with a rapid hematopoietic recovery occurred without any undesired reaction related to the infusion of MSCs (133).

Another interesting result was obtained in a 20-year-old woman suffering from myelogenous leukemia. The expanded haploidentical MSCs were infused after transplantation of haploidentical HSCs ($CD34^+$ cells) which resulted in a rapid engraftment and did not show acute or chronic GVDH and complete remission from leukemia (134).

A multicenter trial explored the safety of MSC infusion also in recipients of allogeneic HSCs. Forty-six patients received HSCs and culture expanded MSCs from their HLA-identical siblings in hematologic malignancy patients. On day 0, patients were given culture-expanded MSCs intravenously (1.0-5.0 $x10^6$/kg b.w.) 4 hours before infusion of either bone marrow or peripheral blood stem cells. Hematopoietic recovery was prompt for most of the patients (135). Consistent with this data, co-transfusion of haplo-identical hematopoietic and mesenchymal stromal cells to treat a patient with severe aplastic anemia improved the engraftment (136). In contrast, it is reported that MSCs do not support hematopoietic engraftment when they are cotransplanted with umbilical cord blood transplantation (UCBT) (137).

Together, these data suggest that MSCs represent an important cellular component of the bone marrow microenvironment.

1.3.2. MSCs in tissue repair and regenerative medicine

The lineage commitment and transdifferentiation properties of MSCs make these stem cells candidates for use in repair/molecular medicine and tissue engineering. Initially, MSCs were thought to mediate tissue and organ repair by virtue of a multilineage differentiation potential that enabled them to replace damaged cells, like differentiation of the donor hMSCs after traumatic brain injury in adult rats in cells that also express the neuronal and astrocytic markers (138), or meniscus regeneration with implanted cells in osteoarthritis (OA) by locally delivered MSCs (139).

The new data, however, ascribe this effect more to the paracrine and autocrine factors, because MSCs secrete a variety of cytokines and growth factors that have both paracrine and autocrine activities. These secreted bioactive factors suppress the local immune system, inhibit fibrosis (scar formation) and apoptosis, enhance angiogenesis (140), and stimulate mitosis and differentiation of tissue-intrinsic reparative mechanisms or stem cells. These effects, which are referred to as trophic effects, are distinct from the direct differentiation of MSCs to repair the damaged tissue (141). Several studies which tested the use of MSCs in models of infarct (injured heart), stroke (brain), or meniscus regeneration models are viewed in the context of MSC-mediated trophic effects in tissue repair (15;141;142). It is now widely believed that in response to tissue injury, MSCs home to the site of damage (143) in mice and swine heart (144;145) and encourage repair processes through production of trophic factors (146), including growth factors, cytokines, and antioxidants (147-149). Transplantation and differentiation of MSCs to functional osteoblasts was demonstrated *in vivo* in an animal model and in humans, which led to treatment for osteogenesis imperfecta (150). Finally, bone engineering with biomaterials seeded with MSCs are effective in replacing lost bone (151).

MSCs show plasticity, based on their ability to transdifferentiate into cells of other germ layers (152). It is reported that MSC are able to differentiate in neurons in mouse brain (153) (154), *in vitro* in hepatocyte- like cells (155) and in rats in muscle cells (156). Data from a recent study indicate that mechanically stimulated MSCs create an angiogenesis-promoting environment (140).

On the basis of many reports and his own experience Prockop concludes that the primary role of the MSCs is to form niches for hematopoietic stem cells (paradigm I); a second paradigm is that the MSCs repair tissues by engraftment and differentiation to replace injured cells (paradigm II); and the more recent paradigm (paradigm III) is that MSCs are engaged in cross-talk with injured tissues and thereby generate microenvironments or 'quasi-niches' that enhance the tissue repair (157).

1.3.3. Immunomodulatory role of MSCs

Although traditionally the regenerative capacity of MSCs through their presumptive plasticity was seen as the driving force behind interest in these cells, their role in modulating the immune response is now attracting greater interest.

T cells are a major executor of the adaptive immune response, and numerous studies have demonstrated that MSCs modulate the function of these cells. MSCs can exert an T cell

immunosuppressive effect *in vitro* and *in vivo* (158;159) by acting on all immune effectors (160). Low immunogenicity of MSCs might be explained with their low expression of major histocompatibility complex (MHC) class I antigens and lack of MHC class II and co-stimulatory molecules such as CD40, CD80 and CD86 (73;76). Expression of MHC class II antigens can be induced by interferon-gamma (IFN-gamma) treatment (73;161). This is relevant because, in many inflammatory milieus IFN-gamma is up-regulated, which in turn may result in an increase in the expression of MHC class II. However, Le Blanc demonstrated that pretreated MSCs with IFN-gamma failed to generate a proliferative response in allogeneic lymphocytes (73). This property is used to expand *ex vivo* generated MSCs from either HLA-identical siblings, haploidentical donors, or third-party mismatched donors for the treatment of GvHD grade 2–4 (78).

Although mostly immune privileged MSCs, may under certain conditions also be subject to immune rejection. Allogeneic MSCs cotransplantated with bone marrow in sublethally irradiated mice induce a memory T cell response resulting in rejection of an allogeneic stem cell graft (158;162;163). However, patients receiving treatment with allogeneic human MSCs did not show anti-allogeneic MSC antibody production or T cell priming (51). The lack of MHC class II and co-stimulatory molecules MSCs protects them from the alloreactive natural killer (NK)-cell-mediated lysis (164).

In addition, human MSCs express HLA-G, a non-classical MHC class I antigen, which may prevent the immune response against MSCs, as shown by blocking experiments, although the expression seems to decrease in culture (165). The mechanisms for such positive therapeutic effects remain partly obscure. However, the antiproliferative properties exerted by MSCs inducing division arrest anergy of activated T cells in the G0 / G1 phase of the cell cycle of activated T cells is demonstrated (166), but not induction of apoptosis (76;77). A possible mechanism of MSCs on inhibition of T cell responses is that by indoleamine 2,3-dioxygenase (IDO)- mediated tryptophan degradation (167;168). In addition, MSCs strongly inhibit dendritic cells (DCs), the most potent antigen-presenting cells (APC) generated from peripheral blood monocytes. MSCs could suppress monocyte differentiation into DCs, whereby differenitated DCs expressed significantly reduced amount of CD83 antigen, suggesting their skew to immature status. This reaction was associated with decreased expression of presentation molecules (HLA-DR and CD1a) and co-stimulatory molecules (CD80 and CD86) and down-regulated IL-12 secretion by monocytes were also observed (169-171). Moreover, prostaglandin E2 (PGE_2) directly added to cultures of monocytes blocked their differentiation toward DCs in a manner similar to MSCs (172).

MSCs can produce a shift from DC1 to DC2 by decreasing TNF-alpha secretion, which leads to a reduced number of IFN-gamma-producing Th1 cells (74), and by inducing DCs to secrete IL-10, which favours IL-4-producing Th2 cells and regulatory T cells (74). Spaggiari and al. (168) showed that MSCs not only inhibit the interleukin-2 (IL-2) induced NK proliferation but also prevent the induction of cytotoxic cells by down-regulation of activating receptors (NKp30, NKp44, and NKG2D) on the surface of NK cells. Moreover, indoleamine 2,3-dioxygenase (IDO) and prostaglandin E_2 (PGE_2) represent key mediators of the MSC-induced inhibition of NK cells. Interestingly, MSCs inhibited interleukin-2 (IL-2)–induced NK-cell proliferation, contrary to the fact that activated NK cells could kill MSCs (173).

MSCs inhibit T cell proliferation by releasing soluble factors such as TGF-β, IGF; VEGF, HGF, NO, IL-10 and PGE_2. Production of nitric oxide (NO) by mouse MSCs has been shown to be involved in suppression of Stat5 phosphorylation and T cell proliferation (174). On the other hand, T regulatory cell population generated in the presence of MSCs in MLR was similar to that generated in the absence of MSCs (74). Some of interactions between MSCs and immune cells as well as soluble factors that mediate their immunosuppressive effects are shown in Figure 1.

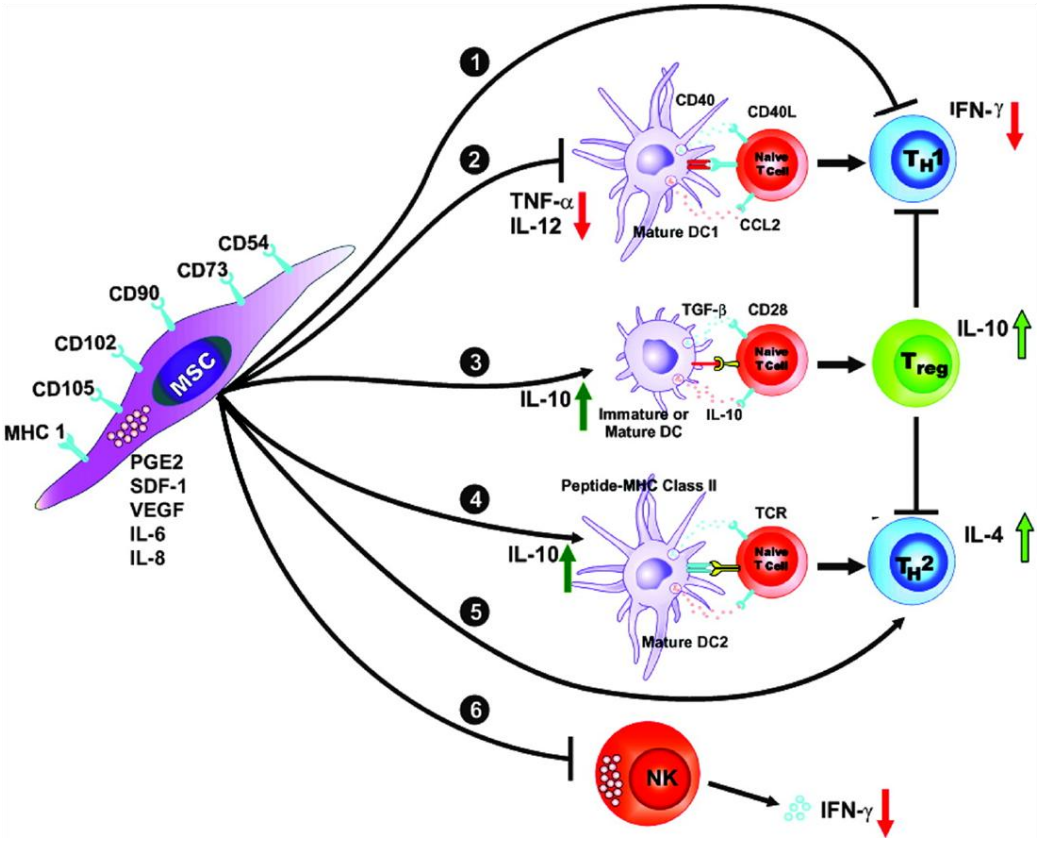

Figure 1. ***Proposed mechanisms of action of MSCs.***
MSCs mediate their immunomodulatory effects by interacting with cells from both the innate (DC, pathways 2-4; NK cell, pathway 6) and adaptive immunity systems (T cell, pathways 1 and 5). MSC inhibition of TNF-α secretion and promotion of IL-10 secretion may affect DC maturation state and their functional properties, resulting in skewing the immune response toward in an anti-inflammatory/tolerant phenotype. Alternatively, when MSCs are present an inflammatory microenvironment, they inhibit IFN-γ secretion from T_H1 and NK cells and increase IL-4 secretion from T_H2 cells, thereby promoting a $T_H1 \rightarrow T_H2$ shift. It is likely that MSCs also mediate their immunomodulatory actions by direct cell-cell contact as well as by secreted factors. Several MSC cell-surface molecules and secreted molecules are depicted. CCL indicates chemokine ligand; TCR, T-cell receptor (74).

2. HYPOTHESIS AND GOALS OF THE STUDY

It is a widely accepted fact that mesenchymal stromal cells generated by plastic adherence (PA-MSCs) represent a heterogeneous cell population concerning their proliferative, differentiation, immunosuppressive and engraftment-promoting potential. So far, there are a few reports on proliferation and differentiation potential of CD271-MSC. However, there are no data on the immunosuppressive and engraftment-promoting potential of these MSCs.

Consequently, the main goal of this study is to find out whether CD271-MSCs possess:

a) Equal or higher proliferative potential compared to PA-MSCs in order to obtain bulk cell numbers for clinical transplantation
b) Equal or higher immunosuppressive or inhibitory potential on allogeneic reaction than PA-MSCs and
c) Equal or higher engraftment-promoting potential *in vivo* than PA-MSCs

An important specific goal of this study will be the investigation of the effect of CD271-MSCs on multilineage differentiation of hematopoietic stem cells into lymphoid lineage, which is decisive for the clinical outcome of hematopoietic stem cell transplantation.

3. MATERIALS AND METHODS

3.1. Materials

3.1.1. Human materials

3.1.1.1. Peripheral human blood

Mononuclear cells were isolated from the peripheral blood of 10 healthy volunteers using a ficoll- density gradient, after their informed consent. These cells were used to study the inhibitory effect of mesenchymal stromal cells on the mitogenic or allogeneic-driven proliferation of mononuclear cells in the mixed lymphocyte reaction (MLR).

3.1.1.2. Human bone marrow

In order to generate mesenchymal stromal cells the bone marrow aspirates from the posterior iliac crest of 10 healthy donors (age 20–40 years) were harvested, using a protocol approved by the University of Frankfurt Institutional Review Board (UFIRB).

3.1.1.3. Mobilized $CD133^+$ hematopoietic stem cells

In order to study the effect of mesenchymal stromal cells on the engraftment of hematopoietic stem cells ($CD133^+$ cells) *in vivo*, these cells were enriched from the apheresis product of a healthy donor using a protocol approved by the University of Frankfurt Institutional Review Board.

3.1.1.4. Platelet concentrates

Platelet concentrates (from 4 donors) has been purchased from the Institute of Transfusion and Immunohematology (Frankfurt am Main, Germany) and were used for production of platelet lysate.

3.1.2. Experimental animals (mice)

3.1.2.1. Immunodeficient NOD/SCID knock-out mice for the gamma chain of the IL-2 receptor (IL-2Rγ^{null})

To study the engraftment-promoting properties of mesenchymal stromal cells *in vivo*, in this work were used five to eight week-old NOD/LtSz-scid IL2Rγ^{null} mice that were purchased from Jackson Laboratories (MA, USA) and housed in microisolators under pathogen-free conditions. They were fed with autoclaved food and water. All experimental procedures were

approved by the Animal Care Committee of Frankfurt am Main University and the Regierungspräsidium Darmstadt (Gen. Nr. F. 133/06).

3.1.3. Equipment

Photometer, 1420 Multilabel Counter, VICTOR^3	Perkin Elmer, Finland
Software	Windows Work Out 2.5
Flow cytometer, FACS Calibur	Becton Dickinson, Heidelberg
CellQuest software	Becton Dickinson, Heidelberg
Cellcounter Coulter AcT-Serie	Beckmann Coulter, Irland
Microscope Olympus CKX 41	Olympus, Japan
iQ™ 5 Multicolor Real-Time PCR detection system	BIO-RAD, Munich
iCycler iQ5 / MYiQ Optical system Software 2.0	Bio-Rad, Munich
BD FACSArray Bioanalyzer	Becton Dickinson, Heidelberg
FCAP Array™ software	Becton Dickinson, Heidelberg
Fluorescence microscope	Olympus IX71, Japan
Centrifuge Heraeus Multifuge 3SR+	Heraeus Instruments GmbH Hanau
Centrifuge Rotina 46	Hettich, Tuttlingen
Incubator, BBD 6220	Heraeus Instruments GmbH Hanau
Sterile bench, Herasafe	Heraeus Instruments GmbH Hanau
Water bath	Memmert, Schwabach
Shaker Incubator SI100	Pharmacia Diagnostics, Staufen
Vortexer Genie 2 ™	Bender & Hobein AG Zürich, Switzerland
Pipettboy comfort	Integra Biosience, Switzerland
Pipettes	Eppendorf, Hamburg
Multipette® plus	Eppendorf, Hamburg
Multichanel pipette	Epperndorf, Hamburg
MilliporeMultiScreenHTS Vacuum Manifold	Millipore, Schwalbach
Stove	Heraeus Instruments GmbH Hanau

3.1.4. Plastic ware

Polystyrencellcultureflasks T-25	Falcon, Becton Dickinson, Heidelberg
Polystyrencellcutureflasks T-75	Corning,
Polystyrencellcutureflasks T-175	Greiner, Solingen
96-Well Mikrotiterplatte	Falcon, Becton Dickinson, Heidelberg
Thermo-Fast 96 Semi Skirted Plate	Thermo Scientific, Dreieich
96-Well Mikrotiterplatte, black	Corning Incorporated, USA
96 well Filter plate for Cytokines	Millipore, Schwalbach
48- Well-Cellculturplatte	Becton Dickinson, Heidelberg
Strippette, 2,5,10 and 25mL	Costar, Fisher Scintific GmbH, Schwerte
Combitips, 0,5ml und 5ml	Eppendorf, Hamburg
Pipettips, steril 10µl,100µl,1000µl	STARLAB, Ahrensburg
Falcon tubes 15ml, 50ml	Greiner, Solingen/Frickenhausen
Eppendorf cups 1.5mL	Sarstedt, Neumrecht
Cryo Tube ™ Vials	Nunc, Denmark
Sterilfilter MILLEX®GV, 0,22µm	MILLIPORE Corporation, USA

S- Monovette Litium –Heparin	Sarstedt, Nümbrecht
FACS Tubes	BD Biosciences, Heidelberg
Petri dishes 10x15mm	Becton Dickinson, Heidelberg

3.1.5. Chemicals and solutions

Biocoll Separating Solution (Ficoll) 1.077	Biochrom KG, Berlin
Ficoll 1.073	GE Healthcare, Uppsala, Sweden
PBS Dulbecco's PBS	PAA Laboratories GmbH, Austria
RPMI 1640 + glutaMAX ™	GIBCO/ Invitrogen, Darmstadt.
DMEM + glutaMAX ™	GIBCO/ Invitrogen, Darmstadt
MSCs Qualified Fetal Bovine Serum	GIBCO/ Invitrogen, Darmstadt
Fetal Bovine Serum (FBS)	GIBCO/ Invitrogen, Darmstadt
Pen Strep (5000U/ml Penicillin + 5000 µg/ml Streptomycin)	GIBCO/ Invitrogen, Darmstadt
Platelet concentrate	Institute of Transfusion and Immunohematology, Frankfurt am Main
Heparin-Natrium 5000UI/mL	Ratiopharm, Ulm
Human serum albumin solution	Baxter, Heidelberg
Bovine serum albumin (BSA)	PAA Laboratories GmbH, Austria
EDTA-Solution (0.5 M)	AppliChem GmbH, Darmstadt
Dimethyl sulfoxide, minimum 99,5% GC	Sigma ALDRICH, Steinheim
Trypan Blue Stain 0,4%	GIBCO/ Invitrogen Corporation,UK
Trypsin,TrypLE ™ select	GIBCO/ Invitrogen Corporation,U.K
NH AdipoDiff Medium	Miltenyi Biotec, Bergisch Gladbach
NH OsteoDiff Medium	Miltenyi Biotec, Bergisch Gladbach
NH ChondroDiff Medium	Miltenyi Biotec, Bergisch Gladbach
H_2O, Ampuwa	Fresenius Kabi, Bad Homburg
Proleukin, IL-2	PeproTech, Hamburg
Phytohemagglutinin (PHA-P)	SIGMA, Munich
Concanavalin A (Con-A)	SIGMA, Munich
Pokeweed mitogen (PWM)	SIGMA, Munich
Staphylococcal Enterotoxin B Fragment (SEB)	SIGMA, Munich
Indomethacin	Sigma, Munich
Collagenase	Sigma, Munich
Krebs Ringer Bicarbonate	Sigma, Munich
$NaHCO_3$	Roth, Karlsruhe
$CaCl_2$ Anhydrous	Merck, Darmstadt

3.1.6. Media and buffers

3.1.6.1. Culture media

Serum-containing culture medium for mesenchymal stromal cells:

Culture medium with FBS: DMEM + glutaMAX^{TM} + 10% MSCs Qualified FBS + 1% P/S

Serum-free culture medium with platelet lysate (PL):

Platelet lysates were obtained from fresh platelet concentrates of 4 donors with a concentration of 1x10^{9} platelets/ 1 ml suspension. Platelets were frozen in Eppendorf cups at -80°C until use. Shortly before use platelets were thawed in a water bath at 37°C and thereafter centrifuged for 5 minutes at 13 000 x g. After centrifugation 50 µL supernatants were added to 1mL DMEM containing 5 units Heparin. On this basis the appropriate volumes of serum-free medium for MSCs were generated: DMEM + glutaMAX^{TM} + 5% PL + 5 UI Heparin/mL DMEM + 1% P/S.

Culture medium for peripheral blood mononuclear cells:

This medium was prepared by supplementation of RPMI 1640 glutaMAX ^{TM} with 10% FBS and 1% Penicillin/Streptomycin.

3.1.6.2. Freezing media

1. Freezing media for MSCs

a) DMEM + glutaMAX^{TM} + 30% FCS + 10%DMSO (for expanded MSCs with FBS)

b) DMEM + glutaMAX^{TM} + 5% HSA + 10%DMSO (for expanded MSCs with PL)

2. Freezing medium for PB-MNCs or BM-MNCs

a) RPMI 1640 + glutaMAX^{TM} + 30% FBS + 10% DMSO

3.1.6.3. Solution for digestion of mouse organs

Krebs Ringer bicarbonate buffer:

900mL Ampuwa water
9.5g Krebs Ringer bicarbonate
1.26g $NaHCO_3$
39.95 mg $CaCl_2$
pH=7.4
Fill to 1000 mL with destilled water.

Krebs Ringer bicarbonate buffer + Collagenase

491.6 mLKrebs Bicarbonate Buffer
+8.33 mL 30% BSA (f.c.0.5%)
+50 µL Collagenase

3.1.7. Material for isolation of cells

3.1.7.1. Material for isolation of CD271^{+}BM-MNCs

CD 271(LNGFR) MicroBead-Kit	Miltenyi Biotec, Bergisch Gladbach
Magnetic field of a MACS Separator	Miltenyi Biotec, Bergisch Gladbach
MACS MS- and LS-Columns	Miltenyi Biotec, Bergisch Gladbach
PBS (+ 2mM EDTA + 0,5 % BSA)	PAA Laboratories GmbH, Austria

3.1.7.2 Material for isolation of CD133^{+} hematopoietic stem cells

CD133 MicroBead Kit	Miltenyi Biotec, Bergisch Gladbach
MACS Separator	Miltenyi Biotec, Bergisch Gladbach
MACS MS- and LS-Columns	Miltenyi Biotec, Bergisch Gladbach
PBS (+ 2mM EDTA + 0,5 % BSA)	PAA Laboratories GmbH, Austria

3.1.8. Material for staining of cells

3.1.8.1. Solutions for staining of CFU-F

Giemsa's Azur Eosin Methylenblue solution	Merck, Darmstadt
Methanol	Sigma-Aldrich, Steinheim

3.1.8.2. Material for staining of osteoblasts

SIGMA FAST™ BCIP/NBT Substrate Tabletts	Sigma, Munich

3.1.8.3. Material for staining of adipocytes

Oil Red O Solution	Millipore
IC Fixation Buffer (Paraformaldehyd 4%)	e-Bioscience, Frankfurt

3.1.8.4 Material for staining of chondrocytes

Formalin 37%	Merck, Darmstadt
Ethanol, 100%	Roth, Karlsruhe
Roti-Histol	Roth, Karlsruhe
Alcian blue-solution	Merck, Darmstadt
Nuclear FAST RED Solution	Sigma-Aldrich, Steinheim
Entellan	Merck, Darmstadt
Roti®-Plast, Paraffin	Roth, Karlsruhe

3.1.9. Other kits

Cell Proliferation ELISA, BrdU-Assay-Kit	Roche Applied Science, Mannheim
Parameter™ PGE_2 Assay kit,	R&D Systems, Wiesbaden
Nitric Oxide Assay Kit	BioChain Institute, USA
Cytokine Kit, which contains two kits:	
BD™ CBA Human Flex Set for IL-2, IL-10, INF-γ, TNF, VEGF, Fas-ligand and Angiogenin	BD Biosciences, Heidelberg
Master Buffer Kit	BD Biosciences, Heidelberg
sHLA-G ELISA	BioVendor, Heidelberg
QIAamp DNA mini Kit	Qiagen, Hilden
Mouse Erythrocyte Lysing Kit	R&D Systems, Wiesbaden

3.1.10. Antibodies

Antibodies	Fluorochroms	Company
IgG1	FITC,PE,PerCP,APC	BD Biosciences, Heidelberg
CD3	FITC, PerCP, APC	BD Biosciences, Heidelberg
CD4	FITC, APC	BD Biosciences, Heidelberg
CD8	PerCP	BD Biosciences, Heidelberg
CD14	APC	BD Biosciences, Heidelberg
CD15	PE	BD Biosciences, Heidelberg
CD25	PE	BD Biosciences, Heidelberg
CD29	PE	BD Biosciences, Heidelberg
CD33	PerCP	BD Biosciences, Heidelberg
CD34	FITC	BD Biosciences, Heidelberg
CD38	APC	BD Biosciences, Heidelberg
CD44	APC	BD Biosciences, Heidelberg
CD45	FITC,PE,PerCP,APC	BD Biosciences, Heidelberg
CD45RA	PerCP	BD Biosciences, Heidelberg
CD45RO	PerCP	BD Biosciences, Heidelberg
CD56	PE	BD Biosciences, Heidelberg
CD62L	PerCP,APC	BD Biosciences, Heidelberg
CD73	PE	BD Pharmingen, Heidelberg,
CD90	FITC	BD Pharmingen, Heidelberg,
CD105	APC	Caltag, Heidelberg
CD127	PE	BD Biosciences, Heidelberg
CD133-2	PE	Miltenyi Biotec, Germany
CD146	PE	BD Biosciences, Heidelberg
CD166	PE	BD Biosciences, Heidelberg
CD184	PerCP-Cy5	BD Biosciences, Heidelberg
CD271	APC, PE	Miltenyi Biotec, Germany
HLA-A,B,C	FITC	BD Biosciences, Heidelberg
HLA-DR	PE	BD Biosciences, Heidelberg
SSEA-1	PE	R&D Systems, Wiesbaden
SSEA-4	PE	R&D Systems, Wiesbaden

3.2. Methods

3.2.1. Isolation of peripheral blood mononuclear cells (PB-MNCs)

PB-MNCs were isolated using ficoll with a density gradient 1.077. One volume of peripheral blood was diluted with one volume PBS and thereafter layered over one volume ficoll in a 50 ml conical tube. The tubes were centrifuged for 20 minutes at 700 x g without brake. After centrifugation, the PB-MNCs were collected from the interface and washed twice with PBS and centrifuged at 400 x g for 10 min. These cells were used at appropriate concentrations in MLR experiments.

3.2.2. Isolation of mobilized CD133$^+$ hematopoietic stem cells

CD133 positive hematopoetic stem cells were isolated from PB-MNCs of a healthy donor with informed consent who was administered granulocyte colony-stimulating factor (G-CSF) to mobilize hematopoietic stem cells from bone marrow into the peripheral blood. For this purpose, $1x10^9$ of mobilized peripheral blood cells were diluted with PBS (1:3) and then proceded as for isolation of peripheral blood mononuclear cells. As the percentage of these cells in this sample was pretty low (about 1%) CD133$^+$ cells were positively selected by means of immunomagnetic separation using CD133 isolation kit from Miltenyi.

Principle of the MACS® (Magnet-activated cell sorting) Separation

First, the CD133$^+$ cells are magnetically labeled with CD133 MicroBeads. Then, the cell suspension is loaded onto a MACS Column, which is placed in the magnetic field of a MACS Separator. The magnetically labeled CD133$^+$ cells are retained within the column. After removing the column from the magnetic field, the magnetically retained CD133$^+$ cells can be eluted as the positively selected cell fraction. To increase the purity, the positively selected cell fraction containing the enriched CD133$^+$ cells is separated over a second column. These highly purified hematopoietic stem cells were frozen until use. After thawing they were co-transplanted with CD271-MSCs into immunodeficient NOD/SCID mice at different ratios for engraftment studies.

The CD133 enrichment procedure is presented below.

Labeling of PB-MNCs with CD133 MicroBeads

1.	$1x10^8$ PB-MNCs /300µl CliniMACS buffer		work fast and keep cell suspension (buffer pre-cooled on ice)
2.	labeling	100µl FcR Blocking reagent 100 µl CD133 MicroBeads	mix well and incubate for 30' at +4°C
3.	washing	10ml buffer/10^8 cells	centrifuge 300 x g 10' at RT
4.	resuspend the cell pellet in	500µl buffer	

Magnetic separation

1. Place MS column in the magnetic field of a suitable MACS Separator
2. Prepare column by rinsing with 500µl buffer
3. Apply cell suspension into column
4. Wash column 3 x 500µl. Add new buffer when the column is empty
5. Remove column from separator and place it on a suitable collection tube
6. Pipette 1ml buffer into the column and immediately flush out the magnetically labeled cells by firmly pushing plunger into the column.

To increase the purity of $CD133^+$ cells, enrich the eluted fraction over a second MS Column. Repeat the magnetic separation procedure from step 1 to step 6 by using a new column.

3.2.3. Isolation of BM-MNCs and their phenotypic profile

Bone marrow aspirates were obtained from the posterior iliac crest of 10 healthy donors (age 20–40 years) under whole anesthesia using a protocol approved by the University of Frankfurt Institutional Review Board. Approximately, 50-100 ml of bone marrow aspirates were diluted 1:2 in PBS and after that two volumes of these samples were layered over 1 volume Ficoll (density: 1.073 g/ml) in a 50 ml conical tube and centrifuged at 700 x g for 30 min without brake. Mononuclear cells were collected from the interface, then washed twice with PBS and centrifuged at 400 x g for 10 min. Thereafter, mononuclear cells were counted using a cell counter, whereby a proportion of these cells was used for determination of phenotypic profile of BM-MNCs. A defined number of isolated BM-MNCs was used for generation of MSCs by plastic adherence (PA-MSCs) and CFU-F assay (colony forming unit- fibroblast), whereas the majority of them was used for CD271 enrichment.

To determine the phenotype of $CD271^+$ MSC progenitor cells, BM-MNC were stained with monoclonal mouse anti-human antibodies conjugated to fluorescein isothiocyanate, phycoerythrin, peridinin chlorophyll protein, or allophycocyanin. The following antibodies were used: CD13, CD14, CD15, CD29, CD34, CD44, CD45, CD73, CD90, CD105, CD146, CD133-2, CD166, CD184, CD271, HLA-A,B,C, HLA-DR, SSEA-1 and SSEA-4. Fluorochrome-conjugated mouse immunoglobulins were used as isotype controls. BM-MNCs were incubated at +4°C for 30 min. After two wash steps with PBS + 0.2% BSA the stained

cells were analyzed on a FACSCalibur (Becton-Dickinson) equipped with Macintosh software for data analysis (CellQuest). At least 50.000 events were acquired for each cell population

3.2.4. Isolation of CD271$^+$ BM-MNCs

BM-MNCs were incubated with monoclonal anti-human CD271 antibody conjugated to allophycocyanin (APC) (isotype: mouse IgG1, clone ME 20.4) and FcR blocking reagent (human IgG) at 4 °C for 10 min. After washing, the cells were incubated with FcR blocking reagent (to block non-specific binding) and anti-APC magnetic beads for 15 min at 4°C. After washing cell suspension is loaded onto MACS column that is placed in the magnetic field of MACS Separator. The magnetically labeled CD271$^+$ cells are retained on the column, whereas the unlabeled cells (CD271 negative) run through. After removing the column from the magnetic field, retained CD271 positive cells were eluted. In order to improve enrichment of CD271 positive cells, the eluate was once more applied to the columns. The percentages of CD271 positive cells in the enriched fractions were then assessed by flow cytometry. Recovery of the immunomagnetically separated CD271$^+$ cells was calculated according to the following formula: Number of positive CD271$^+$ cells in final fraction x percentage purity of CD271$^+$ cells/initial number of CD271$^+$ cells).

The enriched cells were used for generation of CD271-MSCs and CFU-F assay, whereas CD271 depleted cells were also tested for CFU-F.

The CD271 enrichment procedure is presented in details below:

Labeling with CD271

1.	1x10^7 BM-MNCs /80µl pre-cooled buffer (0.5%BSA/2mMEDTA/PBS)		work fast and keep the cells cold
2.	labeling	10µl FcR Blocking reagent 10µl CD271 antibody	incubate 10’ at +4°C
3.	washing	10ml buffer/10^7 cells	centrifuge 300 x g 10’ at RT
4.	resuspend the cell pellet in	70µl buffer	
5.	labeling	10µl FcR Blocking reagent 20µl Anti-APC microbeads	incubate 15’ at +4°C
6.	washing	10ml buffer/10^7 cells	centrifuge 300 x g 10’ at RT

Magnetic separation was performed as described for CD133$^+$ hematopoietic stem cells.

3.2.5. Generation of MSCs and determination of their proliferation using FBS-containing media and FBS-free media

3.2.5.1. Generation of PA-MSCs

As the progenitor cells for MSCs have the basic property to adhere to plastic we termed them as plastic adherent- MSCs (PA-MSCs). To generate PA-MSCs $4.2x10^6$ BM-MNCs were resuspended in 6 ml of either FBS or platelet lysate containing medium and plated in a T25 (25 cm^2) tissue culture flask with vent caps. Cells were cultured in an incubator with 5% CO2 and 95% humidity at 37°C. After 48-72 hours, the medium containing non-adherent cells was removed and replaced with fresh medium. The adherent spindle-like cells were further cultured for 10-14 days until the cells reached about 70-80% confluence as evaluated by microscopy. During this time the medium is changed every 3 days (Figure 2). To detach the MSCs the medium was removed and the cells were washed with PBS. Then the cells were incubated for 6 minutes with trypsin and thereafter the effect of trypsin was neutralized with the culture medium. Cell suspension was centrifuged for 7 min at 350 x g and the resulting cell pellets were resuspended with medium and plated at a density of $2x10^3$ MSCs/cm^2. Once the cells reached a 70-80% confluence the MSCs were again trypsinized and used either for further culture (passages) or were frozen for 24h in freezing medium at -80°C and then on the next day at -180°C until use.

3.2.5.2. Generation of CD271-MSCs

Highly purified bone marrow $CD271^+$ cells (1.25×10^5) were seeded in T25 (25 cm^2) culture flasks with vent caps in 6 ml of either FBS-containing or FBS-free medium. The medium was changed after 7 days and later on every 3rd day until the cells reached the confluence 70-80% (10-14 day). After this step the whole procedure was the same as for generation of PA-MSCs. Generated MSCs from $CD271^+$ BM-MNSc were termed as CD271-MSC (Figure 2).

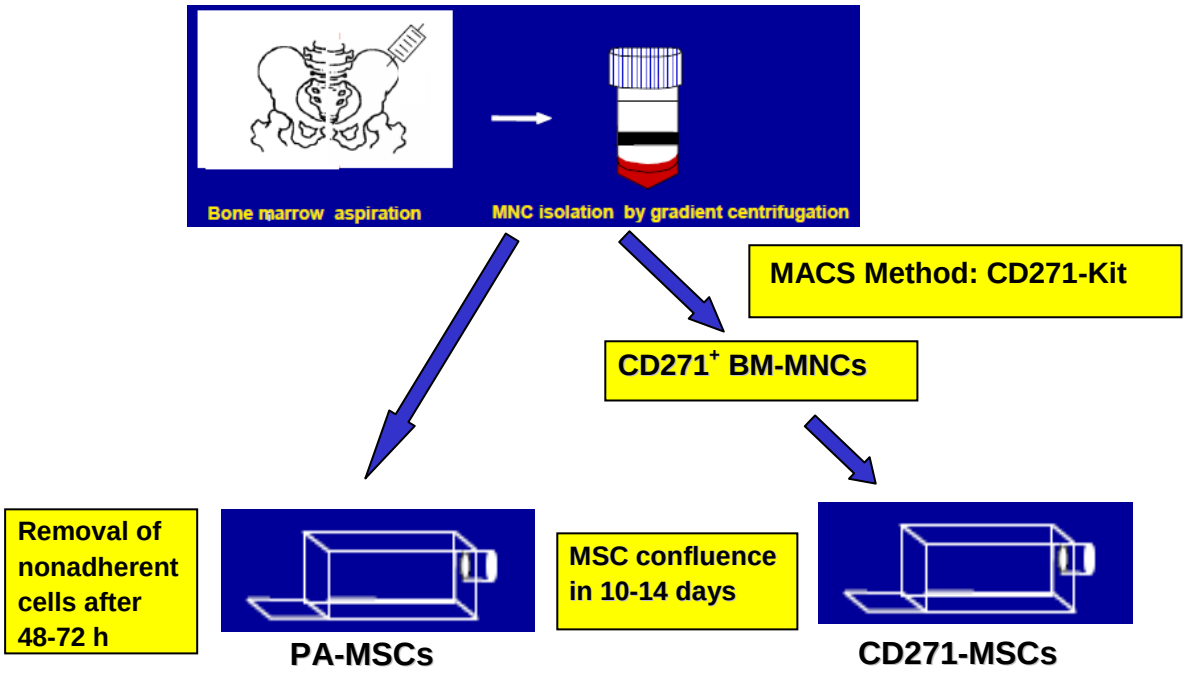

Figure 2. ***Methods for generation of mesenchymal stromal cells.***
In this figure are presented two ways of MSC generation. One proportion of the isolated bone marrow mononuclear cells were used for generation of MSCs by plastic adherence (PA-MSCs) and the other part was positively enriched for CD271$^+$ BM-MNCs which were then used for generation of CD271-MSCs.

3.2.5.3. Freezing and thawing of MSCs

Freezing procedure of MSCs

After trypsinization and centrifugation the cell pellets of MSCs were resuspended in cooled freezing medium containing 30% FCS, 10% DMSO and 60% DMEM or 5% human serum albumin, 10% DMSO and 85% DMEM in serum-free cultured cells. The cells were frozen in a cryobox at -80°C for 24 hours and then on the next day at -180°C in liquid nitrogen.

Thawing procedure of MSCs

The MSCs were thawed quickly in the water bath at 37°C and then resuspended in cooled appropriate media. Thereafter, the cells were centrifuged for 7 minutes at 350xg. The supernatant was removed and cell pellets were resuspended in the appropriate media and the number of the cells was counted in a hemocytometer with trypan blue in order to evaluate cell viability. These cells were plated in the culture flasks and expanded as described above.

3.2.5.4. Proliferation of CD271-MSCs, population doublings and doubling time

To evaluate the proliferative potential of MSCs, 5 x 10^4 cells were generated from bone marrow of 8 donors (CD271-MSCs and PA-MSCs from the same donor) were plated in the T-25 flasks in serum-containing (10% FBS) and MSCs of 3 donors in serum-free medium (5% platelet lysate). The cultured MSCs were grown until they reached 70-80% confluence from the first to the end of the passage 4 or 5.

Proliferation potential of MSCs was calculated by using population doubling as presented below:

Population Doubling (PD)

Population doublings were calculated according to Cristofalo et al. (175) by the following equation: $\mathrm{PD} = \frac{log\ NH - logNI}{\log 2}$, where $NH = \text{Harvested cells}$ and $NI = \text{Inoculated cells}$.

This number shows the number of cell doublings from first day of cell seeding until the day of cell harvest.

Doubling time (DT) is the time within which the cells duplicate themselves and is calculated by this formula: $DT = \frac{log2 \times t}{logNH - logNI}$, where $t = \text{time(days)}$, $NH = \text{Harvested cells}$ and $NI = \text{Inoculated cells}$.

3.2.6. Determination of the frequency of progenitor cells for MSCs using Colony Forming Units-Fibroblast (CFU-F) assay

3.2.6.1. Determination of CFU-F number in unselected BM-MNCs

The frequency of progenitor cells for MSCs in unselected BM-MNCs, highly purified $CD271^+$ BM-MNCs or negative fraction (CD271negative BM-MNCs) was assessed in a conventional CFU-F assay Castro-Malaspina (10). To determine frequency of progenitors for MSCs in freshly isolated BM-MNC, different concentrations of these cells ($1x10^6$, $0.5x10^6$ and $0.25x10^6$) were plated onto T-25 tissue culture flasks with 6 mL of the appropriate media (DMEM+10% MSCs-qualified FBS or DMEM+5% PL). After 7 days the culture medium together with nonadherent cells was removed and replaced with fresh medium. The medium was changed every 3rd day until day 13 when the CFU-Fs were enumerated and then trypsinized in order to determine their cellularity.

Staining and enumeration of CFU-Fs

At the end of cell culture formed colonies were gently washed twice with PBS to remove the residual FBS or platelet lysate and than allowed to dry for 5 minutes. Colonies were fixed with methanol for 3 minutes and after that it was removed and culture flasks have been dried and stained with diluted 1:20 Giemsa's azur eosin methylene blue solution for 15 minutes. Cell clusters containing >50 cells were scored as CFU-Fs under an inverse microscope. The results are presented as number of colonies per $1x10^6$ BM-MNCs.

Colony-forming efficiency (CFE) was calculated using the following formula:

$$\mathrm{CFE}(\%) = \left(\frac{\text{Number of colonies formed}}{\text{Number of plated cells}}\right) \times 100$$

3.2.6.2. Determination of CFU-F number in CD271$^+$ BM-MNCs

To determine the number of CFU-Fs in highly purified CD271$^+$ BM-MNC different concentration of these cells ($1x10^5$, $0{,}5x10^5$ and $0{,}25x10^5$ CD271$^+$ BM-MNCs) were seeded onto T-25 tissue culture flasks with 6 mL of appropriate media (DMEM+10% MSCs-qualified FBS or DMEM+5% PL). After 7 days the culture medium together with nonadherent cells was removed and replaced with fresh medium. The medium was changed every 3rd day until day 13. To stain these colonies was used the same staining procedure as for CFU-Fs generated by unselected BM-MNCs (3.2.6.1).

3.2.6.3. Determination of CFU-F number in cell fraction depleted from CD271$^+$ cells

Ten million of BM-MNCs depleted from CD271$^+$ cells were plated into a T-25 tissue culture flask with 6 ml of appropriate media (DMEM + 10% MSCs-qualified FBS or DMEM + 5% PL) and after 7 days the culture medium was removed and replaced with fresh medium. During 13 days of cell culture the medium was changed every 3rd day. The staining procedure was the same as for CFU-F generated by unselected BM-MNCs (3.2.6.1)

3.2.7. Determination of the phenotype of CD271-MSCs and PA-MSCs

CD271-MSC and PA-MSC of different passages (from passage 1 to passage 4) were labelled with fluorochrome-conjugated mouse anti-human antibodies against non-hematopoietic antigens CD73, CD90, CD105, CD146, CD44, CD29, CD166, hematopoietic antigens CD45, CD34 and CD14 and HLA-Class I and HLA Class II molecules and incubated at 4°C for 30 minutes. After two wash steps with PBS + 0.2% BSA the stained cells were analyzed on a

FACSCalibur (Becton-Dickinson) equipped with Macintosh software for data analysis (CellQuest). At least 50.000 events were acquired for each cell population

3.2.8. Differentiation potential of CD271-MSCs

3.2.8.1. Differentiation into osteoblasts

To analyse differentiation potential of MSCs into osteoblasts, expanded MSCs in FBS-containing or FBS-free medium of passage 2 or 4 were cultured in the special NH OsteoDiff medium from Miltenyi Biotec (Germany). For this purpose $4{,}5x10^4$ MSCs were resuspended in 1,5 ml in NH OsteoDiff Medium and transferred into the 35 mm diameter cell culture dishes. The cells were cultured in an incubator at 37°C, with 5% CO_2 and 95% humidity. The medium was replaced every 3rd day by day 10 in culture. On day 10 osteoblasts can be identified by their cuboidal apparence and their association with newly synthesized new bone matrix. Furthemore, committed osteogenic cells are characterized by expression of high levels of alkaline phosphatase (AP), an enzyme that is involved in the bone matrix mineralization, which can be detected using SIGMA FAST™ BCIP/NBT (5-bromo-4-chloro-3-indolyl phosphate/nitro blue tetrazolium) tablets as an insoluble substrate for the detection of alkaline phosphatase.

Staining steps:

- Aspirate OsteoDiff Medium from culture dishes.
- Wash cells with 2x2 mL PBS
- Remove PBS and incubate cells with 2 mL of pre-cooled methanol for 5 minutes at -20°C.
- Remove methanol completely.
- Wash cells with 2 mL of deionized H_2O .
- Remove H_2O completely.
- Add 2 mL SIGMA FAST BCIP/NTB substrate to the culture dishes and agitate slowly on a plate shaker at room temperature for 10 minutes. As alkaline phosphatase expressed by osteoblasts processes the substrate, cells stain dark purple.
- Aspirate the substrate solution and wash cells with 2 mL deionized H_2O.
- Keep the cells mist. If necessary add 300 µL dH_2O
- Immediately after staining examine the cells under microscope.

3.2.8.2. Differentiation into adipocytes

The NH AdipoDiff Medium from Miltenyi Biotec (Germany) promotes differentiation and further maturation of MSCs into adipocytes (fat cells). For differentiation into adipocytes were tested both CD271-MSCs and PA-MSCs expanded in appropriate media, DMEM with 10% FBS or 5% PL. For this purpose $7.5x10^4$ MSCs resuspended in 1.5mL NH AdipoDiff Medium and plated in 35 mm diameter cell culture dishes. The cells were cultured in an

incubator with 5% CO_2 and 95% humidity. The medium was changed carfully (because adipocytes are very fragile) every 3rd day. After 2-3 weeks, lipid vacuoles start to appear and on day 21 they were stained with Oil Red O solution. The staining procedure of adipocytes is described below:

Staining steps:

- Carfully aspirate medium from culture dishes.
- Wash cells with 2x2 mL PBS
- Fix adipocytes by incubating in 4% paraformaldehyde for 35 minutes at room temperature.
- Aspirate carefully fixative and rinse three times (5-10 minutes each) with 2 mL PBS
- Aspirate and rinse with water.
- Aspirate water and add 2 mL Oil Red O staining solution to cell culture dish and incubate at room temperature for 50 minutes.
- Remove Oil Red O solution and wash the cells three times with 2 mL water.
- Keep the cells moist. If necessary add 300 µL dH_2O
- Immediately after staining examine the cells under microscope. Adipocytes containing lipid droplets will be stained red by the Oil red solution.

3.2.8.3. Differentiation into chondrocytes

To induce differentiation of MSCs into chondrocytes was used NH ChondroDiff Medium from Miltenyi Biotec (Germany). For this purpose, $2.5x10^5$ cells of each type of MSCs (CD271-MSCs and PA-MSCs) expanded either in medium with FBS or PL were resuspended in 1 ml of expansion medium and then placed in a 15 mL conical polypropylene tubes.

Cell differentiation procedure:

- Centrifuge the cell suspension for 5 minutes at 150xg at room temperature.
- Aspirate expansion medium completely.
- Add 1mL of pre-warmed NH ChondroDiff Medium and resuspend cells
- Repeat step 1. Do not resuspend cells.
- Replace cap of the tube but do not tighten to permit the circulation of air. Place the tubes up right and incubate at 37°C in an incubator with 5% CO_2 and humidity >95% humidity.
- Change the medium every 3rd day
- On day 24 proceed with detection of chondrocytes.

Preparation of fixation and embedding reagents

1. Dilute formalin with PBS to final concentration 3.7% (neutral buffered formalin)
2. Prepare Ethanol series (70%, 80% 96% and 100%)
3. Heat Roti–Plast at +60°C in oven until completely melted

Preparation slides of chondrocyte nodules

1. Aspirate NH ChondroDiff Medium from micromass culture (cells in 15 mL tubes)
2. Wash chondrocyte nodules 1x with 1 mL PBS
3. Fix chondrocyte nodules by immersion in neutral buffered Formalin (3.7% /PBS) overnight (6-12h) in room temperature with agitation (on the shaker).
4. Place nodules in an embedding cassette with filter paper and dehydrate by applying the following ethanol dilution series:
   - 2x30 min 70% ethanol
   - 2x30 min. 80% ethanol
   - 2x30 min. 96% ethanol
   - 2x30 min 100% ethanol
5. Incubate embedding casete 2x30 min in Roti-Histol.
6. Incubate embedding casete 3x30 min in 58°C Roti-Plast.
7. Remove chondrocyte nodules from embedding cassette and embed with pre-heated Roti-Plast in Bio-mold.
8. Cool overnight at -20°C
9. Generatete 5 µm thick tissue sections using a microtome and transfer to a +40°C waterbath.
10. Place tissue sections on HistoBond slides and incubate at 52°C for 3h.
11. Cool to room temperature before proceeding or storage at room temperature.

Staining with alcian blue solution

Alcian blue stains acid mucosubstances and acid mucines. Therefore, with this method acid mucosubstances are stained blue, nuclei are stained red, and cytoplasm is stained pale pink.

The staining procedure:

- Deparafinize the sections using Roti-Histol and a descending ethanol dilution series and rehydrate.
  - 2x5 min Roti-Histol
  - 2x5 min 100% ethanol
  - 2x5 min 96% ethanol
  - 2x5 min 80% ethanol
  - 2x5 min 70% ethanol
  - 2x briefly rinse in deionized water.
  - 2x5 min in PBS
- Incubate sections 15 min in Alcian blue solution
- Wash sections in running tap water 3 min.
- Rinse in distilled water
- Incubate 10 min with Nuclear fast red solution
- Wash sections in running tap water for 3 min.
- Rinse in destilled water
- Repeat ascendant ethanol series 2x and Roti histol 2x
- Mount with Entelan
- Microscope
- Nuclei are red stained and acid mucosubsatances are light blue.

3.2.9. Transfection of MSCs with green fluorescent protein (GFP)

The packaging plasmid pCMVΔR8.91 encodes the human immunodeficiency virus-1 regulatory proteins *tat* and *rev* as well as Δplasmid pCMV *gag* and *pol* precursors. Plasmid pMD.G expresses vesicular stomatitis virus glycoprotein G. Pseudotyped lentiviruses were

produced by transient calcium-phosphate transfection of 293T cells with pCMVΔR8.91, pMD.G, and the lentiviral transfer vectors (SIEW) into which cDNAs encoding RhoV14 or C3 transferase were subcloned. Viral supernatants were collected 48–72 hours after transfection. Viral titers were determined on 293T cells and amounted to 0.1–1 × 10^8 titer units/ml. Lentiviral transduction of human MSCs was performed by seeding the cells in a 6-well plate (1 × 10^5 cells per well) in DMEM/10% FBS. The cells were allowed to attach for 24 hours. Viral supernatants of different vectors containing multiplicity of infection 1–5 were added to the cells in the presence of polybrene (4μg/ml). After 24 hours, the cells were washed and incubated with fresh medium. The cells were split 72 hours later and expanded. Percentage of transduced MSCs (presence of green fluorescent protein reporter gene) was estimated by flow cytometry. In order to obtain a highly pure cell population of MSCS these cells were subsequently sorted by the FACSAria cell sorter.

3.2.10. Evaluation of immunosuppressive potential of MSCs

3.2.10.1. Mixed lymphocyte reaction (MLR)

To study the effect of mesenchymal stromal cells on the allogeneic reaction, 1x 10^5 peripheral blood mononuclear cells (PB-MNCs) from two unrelated healthy donors (5x10^4 PBMNCs each) isolated using ficoll-gradient were plated in triplicates in 96-well black plates with opaque flat bottom in 100 μL RPMI 1640 with 10% FBS per well. In the wells were added 1x10^5; 5x10^4; 1x10^4 of lethally irradiated (30 Gy) CD271-MSC or PA-MSCs resuspended in 100 μL of RPMI 1640 with 10% FBS which generated a MSCs to PB-MNCs ratio: 1:1, 1:2 and 1:10. In order to investigate the possible inhibitory effect of MSCs mediated by PGE2, some triplicates were treated with 2μL of PGE2 inhibitor indomethacin (5μM final concentration). The cells were incubated in an incubator at 37°C in 5% CO_2 and 95% humidity. On day 5 the cells were labeled with 5-bromo-2'-deoxyuridine (BrdU) and further incubated for another 24 hours in the incubator. The inhibitory effect of MSCs on proliferation of PB-MNCs on day 6 was quantified by cell proliferation assay (BrdU chemiluminescent assay) as Relative Light Units (RLU/sec) using the luminometer 1420 Multilabel Counter Victor[3]. In parallel, the same experimental design was set in a 48 well plate with a three-fold greater number of cells in order to obtain enough volume of the supernatants for investigation of solubile molecules (PGE_2, NO, HLA-G, and cytokines) and a sufficient number of the cells for determination of the phenotype changes of PB-MNCs in MLR. On day 6 the non-adherent cells (PB-MNCs) incubated in 48 well plates were

resuspended in wells and then collected in 15 ml tubes and centrifuged for 10 min in 400xg. Supernatants were frozen at -80°C until determination of solubile molecules, whereas the cell pellets were used for determination of their phenotype by flow cytometry (T regs). As control group in each experiment were used PA-MSCs.

3.2.10.2. Effect of MSCs on the mitogenic stimulation of peripheral blood mononuclear cells

Peripheral blood mononuclear cells (PB-MNC) from healthy donors were isolated by gradient centrifugation, plated in triplicates in 96-well black plates with opaque flat bottom at a concentration of 10^5 cells/100 µL in RPMI 1640 with 10% FBS, and stimulated with the following mitogens at these final concentrations: phytohemagglutinin-P (10 µg/mL), concanavalin A (5 µg/mL), pokeweed mitogen (10 µg/mL), and staphylococcal enterotoxin B (1 µg/mL) and interleukin-2 (IL-2) (500 IU/mL). Non-proliferative, lethally irradiated (30 Gy) MSC (10^5) were resuspended in 100 µL of RPMI 1640 with 10% FBS, and were added to the total number of responder MNCs at a ratio of 1:2. Cultures were incubated at 37°C in 5% CO_2 for 5 days, and then labelled with 5-bromo-2'-deoxyuridine (BrdU) for 24 hours. Relative light units (RLU/sec) were measured the following day by cell proliferation assay (described below) using the luminometer 1420 Multilabel Counter Victor^3 . The inhibitory effect of MSC on the proliferation of PB-MNC was calculated using the formula: %inhibition of PB-MNCs proliferation = (proliferation of PB-MNCs with mitogens in the presence of MSCs/proliferation of PB-MNCs without MSCs) x 100.

3.2.10.3 Cell proliferation assay (BrdU chemiluminescent assay)

This immunoassay is based on the measurement of 5-bromo-2'-deoxyuridine (BrdU) incorporation instead of thymidine during DNA synthesis in proliferating cells and represents a non-radioactive alternative to the [^{3}H]–thymidine incorporation assay. In this study was used Cell proliferation ELISA, BrdU (chemiluminescent) Kit from Roche (Roche Diagnostics GmbH, Mannheim, Germany). Briefly, the cells are cultured in 96-well opaque flat bottom plates in presence of the respective cells and test substances for 5 days in an incubator with 5% CO2 at 37°C. On day 5 BrdU is added to the cells and the cells are re-incubated for 24 h. During this labelling period, the pyrimidine analogue BrdU is incorporated instead of thymidine into the DNA of proliferating cells. After removing the culture medium the cells are fixed and the DNA is denatured in one step by adding FixDenat (the denaturation of the DNA is necessary to improve the accessibility of the incorporated BrdU for detection by the

antibody). The anti-BrdU-POD antibody (antibody from mouse-mouse hybrid conjugated with peroxidase) is added and this antibody binds to the BrdU incorporated in newly synthesized cellular DNA. The immune complexes are detected by the subsequent substrate (which contain H_2O_2 and luminol) reaction. POD in the presence of hydrogen peroxide catalyzes the oxidation of diacylhydrazides like luminol. A reaction product in an excited state is formed, which decays to the ground state by emitting light. Thus the signal (photons) generated in enzyme-catalyzed light emitting reactions (luminescence) is identical with the signal during radioactive decay in scintillation counting. Therefore, chemiluminescence detection has features and advantages comparable to radioactive methods. That means, it provides a rapid and constant signal over a large logarithmic measuring range. This signal is quantified by measuring the photons using a microplate luminometer with photomultiplier technology. The relative light units/second (rlu/s) directly correlates to the amount of DNA synthesis and hereby to the number of proliferating cells in the respective microcultures.

Steps of the BrdU assay:

1.	Labelling with BrdU	20 µL BrdU/well (f.c.10µM)	24h in Incubator 37°C
2.	Centrifuge the plates		10 min 400xg
3.	Remove labeling medium by flicking off		
4.	Dry the plates in oven		60°C for 1h
5.	Fix the cells with 200µL/ well FixDenat		30' at RT
6.	Remove FixDenat by flicking off and tapping		
7.	Add 100 µL/ well Antibody conjugate (BrdU POD) Monoclonal mouse-mouse antibodys conjugated with peroxidase		90 min RT
8.	Remove Antibody conjugate by flicking off		
9.	Wash the wells 3 x with 250 µL Washing solution		5 min each
10.	Remove Washing solution by tapping		
11.	Add 100 µL/ well substrate solution (containing luminol and stabilized form of H_2O_2)		
12.	Incubate on dark on a shaker		at least 3 min.
13.	Measure the light emission of samples in a microplate luminometer with photomultiplier technology		

3.2.11. Determination of prostaglandin E2 (PGE2 assay)

The concentration of PGE2 in the supernatants of MLR was measured using ELISA method: Parameter™ PGE2 Assay. For this purpose, the frozen supernatants of day 6 of MLR were thawed and used for PGE2 determination. Briefly, the principle of this assay is based on competitive binding technique in which PGE2 present in a sample competes with horseradish peroxidase (HRP)-labeled PGE2 for a limited number of binding sites on a mouse monoclonal antibody. PGE2 in the sample is allowed to bind to the antibody in the first incubation. During the second incubation, HRP-labeled PGE2 binds to the remaining antibody sites. Following a wash to remove unbound materials, a substrate solution is added to the wells to determine the

bound enzyme activity. The color development is stopped, and the absorbance is read at 450 nm in a microplate reader. The intensity of the color is inversely proportional to the concentration of PGE2 in the sample. The standard curve was generated from 7 calibrator concentrations: 2500; 1250; 625; 313; 156; 78; 39 pg/mL.

Assay procedure:

1. Dilute the samples with calibrator diluent 1:3.
2. Prepare the needed number of 96 well polystyrene microplate coated with goat Anti-mouse polyclonal antibody.
3. Add 150µL of Calibrator diluent RD5-56 to the non-specific binding (NSB) wells.
4. Add 150µl of calibrator diluent to the zero standard (B0) wells.
5. Add 50 µL of Standard and sample to remaining wells.
6. Add 50 µL of the primary antibody solution (mouse monoclonal antibody to PGE2 with blue dye) to each well (excluding the NSB wells).
7. Cover plate with sealer and incubate for 1 hour at room temperature on a microplate shaker (500 rpm).
8. Add 50 µL of PGE2 conjugate (PGE2 conjugated to horseradish peroxydase with red dye) to each well. All wells except the NSB wells will now be violet in color.
9. Cover with adhesive strip provided, and incubate for 2 hours at room temperature on the shaker.
10. Aspirate each well and wash three times for total of four washes with 300 µl wash buffer with multichannel pipette.
1. Remove completely the liquid after each wash step and after the fourth wash (last wash) invert the plate and blot it against clean paper towels.
11. Add 200 µL of substrate (a mix of 1 volume hydrogen peroxide +1 volume chromogen) to each well and incubate for 30 minutes at room temperature protected from light.
12. Add 100 µL Stop Solution (2N sulfuric acid) to each well and gently tap the plate to ensure thorough mixing.
13. Determine the absorbance by microplate reader at 450 nm.

3.2.12. Determination of solubile HLA-G (sHLA-G)

sHLA-G ELISA is a sandwich enzyme immunoassay for the quantitative measurement of soluble forms of human leukocyte antigen-G (sHLA-G) as an immunosuppressive molecule. Briefly, calibrators and thawed samples of day 6 of MLR were incubated in microplate wells pre-coated with monoclonal anti-sHLA-G antibody. After 16-20 hours incubation and washing, monoclonal anti-human β2-microglobulin antibody labelled with horseradish peroxidase (HRP) is added to the wells and incubated for 60 minutes with captured sHLA-G. Following another washing step, the remaining HRP conjugate is allowed to react with the substrate solution (TMB, 3,3′,5,5′-tetramethylbenzidine) as a chromogen. This yields a blue color when oxidized, typically as a result of oxygen radicals produced by the hydrolysis of hydrogen peroxide by HRP. The reaction is stopped by addition of acidic solution and absorbance of the resulting yellow product is measured. The absorbance is proportional to the concentration of sHLA-G. A calibration curve is constructed by plotting absorbance values

against concentrations of calibrators, and concentrations of unknown samples are determined using this calibration curve.

Steps:

1. Reconstitute calibrator with 1 ml distilled water with resulting of stock solution of 625.00 Units /ml. Dilute it with Dilution Buffer from 125.00units to 3.91 units (create 5 concentrations).
2. Pipet 100 µl of calibrators, samples (diluted 1:4) and Dilution Buffer (= blank) into duplicate microplate wells pre-coated with monoclonal anti-sHLA antibody.
3. Incubate plate at 2-8 °C for 16-20 hours.
4. Wash the wells 5- times with Wash Solution (300 µl /well). After final wash, invert and tap the plate strongly against paper towel.
5. Add 100 µl of Conjugate Solution (monoclonal anti-human β2- microglobulin antibody labelled with horseradish peroxidise (HRP)).
6. Incubate the plate at room temperature for 1 hour by shaking ca. 300 rpm on a micropate shaker.
7. Repeat step 4
8. Add 100 µl of Substrate Solution (TMB-3.3',5,5 'tetramethylbenzidine) into each well.
9. Incubate for 25 minutes at room temperature in dark
10. Add 100 µl of Stop solution (phosphoric acid) to stop the color development.
11. Determine the absorbance by microplate reader at 450 nm, with a reference walenlength at 630 nm.

3.2.13. Determination of the cytokine profile of MLR supernatants

For determination of the cytokines (IL-2, IL-10, INF-γ, TNF-alpha, VEGF, Fas-ligand and angiogenin) in the MLR supernatants of day 6 was used BD™ Cytometric Bead Array (CBA), which is a flow cytometry application that allows quantification of multiple proteins simultaneously. The BD CBA system uses the broad dynamic range of fluorescence detection offered by flow cytometry and antibody-coated beads to efficiently capture analytes. Human Soluble Protein Flex Sets and Human Soluble Protein Master Buffer Kits employ particles with discrete fluorescence intensities to detect soluble analytes. The kit for estimation of cytokines contains 2 components:

1. BD^{TM} CBA Human Flex Set which contains capture beads, detection reagent and standards.
2. BD^{TM} CBA Flex Set Master Buffer Kit which contains assay reagents (Assay diluent, Capture bead diluent , Detection reagent diluent and wash buffer) instrument setup beads (Set up beads A1, A9,F1, F9; PE instrument setup bead F1 and PE positive control detector) configurated from compatible BD CBA Flex Sets.

Principle of the test

A BD™ CBA Human Soluble Protein Flex Set capture bead is a single bead population with distinct fluorescence intensity and is coated with a capture antibody specific for a soluble protein. The bead population is resolvable in the NIR and Red channels of a BD

FACSArray™ bioanalyzer or the FL3 and FL4 channels of a BD FACSCalibur™ flow cytometer. Each bead population is given an alphanumeric position designation indicating its position relative to other beads in the BD CBA Flex Set system. Beads with different positions can be combined in assays to create a multiplex assay. In a BD CBA Flex Set assay the capture bead, PE-conjugated detection reagent, and standard or test samples are incubated together to form sandwich complexes. Following acquisition of sample data using the flow cytometer, the sample results are generated in graphical and tabular formats using the FCAP Array™ Software.

Preparation of reagents:

---

1. Perform instrument setup procedure.
2. Prepare standards by mix of all lyophilized standard spheres into one tube and reconstitute them with 4 mL of Assay diluent. This is the top Standard 2500 pg/ml. Perform a serial dilution of standards by dilution with Assay diluent from 1:2, 1:4, 1:32, 1:64, 1:125, 1:256 (Standards from 2500-10 pg / mL)
3. Dilute samples 1:2 and 1:10 using Assay Diluent.
4. Prepare Capture Beads: After vortexing for 15 seconds 50x concentrated capture beads needed for determination of cytokines, they are diluted 1:50 (1µL capture beads :50 µL Capture Beads diluent x number of tests (samples) = Mixed capture beads)
5. Prepare PE detection reagent; Dilute PE- Detection Reagent with Detection Reagent Diluent (1:50) x number of tests (samples) = Mixed PE detection reagent. After preparing of standards, samples and reagents these reagents are pipetted into the plates

---

BD CBA Human Soluble Protein Flex Set Assay Procedure:

---

1. Pre- wet the clear non-sterile filter plates by adding 100 µl of wash buffer to each well. Aspirate with vacuum manifold, do not exceed 10'' Hg of vacuum pressure for 2-10 seconds) and blot the bottom of the plate on paper towels.
2. Add 50 µl of the mixed capture beads to each assay well.
3. Add 50 µl of standard or samples and negative control (Capture Beads, Assay Diluent, PE Detection Reagent) to the assay wells.
4. Mix the plate for 5 minutes using a digital shaker at 500 RPM and incubate for 1 hour at room temperature (RT) in dark.
5. Add 50 µL of mixed PE Detection Reagent to each assay well.
6. Mix the plate for 5 minutes using shaker at 500 RPM and incubate for 2 hours at RT in Dark.
7. Aspirate the wells (do not exceed 10'' Hg of vacuum pressure) until the wells are drained then blot the bottom of the plate on paper towels after aspiration.
8. Pipet 150 µL Wash buffer and resuspend carefully and shake at 500 RPM for 5 minutes.
9. Start analyzing samples on a flow cytometer.

Following acquisition on the BD FACSArray bioanalyzer, data files are exported and analyzed using FCAP Array™ software, which comes installed on the BD FACSArray workstation

---

3.2.14. Determination of nitric oxide (NO)

Since NO is oxidized to nitrite and nitrate, it is a common practice to quantitate total $NO2^-$ /$NO3^-$ as a measure for NO level. This assay was used to accurately measure NO levels in the supernatants of day 6 of MLR using reduction of nitrate to nitrite (improved Griess method).

Procedure:

1. Prepare 6 concentrations of standards: from 0-50 µM Nitrite standards diluting with distilled water in centrifuge tubes.
2. Add 50 µL of glycine buffer per tube.
3. Transfer 100 µL into wells of a clear bottom 96-well plate.
4. Deproteination of samples: mix 100µL sample with 80 µl 75mM ZNSO4 in 1.5 eppendorf cups. If precipitation occurs, centrifuge 14000 rpm.
5. Transfer supernatant to a clean tube containing 120 µl 55mM NaOH. Pellet protein precipitates again (dilution factor = 3)
6. Transfer 210 µl supernatant and mix with 70µL Glycine buffer in a 1.5 mL eppendorf cup.
7. Activation of cadmium granules (Cd). The number Cd granules to be used is 3-fold of the number of samples. Transfer Cd granules in a 50 mL centrifuge tube and wash them three times with water. Remove residual water with a pipet.
1. Add 200µL diluted 1x Activation Buffer per granule and incubate 5 min at room temperature. Swirl the tube intermittently. Wash three times with water. Activated Cd should be used within 20 min.
8. Nitrate reduction. Dry activated Cd granules on a filter paper. Add three Cd granules per sample and shake intermittently. Incubate 15min at room temperature. Transfer 2x100 µL samples (duplicate) into wells of 96-well plate.
9. Assay: Add 50 µL reagent A to all wells and tap plate lightly to mix. Add 50 µL reagent B and mix. Incubate 5 min at room temperature. Read OD at 500-570 nm (peak 540nm)
10. Calculation of results:
    Substract blank OD (150 µL Water + 50µl) and reagent A and B (step 9) from the standard values and plot the OD against standard concentrations. Determine the slope using linear regression fitting. The NO is calculated as: (OD Sample-OD Blank) x *n* (µM)/Slope OD Sample and OD Blank are optical density values of the samples and water, respectively. *n* is the dilution factor.

3.2.15. Determination of T regulatory cells (T regs) in the MLR

In order to examine changes of phenotype of allogeneic cells (PB-MNCs) from two HLA-disparate healthy persons in presence or absence of third-party lethally irradiated MSCs in MLR, flow cytometry analysis on day 0 and day 6 as an end-point of this assay was performed. In particular, in order to assess the percentage of T-regulatory cells and their subsets, the MNCs were stained with monoclonal antibodies against CD3, CD4, CD25 antigens as well as CD62L and CD45RA.

3.2.16. Co-transplantation of CD133$^+$ hematopoietic stem cells and CD271-MSCs in immunodeficient NOD/SCID knock-out mice

Immunodeficient NOD/SCID knock-out mice for the gamma chain of the IL-2 receptor (NOD/LtSz-scid IL2Rγ^{null}) were purchased from Jackson Laboratories (MA, USA) and were maintained in microisolator cages under specific pathogen-free conditions. They were sublethally irradiated (300 cGy) 24 h before transplantation. To assist in the identification of human cells after transplantation into mice, green fluorescent protein (GFP) was introduced into passage 4 CD271-MSC and PA-MSC via lentiviral vectors. Transduced MSC, together

with highly enriched mobilized peripheral blood $CD133^+$ cells, were administered to the sublethally irradiated immunodeficient mice via an injection in the lateral tail vein. The first group of mice was given $CD133^+$ cells ($1x10^5$) only, whereas the other groups were co-transplanted with either CD271-MSC or PA-MSC at a ratio of 1:1 (10^5 $CD133^+$ cells and 10^5 MSC) or 1:8 (10^5 $CD133^+$ cells and $7x10^5$ MSC). All procedures were approved by the Animal Care Committee of Frankfurt am Main University and the Regierungspräsidium Darmstadt (Gen. Nr. F. 133/06).

3.2.16.1. Estimation of engraftment of $CD133^+$ cells in the bone marrow by multiparameter flow cytometric analysis

Mice were sacrificed 14 weeks after co-transplantation of hematopoietic and mesenchymal cells. Bone marrow was obtained by flushing the cavities of the tibia and fibula bones with RPMI 1640 supplemented with 5% FCS using a 27 gauge-needle. Single-cell suspensions were treated with mouse erythrocyte lysing buffer to remove erythrocytes (Mouse Erythrocyte Lysing Kit) and then washed 2x with RPMI + 5% FCS. Cell pellet was washed once with PBS+0.5% BSA and then incubated for 30 minutes with anti-human specific antibodies (CD45, CD3, CD19, CD56, CD41a, and CD33) at +4°C. Thereafter, the cells were washed twice with PBS + 0.5% BSA and centrifuged for 10 min ar 400xg. Cell pellets were resuspended in 300 µL PBS + BSA 0.5% and analysed by four-color flow cytometric analysis. The proportion of each lineage was calculated from at least $5x10^5$ to $1x10^6$ events acquired using CellQuest software (Becton Dickinson, San Jose, CA, USA).

3.2.16.2. Quantification of human cells in the organs of NOD/SCID mice by real-time PCR

Fourteen weeks after transplantation, mouse organs were harvested after their sacrification. In order to isolate genomic DNA the organs were sliced and digested with collagenase in Krebs buffer for 30 minutes by rotation. Such treated tissues were thereafter homogenized using cell scraper through a 70 µM cell strainer. The cells which passed the strainer were washed and frozen in mononuclear freezing medium at -180°C until real time PCR analysis. To estimate human DNA in mouse organs a calibrator curve consisted of human DNA isolated from peripheral mononuclear cells mixed with the DNA isolated from mouse of control group (untreated with HSCs or MSCs) at following percentages: 10%; 1%; 0.1% and 0.01%; (from 10^{-1} to 10^{-4}) was created. Genomic DNA was isolated from $5x10^6$ human PB-MNCs with blood and body fluid spin protocol using the QIAamp DNA mini Kit (Qiagen, Hilden,

Germany), whereas for isolation of DNA from mouse cells has been used the same kit but the protocol for DNA isolation from tissues.

The Procedure of DNA isolation from human PB-MNCs:

1. Pipet 20 µL Qiagen Protease into a 1.5 mL microcentrifuge tube.
2. Add 200 µL sample which contain 1-5x10^6 cells / 200 µL PBS
3. Add 200 µL AL buffer (Lysis buffer). Mix by pulse vortexing for 15 sec.
4. Incubate at 56°C for 10 min.
5. Briefly centrifuge microcentrifuge tubes
6. Add 200 µL ethanol (96-100%) and mix by pulse vortexing for 15 sec, and thereafter centrifuge briefly to remove drops from inside of the lid.
7. Apply the mixture from step 6 to the mini-spin column (which is inserted in a 2 mL collection tube), close the cap and centrifuge for 2 min. at 8000 RPM. Place the QIAamp Mini spin column in a clean 2 mL collection tube and discard the collection tube containing filtrate.
8. Add 500 µL Buffer AW (wash buffer 1) into the column. Close the cap and centrifuge at 800 rpm for 2 minutes. Place the column in a clean 2 mL collection tube and discard the collection tube containing filtrate.
9. Add 500 µL Buffer AW2 (Wash buffer 2) into the column. Close the cap and centrifuge full speed (13,000 rpm) for 3 min.
10. Place the column in a new 2 mL collection tube and centrifuge at 13,000 rpm for 1 min.
11. Place the column in a clean 1.5 mL microcentrifuge tube. Carefully open the column and add 30 µL AE (Elutions buffer) and incubate at RT for 5 min.
12. Centrifuge for 1 minute at 8000 rpm.
13. Eluted DNA concentration is measured by Eppendorf Bio Photometer.

The procedure of DNA isolation from mouse cells

1. After thawing of mouse cells, the cells were washed in RPMI medium followed by two washing steps with PBS.
2. In cell pellets up to 10 mg were added 180 µL of ATL buffer (tissue lysis buffer) into 2 mL microcentrifuge tubes and 20 µl Proteinase K. Thereafter the cells were mixed by vortexing.
3. To lyse the cells, samples were placed in a shaking water bath at 56°C and incubated overnight.
4. Next day, the drops were removed from the inside of the lid and the tubes were briefly centrifuged
5. 200µL of AL buffer (Lysis buffer) were added and mixed by pulse vortexing for 15 sec.
6. To dissolve white precipitate after addition of the AL buffer the tubes were incubated at 70°C for 10 min.
7. The drops from the inside of the lid were removed by a brief centrifugation.
8. Continue with the step 6 from The Procedure of isolation DNA from human PB-MNCs.

Real time PCR

To correct for the quantity and quality (amplifiability) of DNA in samples, the gene encoding for human albumin was used (176). Sequences for TaqMan probe, forward primer, and reverse primer, to amplify and detect the albumin gene were: sequences for TaqMan probe: TGCTGAAACATTCACCTTCCATGCAGA,

forward primer: TGAAACATACGTTCCCAAAGAGTTT and

reverse primer: CTCTCCTTCTCAGAAAGTGTGCATAT

For this purpose was used Absolute ^{TM}QPCR ROX Mix from Thermo Scientific, which contained Thermo-StartTaq Polimerase, dNTP's including dTTP to improve reaction

sensitivity and proprietary reaction buffer that provides high sensitive, specific fluorescence readings for real-time and end-point analysis. In the Thermo-Fast 96- Semi Skirted Plate was pipetted reaction mix which was composed of following substances:

	Volume	Final Concentration
ABsolute QPCR ROX Mix (2X)	10 µL	1x
Forward primer (100 µM)	0. 08 µL	400nM
Reverse primer (100 µM)	0, 08 µL	400 nM
Probe (T-Sonde) (5 µM)	0, 4 µL	100 nM
Water (PCR grade)	7, 44µL	
Tamplate DNA	2 µL	200 ng
Total volume	20 µL	

The products were amplified by iQ^{TM} 5 Multicolor Real-Time PCR detection system, while the amplified products were analysed by iCycler iQ5 / MYiQ Optical system Software 2.0.

QPCR thermal cycling program: Enzyme activation

	Temp.	Time	Number of cycles
Enzyme activation	95°C	15 min.	1 cycle
Denaturation	95°C	15 sec	50 cycles
Anealing/Extension	60°C	60 sec	

3.2.16.3. Analysis of the MSC-presence in the mouse organs by immunochistochemistry

In situ analysis of mouse organs to detect resident human cells

In order to track in vivo human GFP-positive MSC in different organs, frozen tissue sections were washed twice with PBS, fixed with 4% paraformaldehyde for 10 min, and permeabilized with 0.1% Triton X-100 in PBS containing 3% BSA. After 30 min of pre-incubation at room temperature, the slides were stained with an anti-GFP primary antibody (1:400, Molecular Probes, Invitrogen, Germany) for 60 minutes at room temperature. Unbound anti-GFP antibodies were removed by washing the slides three times with PBS. The samples were incubated with anti-rabbit Alexa Fluor 488-conjugated secondary antibodies (1:1000, Molecular Probes) and phycoerythrin-labeled anti-human HLA-A, HLA-B, and HLA-C antibodies (1:100) (BD Biosciences) for another 60 min at room temperature in the dark. After washing with PBS and mounting on coverslips in VectaShield mounting medium containing 4,6-diamino-2-phenylindole (DAPI) (Biozol Diagnostica Vertrieb GmbH, Eching, Germany), the results were evaluated using an Olympus IX71 microscope.

3.3. Statistics

Statistical significance was analyzed using GraphPad Prism 5 software (GraphPad Software, San Diego, CA, USA). Significance was assessed with a Mann-Whitney rank sum or Student's *t* test. A *P* value less than 0.05 was considered statistically significant.

4. RESULTS

4.1. *In vitro* studies

4.1.1. Phenotypic characterization of CD271$^+$ bone marrow mononuclear cells

To determine the phenotype of CD271$^+$ MSC progenitor cells, BM-MNC were stained with monoclonal antibodies against typical MSC antigens. Gating on all CD271$^+$ BM-MNC (Figure 3A), we found that most of these cells (60–95%) expressed CD29, HLA-A, HLA-B, HLA-C, HLA-DR, and CD166. A considerable proportion of cells (20–30%) expressed CD105, CD15, CD13, SSEA-1, CD184, CD56, CD34, and CD133. However, only a small proportion of cells (10–20%) expressed CD146, CD73, CD90, and early stage-specific embryonic antigen-4 (SSEA-4) (Figure 3B).

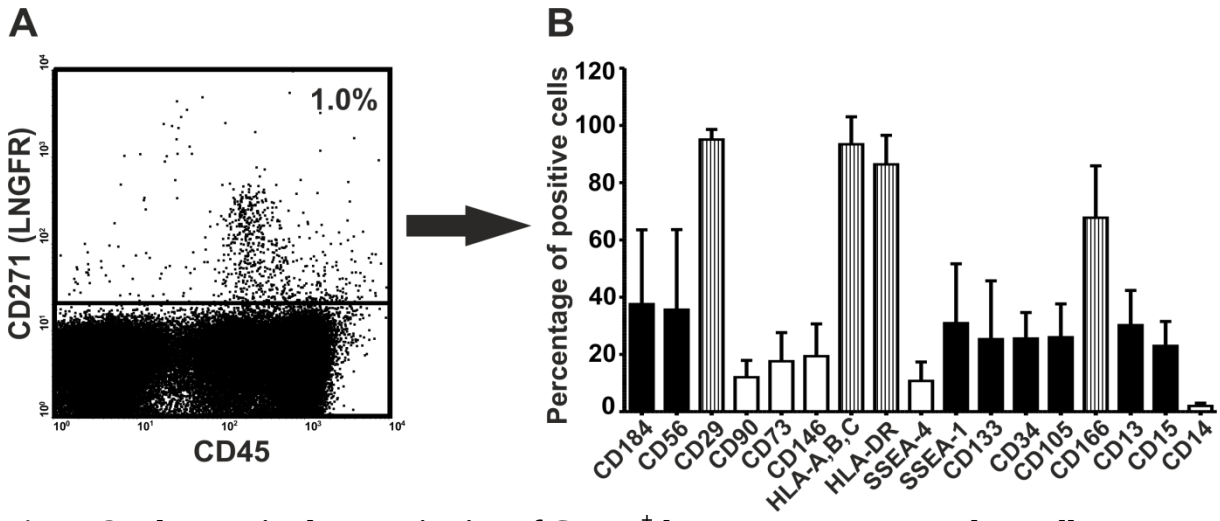

Figure 3. ***Phenotypic characterization of CD271$^+$ bone marrow mononuclear cells.***
(A) A representative dot plot of CD271$^+$ bone marrow mononuclear cells. (B) Cell surface profile of CD271$^+$ bone marrow mononuclear cells after density gradient separation. The positivity for analyzed antigens was determined by gating on all CD271$^+$ BM-MNC.

As assessed by flow cytometry, the frequency of CD271$^+$ cells in the BM-MNC samples used in this study was 0.6±0.1% (range, 0.2% to 1.2%; median 0.5%).The frequency of CD271$^+$ BM-MNCs varied from donor to donor and no correlation between the donor age and frequency of this cell fraction in the bone marrow samples has been observed (Figure 4).

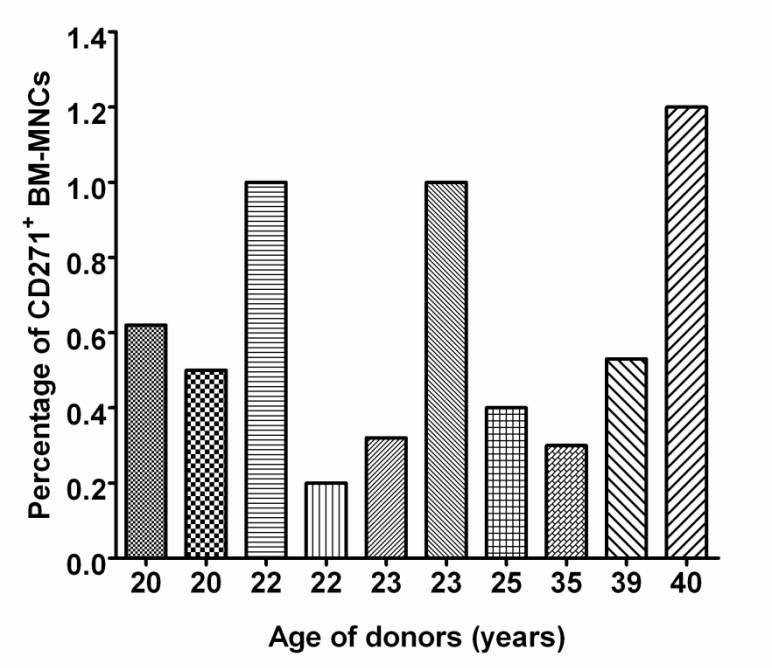

Figure 4. ***Frequency of CD271$^+$ bone marrow mononuclear cells.***
Bone marrow mononuclear cells of healthy donors (n=10) isolated by ficoll-gradient were labeled with the phycoerythrin (PE)-conjugated mouse anti-human CD271 antibody. The percentage of CD271$^+$ BM-MNCs was determined by means of flow cytometry.

4.1.2. Clonogenic and proliferative potential of mesenchymal stromal cells derived from CD271$^+$ bone marrow mononuclear cells

As mentioned above the mean frequency of CD271$^+$ BM-MNCs in our sample from 10 donors was 0.6%. The purity of positively selected CD271$^+$ BM-MNC by immunomagnetic selection was 92.3±5.9% (range 80% to 98%) (Figure 5) with a recovery of 75±20%. These highly purified cells were used for generation of CFU-Fs as an assay for enumeration of progenitor cells of MSCs (Figure 6) as well as for generation of bulk quantities of CD271- MSC that have been used throughout the study. In all experiments performed in this study PA-MSCs were used as a control.

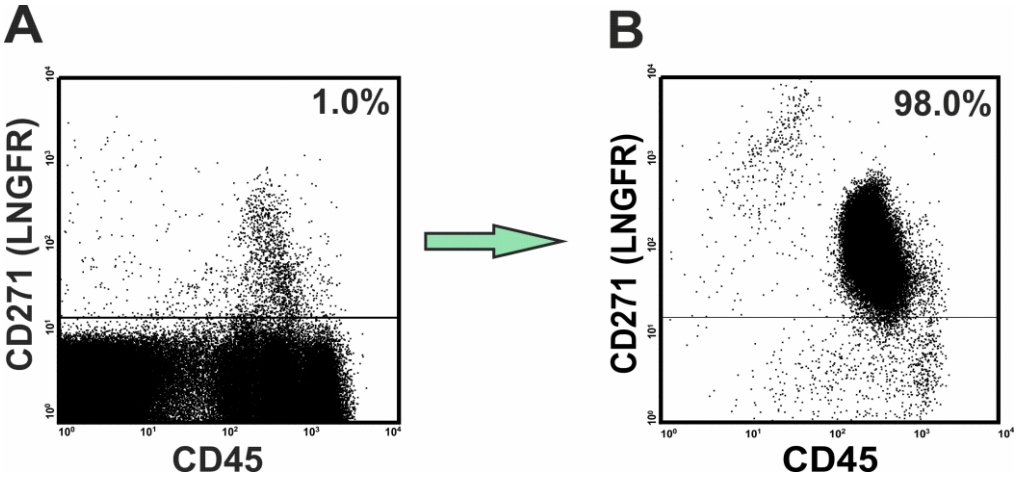

Figure 5. ***Positive selection of CD271$^+$ bone marrow mononuclear cells.***
(A) A representative dot plot of CD271$^+$ bone marrow mononuclear cells before enrichment. (B) A representative dot plot of positively selected CD271$^+$ BM-MNCs. BM-MNCs (n=10) were incubated with monoclonal anti-human CD271 antibody conjugated to allophycocyanin (APC) (clone ME20.4) and thereafter with anti-APC magnetic beads. The enrichment of CD271$^+$ cells was performed by a MACS separator. Highly purified CD271$^+$ BM-MNCs were collected and used for further analysis.

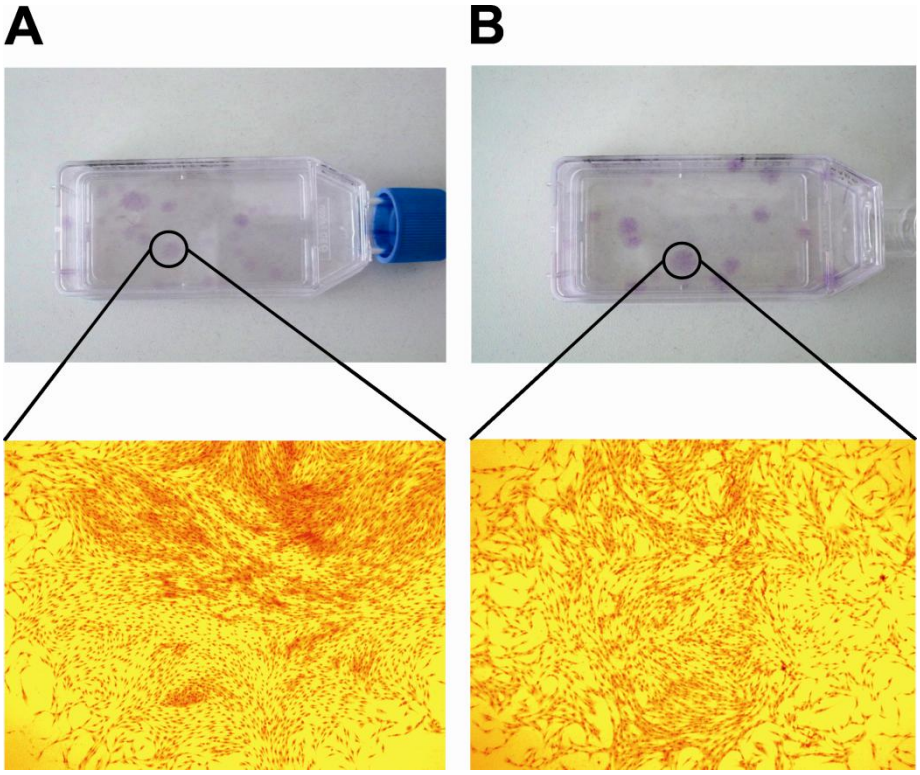

Figure 6. ***Generation of colony forming unit-fibroblast (CFU-F).***
(A) 2.5x10^4 of purified CD271$^+$ BM-MNCs were plated into tissue culture flasks. After 13 days in culture, staining with Giemsa's azur eosin methylene blue solution showed the presence of spot-like formations in the flasks. Enumeration of these formations by microscopy demonstrated that they consist of spindle-shaped cells: MSCs. (B) Generation of CFU-Fs with unseparated BM-MNCs (2.5x10^5 cells/flask). Magnification for both microscopic pictures: 40x.

To estimate the number of progenitor cells for MSCs by means of CFU-F assay, highly purified $CD271^+$ BM-MNCs ($1x10^5$, $0.5x10^5$, and $0.25x10^5$) were cultured in both FBS-containing culture medium (Figure 7A) as well as in the animal serum-free medium (platelet lysate) (Figure 7B) and colony-forming efficiency (CFE) was calculated.

An average of 0.2 ± 0.04 CFU-F/10^2 cells (1 progenitor cell for MSCs in 500 enriched $CD271^+$ BM-MNCs) was observed in the $CD271^+$ fraction cultured with FBS-containing medium compared to $CD271^+$ fraction cultured with platelet lysate-containing medium (serum-free) whereby the CFE was 0.15 ± 0.024 CFU-F/10^2 cells (0.75 progenitors for MSC in 500 enriched $CD271^+$ BM-MNCs). However, compared to the unseparated BM-MNCs cultured in FBS-containing medium this frequency represented a 26-fold enrichment of CFU-Fs (MSC-progenitors) within the $CD271^+$ cell fraction ($P<0.0001$) (Figure 7A). In addition, the number of CFU-Fs was also significantly enriched (20.3-fold) in the $CD271^+$ BM-MNC fraction cultured in the medium supplemented with platelet lysate compared to unseparated BM-MNCs ($P<0.0001$) (Figure 7B). No colonies were formed by $CD271^-$ cells plated at a 100-fold higher density than enriched $CD271^+$ BM-MNCs (data not shown).

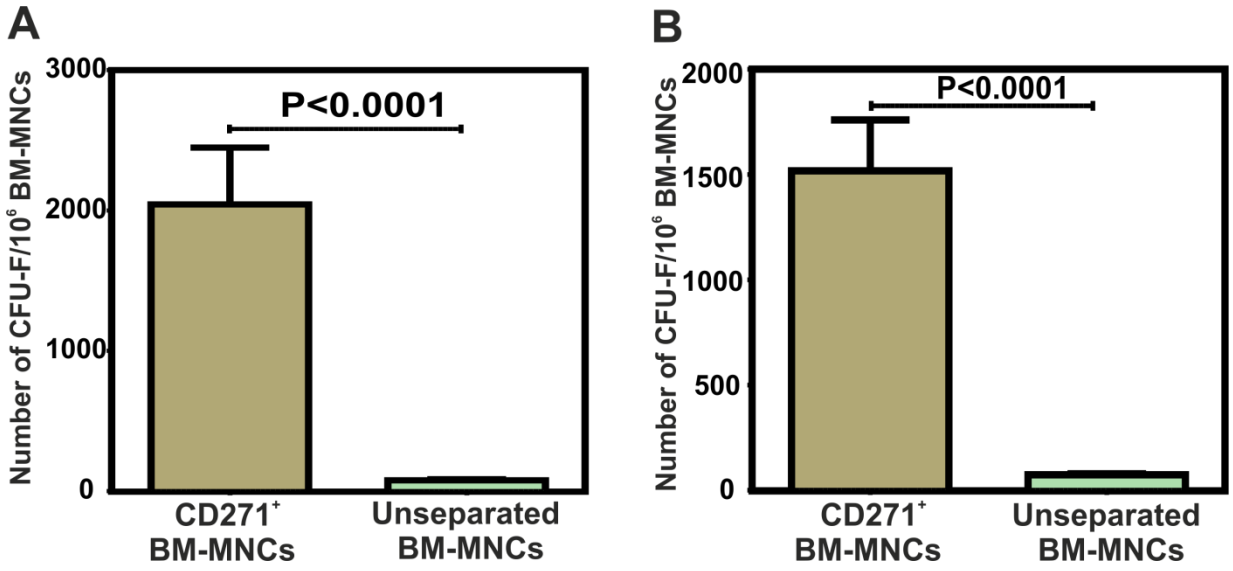

Figure 7. ***Number of progenitor cells for MSCs (CFU-Fs) in culture medium supplemented with fetal bovine serum or platelet lysates.***

Enriched $CD271^+$ BM-MNCs as well as unseparated BM-MNCs were cultured for 13 days in the DMEM culture medium supplemented with 10% fetal bovine serum (A) and in DMEM supplemented with 5% platelet lysate (B). On day 13, the number of fibroblast-like colonies was scored and the frequency of CFU-F per $1x10^6$ of $CD271^+$ BM-MNCs and unseparated BM-MNC was calculated. The results are presented as mean values ± SEM (n=10).

Analysis of the cellularity of CFU-Fs at day 13 revealed that although the number of colonies derived from $CD271^+$ BM-MNCs cultured in FBS-containing medium was 26-fold higher, they contained only 7-fold more cells than CFU-Fs generated by BM-MNCs ($P<0.03$). The cellularity of all CFU-Fs generated from $CD271^+$ BM-MNCs varied from 7.5×10^5 to 16×10^6 (Figure 8). In addition, the cellularity of CFU-Fs at day 13 demonstrated that although the number of colonies derived from $CD271^+$ BM-MNCs cultured in the medium supplemented with platelet lysate was 20.3-fold higher than the number of CFU-Fs formed by BM-MNCs, they contained only 8-fold more cells ($P<0.005$). The cellularity of all CFU-Fs generated from $CD271^+$ BM-MNCs varied from 5.4×10^4 to 2.1×10^6 (Figure 8).

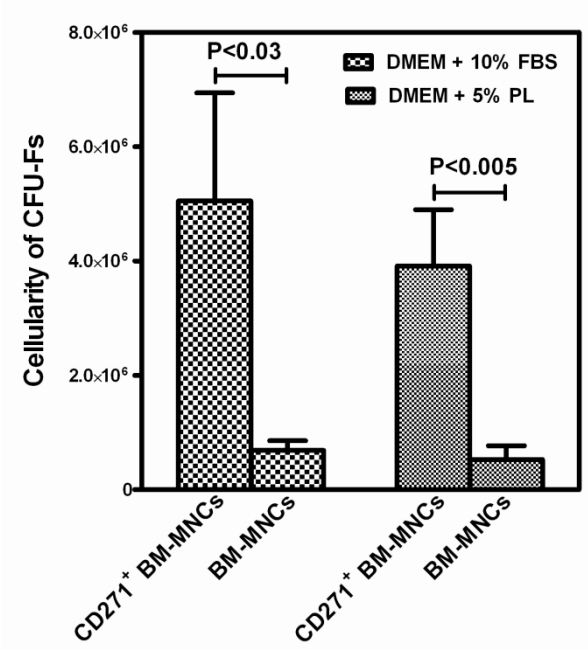

Figure 8. ***Cellularity of CFU-Fs generated by $CD271^+$ BM-MNCs and unseparated BM-MNCs.*** *Hundred-thousand of enriched $CD271^+$ BM-MNCs were cultured either in DMEM supplemented with 10% FBS or DMEM supplemented with 5% platelet lysate (PL). In addition, $1x\ 10^6$ BM-MNCs were cultured in either of these media. On day 13 the number of CFU-Fs was estimated by microscopy. Thereafter, the cells were detached by trypsin and the number of viable MSCs was determined by trypan blue staining. Number of MSCs were calculated to $1x10^6$ $CD271^+$ BM-MNCs or unseparated BM-MNCs. Results are presented as mean values ± SEM (n=10).*

Comparative analysis of the number of CFU-Fs and the age of bone marrow donors, demonstrated no correlation between these two parameters neither for CFU-Fs generated by enriched $CD271^+$ BM-MNCs (Figure 9A) nor for CFU-Fs generated by unseparated BM-MNCs (Figure 9B). Neither was found a correlation between the frequency of $CD271^+$ BM-MNCs and age of the donors, nor between these two parameters and the potential to generate CFU-Fs. For instance, one 22-year old donor whose bone marrow expressed 1% CD271

antigen generated only 602 CFU-Fs. The other donor of the same age (22 years) whose bone marrow expressed only 0.2% of $CD271^+$ cells generated 4.6- fold more colonies (2.800 CFU-F).

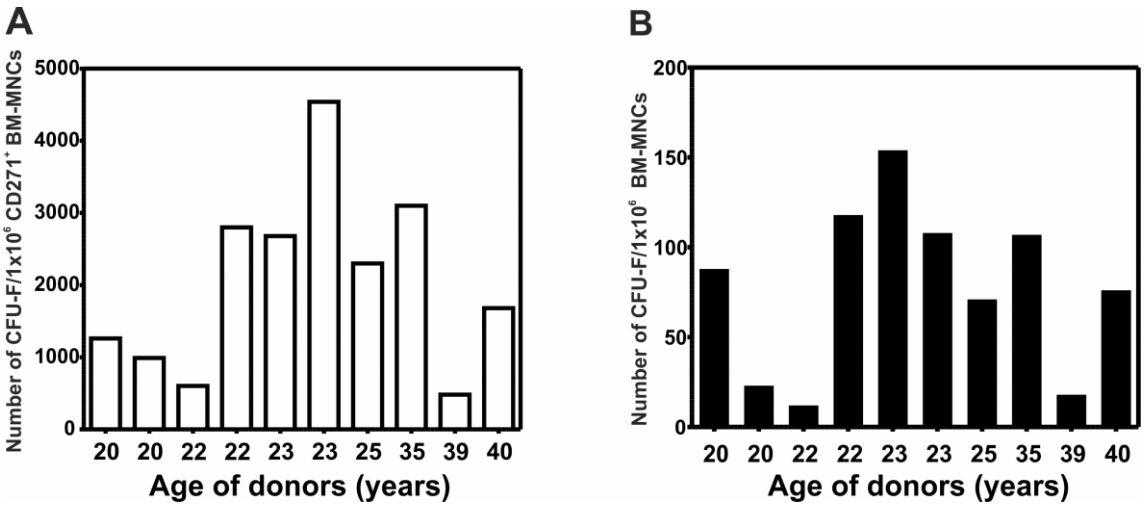

Figure 9. ***CFU-F potential and the age of donors.*** *(A) Potential of enriched $CD271^+$ BM-MNCs from individual donors of different ages to give rise to CFU-Fs. (B) Potential of unseparated BM-MNCs from individual donors of different ages to generate CFU-Fs.*

In order to evaluate the potential of the enriched $CD271^+$ BM-MNCs to give rise to mesenchymal stromal cells (CD271-MSCs) and their consequent proliferation, these cells were cultured in DMEM-low glucose culture medium supplemented either with 10% MSC-qualified FBS or 5% platelet lysate (animal serum-free medium). In parallel, potential of unseparated BM-MNCs to give rise to mesenchymal stromal cells (PA-MSCs) and proliferate under the same culture conditions was used as a control. Estimation of population doublings (PD) over a period of 30 days revealed no significant differences in the proliferative potential of CD271-MSC compared to PA-MSC. Both types of MSCs demonstrated very similar growth kinetics by day 30 in the culture medium supplemented either with FBS (CD271-MSCs: 19.5 ± 1.3 PD; PA-MSCs: 19.3 ± 1.0 PD) (Figure 10A) or with platelet lysate (CD271-MSCs: 17.0 ± 1.2; PA-MSCs: 14.7 ± 2.6) (Figure 10B).

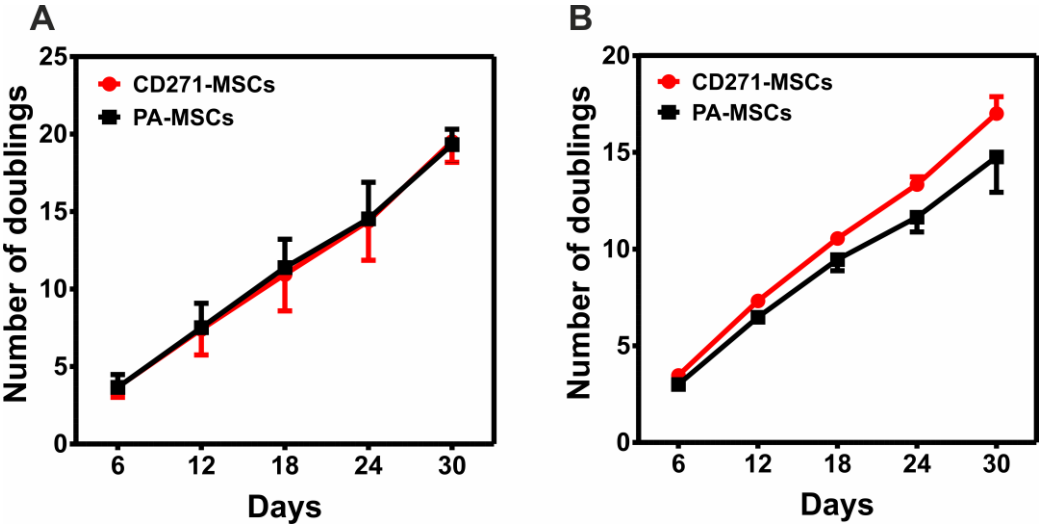

Figure 10. ***Growth kinetics of CD271-MSCs and PA-MSCs.***
(A) Growth kinetics of MSCs in culture medium DMEM supplemented with 10% FBS (n=8). To estimate the number of population doublings, cultured MSCs were trypsinized in weekly intervals and the viable number of MSCs was determined by trypan blue staining. (B) The number of population doublings in both types of MSCs cultured in DMEM supplemented with 5% platelet lysates (n=3). Results are presented as mean values ± SEM.

Determination of doubling time demonstrated that CD271-MSCs need a shorter time to duplicate themselves when cultured in serum-free medium (Figure 11A). In addition, the doubling time was prolongated by the time in culture, e.g. while at passage 1 and 2 the doubling time of these MSCs was in average 1.6 days (38.4 hours), by passage 4 the doubling time became significantly longer (2.3 days or 55.2 hours). PA-MSCs at passage 4 cultured under the same conditions needed in average 2.96 days (71 hours) to duplicate themselves. However, the differences were not statistically significant, because of large variations between donors. These doubling times were comparable to the doubling times of CD271-MSCs and PA-MSCs cultured in presence of animal serum (10% FBS) (Figure 11B), suggesting that platelet lysate has equal stimulatory properties for proliferation of both types of MSCs as FBS. Therefore, FBS can be freely replaced by platelet lysate in order to generate bulk quantities of animal serum-free MSCs for clinical application.

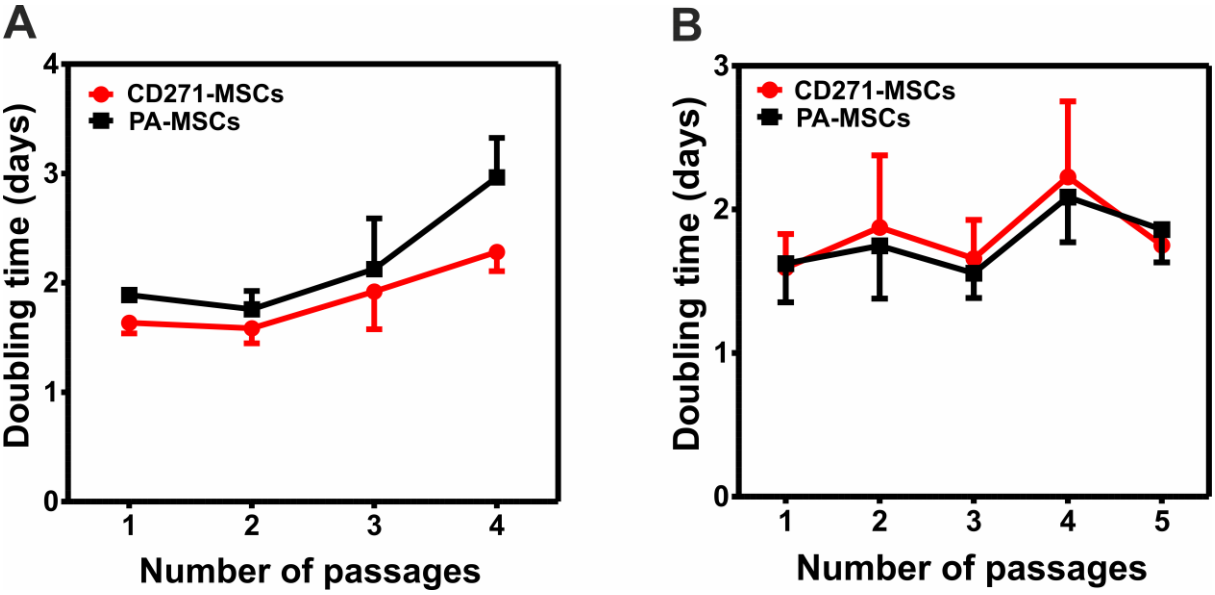

Figure 11. ***Doubling time of CD271-MSCs and PA-MSCs in serum-containing and serum-free media.*** *(A) Doubling time of both types of MSCs in serum-free medium (DMEM supplemented with 5% platelet lysate) (n=3) and (B) serum-containing medium (DMEM supplemented with 10% FBS) (n=8). Results are presented as mean values ± SEM.*

4.1.3 Phenotype and differentiation potential of the expanded mesenchymal stromal cells derived from CD271$^+$ BM-MNCs (CD271-MSCs)

Passage 4 CD271-MSC expressed typical mesenchymal cell surface markers, such as CD73, CD90, CD105, CD146, CD44, CD29, CD166, and HLA class I molecules. However, they were negative for the hematopoietic cell markers CD14, CD45, hematopoietic stem cell marker CD34 as well as class II HLA-antigens (HLA-DR) (Figure 12). This phenotypic profile was observed in both CD271-MSCs cultured in FBS-containing medium and medium supplemented with platelet lysate (serum-free). In addition, mesenchymal stromal cells generated through plastic adherence of unselected BM-MNCs (PA-MSCs) at passage 4 expressed the same typical MSC antigens at the same level as CD271-MSCs, either.

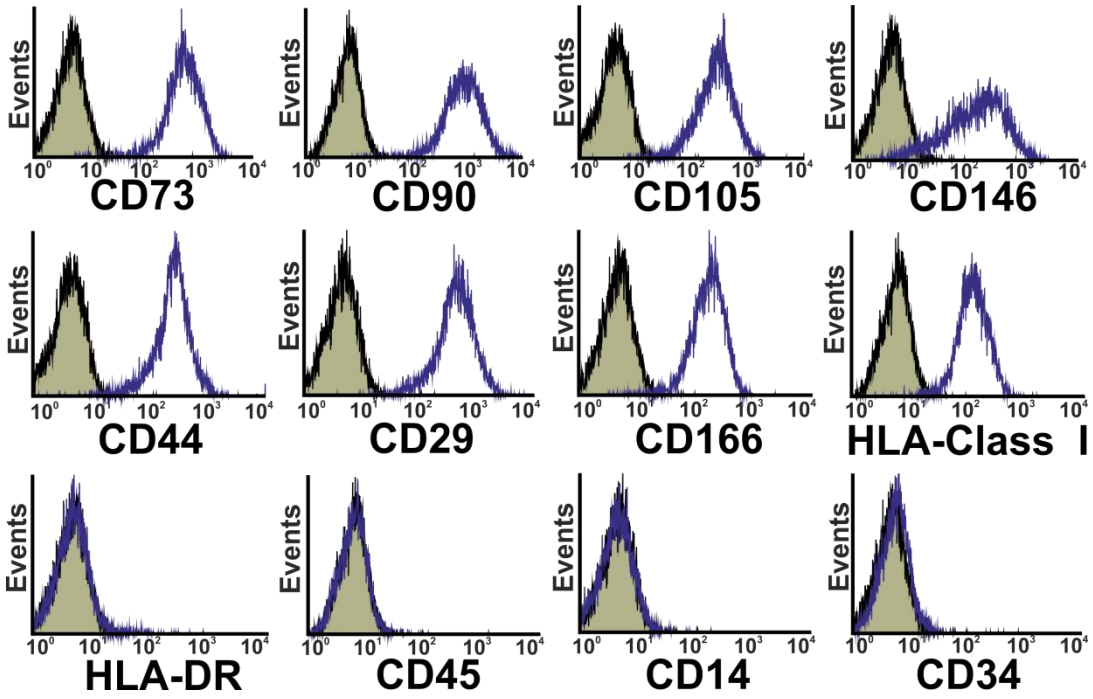

Figure 12. ***Characterization of adult bone marrow-derived CD271-MSCs.***
CD271-MSCs of passage 4 were labelled with fluorochrome-conjugated mouse anti-human antibodies against non-hematopoietic and hematopoietic antigens. After an incubation step and washing, the cells were analyzed for cell surface marker expression. Isotype controls are presented as shaded histograms and analyzed markers as open histograms.

One of the important criteria that the cells should fulfil in order to be defined as mesenchymal stromal cells is their capacity to differentiate along three lineages: adipocytes, osteoblasts and chondrocytes. In order to study the differentiation potential of CD271-MSCs to adipogenic, osteogenic, and chondrogenic lineages, MSCs of passage 4 were cultured in tissue-specific media according to the manufacturer's instructions (Miltenyi Biotec GmbH). Culture of the expanded CD271-MSC in tissue-specific media demonstrated that these MSCs possess an equal potential as PA-MSCs to differentiate along adipogenic, osteogenic, and chondrogenic lineages (Figure 13).

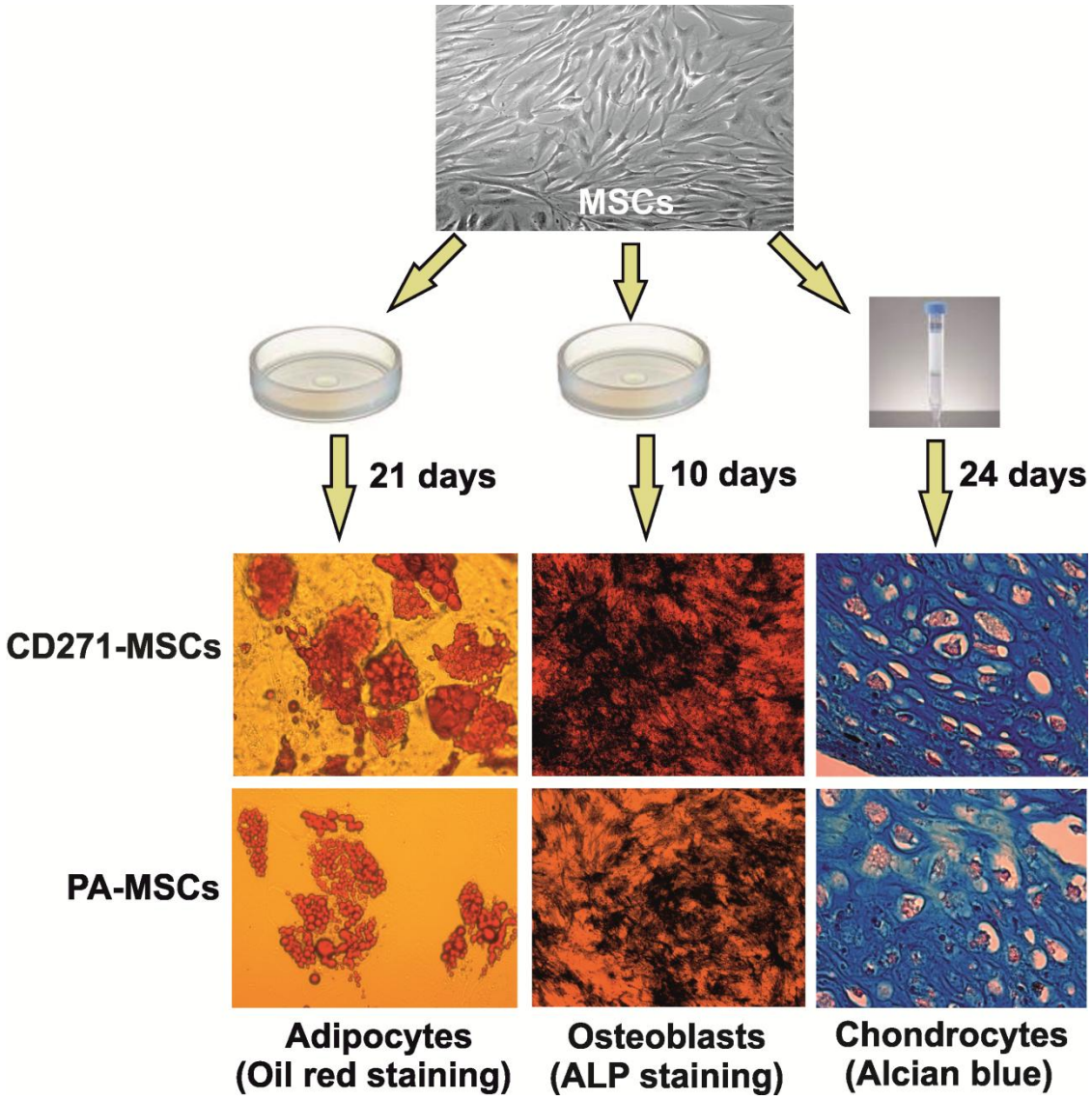

Figure 13. ***Differentiation potential of CD271-MSCs.***
Like PA-MSCs, CD271-MSCs differentiate into adipocytes, osteoblasts and chondrocytes. Accumulation of intracellular lipid vacuoles was shown by oil red-O staining after 21 days in culture with NH AdipoDiff medium, while osteoblast differentiation was detected by alkaline phosphatase activity after 10 days in NH OsteoDiff medium. Cartilage matrix deposition along with chondrocytes in lacunae was demonstrated by alcian blue staining after 24 days in NH ChondroDiff medium. Magnification for microphotographs of MSCs and osteoblasts was 40x; the magnification for adipocytes was 200x and for chondrocytes 400x.

4.1.4. Immunomodulatory potential of CD271-MSCs

4.1.4.1. Potential of CD271-MSCs to inhibit the proliferative response of peripheral blood mononuclear cells (PB-MNCs) to mitogens

To determine whether CD271-MSC may affect the proliferative response of PB-MNC to mitogenic stimulation, both types of lethally irradiated MSC were cultured with PB-MNCs at

a 1:1 ratio (Figure 14A). Third-party CD271-MSC markedly inhibited the proliferation of PB-MNC after mitogenic stimulation with phytohemagglutinin (41.3±2.9% of control, $P<0.03$) and concanavalin-A (34.3±8.0% of control, $P<0.0001$) as specific mitogens for stimulation of T cells and pokeweed mitogen (48.1±9.1% of control, $P<0.002$) as a mitogenic stimulator of both T and B cells. In contrast, they were unable to inhibit proliferation of PB-MNC after stimulation with the superantigen staphylococcal enterotoxin B (108.8±15.6% of control, $P<0.9$) like PA-MSC (Figure 14B).

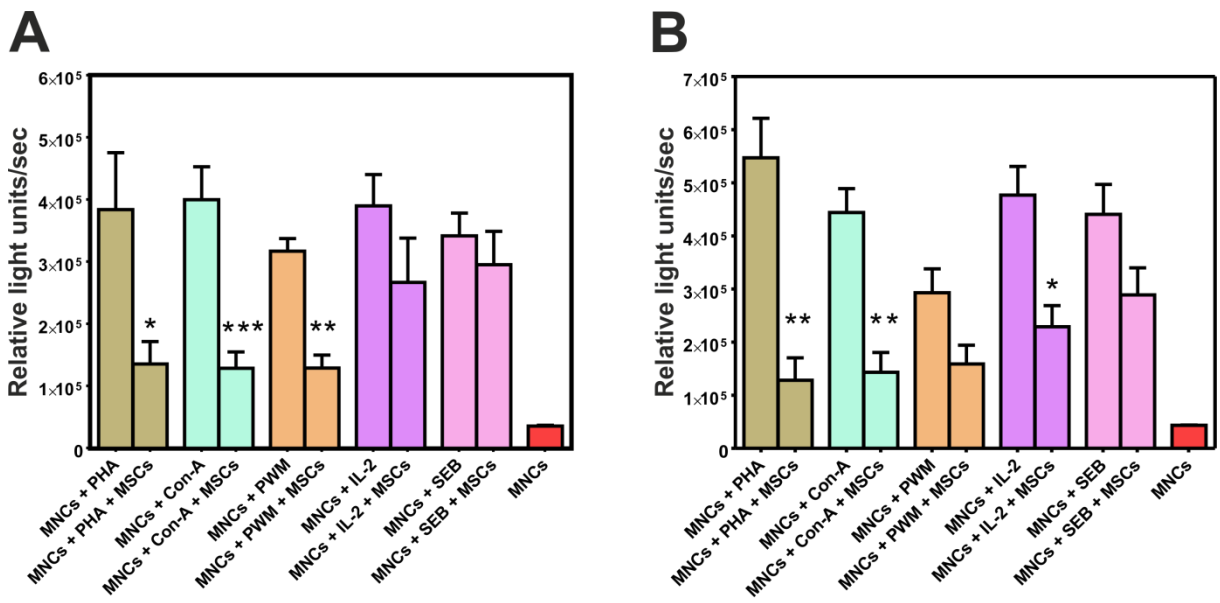

Figure 14. ***The effect of CD271-MSC on proliferation of mitogen-activated lymphocytes.*** *The figure shows the inhibitory effect of the CD271-MSC population (A) and PA-MSC population at passage 4 at ratio 1:1 (B). In each experiment, 100,000 peripheral blood lymphocytes were stimulated in triplicate with phytohemagglutin (PHA), concanavalin A (con-A), pokeweed mitogen (PWM), interleukin- 2 (IL-2) and staphylococcal enterotoxin B (SEB) in the presence or absence (control group) of lethally irradiated mesenchymal stromal cells (10^5). The values represent the mean of the triplicate experiments ± standard error of mean (SEM) (n=7). Statistically significant differences between groups were assessed with a Student's t test. P values of less than 0.05 were considered to be statistically significant: *P<0.02; **P<0.003;*** P<0.0001.*

4.1.4.2. Inhibition of allogeneic reaction through CD271- MSC

As MSCs are often used for the treatment of graft-versus-host disease, it is preferable to expand these cells in serum-free media. This was the major reason to expand CD271-MSCs either in FBS-containing or platelet lysate-containing media and assess their allosuppresive effect in mixed lymphocyte reaction. CD271-MSCs expanded in FBS-containing medium demonstrated a significant inhibitory effect on allogeneic driven proliferation of MNCs from two randomly chosen unrelated donors. CD271-MSCs were most effective at the MSC:MNC

ratios of 1:1 (P< 0.0009) and 1:2 (P< 0.001), and to a lesser extent at the ratio 1:10 (P< 0.01) (Figure 15A). Interestingly, indomethacin, an inhibitor of cyclooxygenase-1 and 2 necessary for the biosynthesis of PGE2, was not able to significantly abrogate the inhibitory effect of MSCs on proliferation of MNCs at the ratios 1:2 and 1:10. However, it reduced significantly this effect of CD271-MSCs at the ratio MSCs:MNCs=1:1. In contrast, PA-MSCs were able to suppress the alloantigen-induced proliferation of MNCs only at MSC:MNC ratios 1:1 and 1:2, but not at 1:10 ratio (Figure 15B).

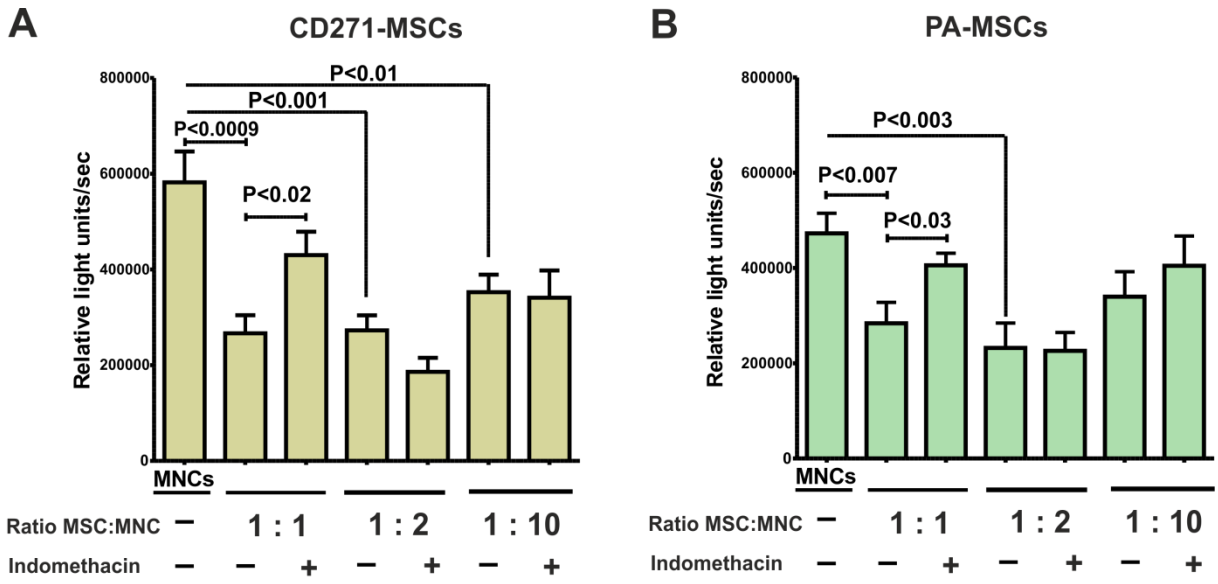

Figure 15. ***Allosuppressive effect of CD271-MSCs cultured in serum-containing medium.*** *In this figure is presented the inhibition of allogeneic reaction through CD271-MSCs (A) and PA-MSCs (B). MNCs of two unrelated donors were cultured for 5 days either alone (control group) or with lethally irradiated third-party MSCs at the MSC:MNC ratio of 1:1, 1:2 and 1:10. To demonstrate the MSC-mediated inhibition by prostaglandin E2 (PGE2), the MSCs were cultured with MNCs in the presence or absence of the PGE2 inhibitor, indomethacin (IM, final concentration: 5 μM). Proliferation levels of MNCs were determined on day 6 by means of the BrdU assay. The significance of inhibition of proliferation of allogeneic cells by MSCs and abrogation of this effect by indomethacin was assessed with a Student's t test. P values of less than 0.05 were considered to be statistically significant. The experiment was performed with eight unrelated MSC-MNC donor pairs.*

In addition, CD271-MSCs were successfully expanded in the medium supplemented with 5% of platelet lysate. These MSCs demonstrated a significant allosuppressive effect on allogeneic driven proliferation of MNCs from two randomly chosen unrelated donors. CD271-MSCs were most effective at the MNC: MSC ratios of 1:1 (P< 0.03) and 2:1 (P< 0.04) (Figure 16A). Indomethacin, as an inhibitor of cyclooxygenase-1 and 2 necessary for the biosynthesis of PGE2, was able to reverse the inhibitory effect of MSCs at both ratios 1:1 and 2:1. Like CD271-MSCs, PA-MSCs were also able to significantly suppress the alloantigen-induced

proliferation of MNCs only at MNC:MSC ratios 1:1 (P< 0.0001) and 2:1 (P< 0.0009) (Figure 16B).

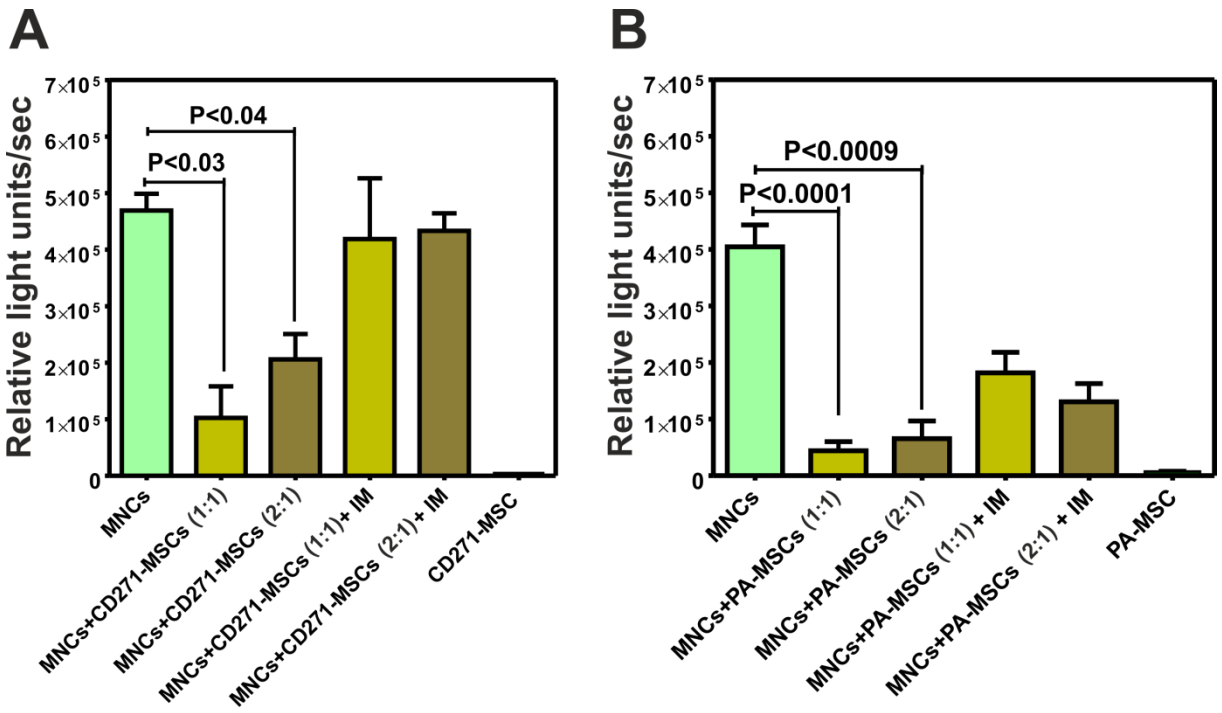

Figure 16. ***Allosuppressive effect of CD271-MSCs cultured in serum-free medium.***
In this figure is presented the inhibition of allogeneic reaction through CD271-MSCs (A) and PA-MSCs (B) previously cultured in the medium supplemented with 5% platelet lysate (serum-free). MNCs of two unrelated donors were cultured for 5 days either alone (control group) or with lethally irradiated third-party MSC at the ratio of 1:1 and 2:1. To demonstrate the MSC-mediated inhibition by prostaglandin E2 (PGE2), the MSCs were cultured with MNCs in the presence or absence of the PGE2 inhibitor, indomethacin (IM, final concentration: 5 μM). Proliferation levels of MNCs were determined on day 6 by means of the BrdU assay. The significance of inhibition of proliferation of allogeneic cells by MSCs was assessed with a Student's t test. P values of less than 0.05 were considered to be statistically significant. Values are presented as mean± SEM (n=3).

4.1.5. Effector soluble molecules of MSC-mediated immunosuppression

4.1.5.1. Prostaglandin E2 (PGE2)

In the MLR as a result of the allogeneic reaction there was a baseline level of PGE2 (3.3±0.68 ng/ml). On the other hand, CD271-MSCs alone produced also low levels of this molecule (5.29±0.71 ng/ml). However, contact of MSCs with the HLA-mismatched mononuclear cells at 1:1 and 1:2 ratio resulted in a significant increase of PGE2 production (23.8±5.04 ng/ml, P<0.007; and 23.14±2.93 ng/ml, P<0.0006, respectively). Remarkably, at a CD271-MSC:MNC ratio of 1:10 there was no increase in PGE2 production (3.52±1.06 ng/ml) (Figure

17A). Indomethacin as a specific blocker of PGE2 synthesis inhibited its production at ratios 1:1 and 1:2 but not at the ratio 1:10. Similar values were obtained when the PA-MSCs were used in MLR (Figure 17B).

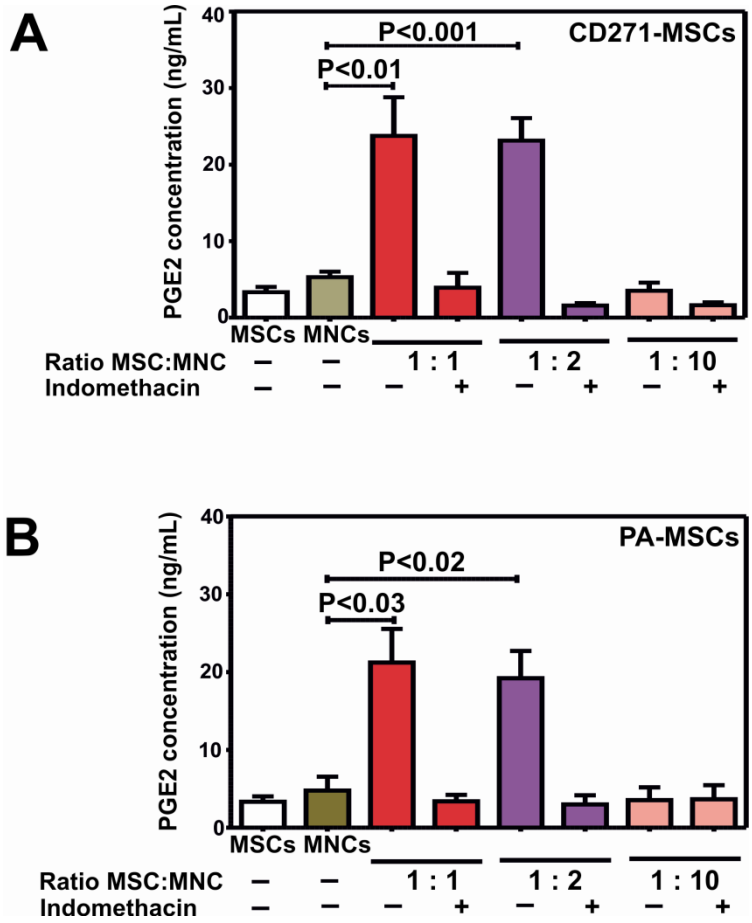

Figure 17. ***Concentration of prostaglandin E2 in the supernatants of MLR.***
Levels of PGE2 in the supernatants of MLR at different CD271-MSC:MNC (A) or PA-MSC:MNC ratios (B). The results are shown as mean values ± SEM of 6 independent experiments.

4.1.5.2. Soluble HLA-G (sHLA-G) and nitric oxide (NO) molecules

In addition to PGE2, the levels of soluble HLA-G and nitric monoxide in the supernatants of MLR in presence and absence of CD271-MSC were assessed. As shown in Figure 18A, no significant differences were observed in the levels of sHLA-G when MNCs were incubated with CD271-MSCs (7.3±0.2 U/ml) or PA-MSCs (6.4±0.3 U/ml) in comparison to the MNCs from two unrelated donors (6.4±0.4 U/ml). Baseline levels for sHLA-G released by CD271-MSCs were equal to the levels of this molecule released by PA-MSCs (6.3±0.7 U/ml or 6.4±0.6 U/ml, respectively).

To further examine the possible role of NO in MSC-mediated immunosuppression, levels of this molecule in the MLR supernatants at the MNC:CD271-MSC or MNC:PA-MSC ratio of 1:1 (Figure 18B) were assessed. No significant differences were found between the levels of NO in the supernatant of MLR either at MNC:CD271-MSC or MNC:PA-MSC ratio 1:1 (25.2±3.3 µM and 24.6±3.8 µM, respectively). In addition, blockade of NO synthesis by means of N-nitro-L-arginine methyl ester (L-NAME) (a NO-synthase inhibitor) did not affect the suppressive effect of either CD271-MSCs or PA-MSCs in MLR (data not shown).

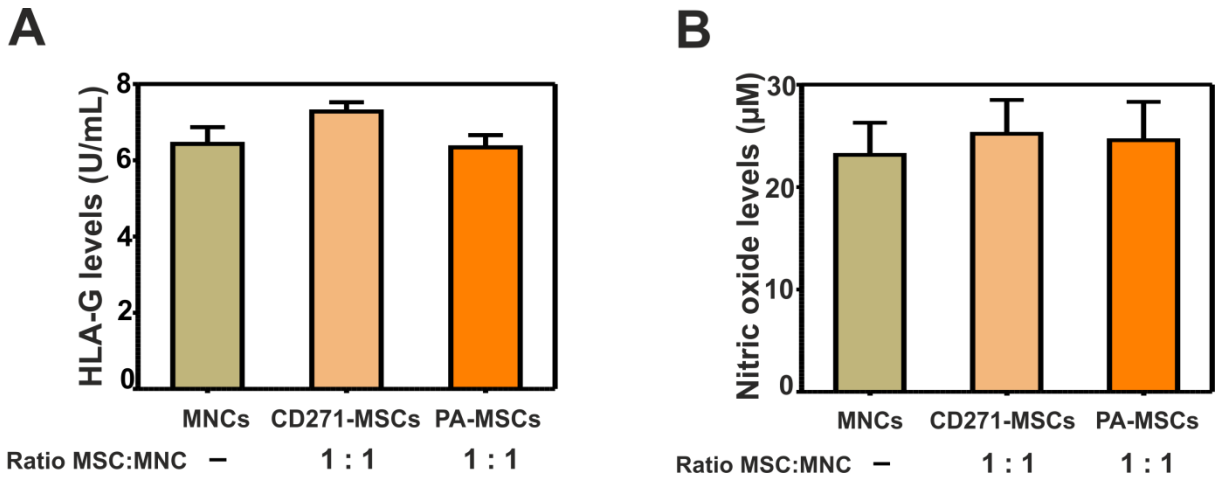

Figure 18. ***Levels of sHLA-G and NO in the supernatants of MLR.***
On day 6 of MLR the supernatants were collected and frozen until use. After thawing the samples were appropriately diluted and the levels of soluble HLA-G (A) and NO (B) in the supernatants of MLR at MNC:CD271-MSC or MNC:PA-MSC ratio of 1:1 were estimated. The results are shown as mean values ± SEM of 5 independent experiments.

4.1.5.3. Cytokine profile of the supernatants of MLR

MSCs have been shown to exert an anti-inflammatory effect in the allogeneic reaction. Determination of cytokines in the supernatants of MLR in the presence of CD271-MSCs revealed a significant decrease of the levels of inflammatory cytokines such as IFN-gamma and TNF-alpha. CD271-MSCs decreased the IFN-gamma levels significantly either at MNC:CD271-MSCs ratio of 1:1 (76.1±24.3 pg/ml, $P<0.02$) or 2:1 (124.8±32.3 pg/ml, $P<0.03$) compared to MNCs alone (612.4±176.1 pg/ml). In contrast, PA-MSCs decreased IFN-gamma levels slightly at 1:1 and significantly at the MNC:PA-MSC ratio of 2:1 ($P<0.03$) (Figure 19A). As a consequence of alloreaction, levels of TNF-alpha were increased in the supernatants of MNCs in MLR (404.3±82.9 pg/ml). However, the presence of CD271-MSCs induced a significant decrease either at ratio MNCs:CD271-MSCs of 1:1 or 2:1 (12.9±3.1 pg/ml, $P<0.003$; or 13.3±0.4 pg/ml, $P<0.003$, respectively) (Figure 19B). No significant changes were observed in the levels of Fas-ligand levels in the presence of CD271-MSCs,

even if CD271-MSCs induced a decrease in the levels of this ligand (Figure 19C). In contrast, co-culture of MNCs with CD271-MSCs resulted in a significant increase of IL-2 levels at the ratio 1:1 (140.6±33.9 pg/ml) and 2:1 (137±35 pg/ml) ($P<0.04$) compared to the levels of this cytokine in the supernatants of MNCs alone (29.8±4.7 pg/ml) (Figure 19D). CD271-MSCs produced high baseline levels of angiogenin (568.6±166.2 pg/ml) and VEGF (20385±6310 pg/ml). In addition, co-incubation of these MSCs with allogeneic MNCs did not change levels of these cytokines (data not shown). Remarkably, no changes in the levels of IL-10 in the supernatants of MLR have been observed (data not shown). PA-MSCs, which were used as a control throughout the study, demonstrated approximately the same potential as CD271-MSCs.

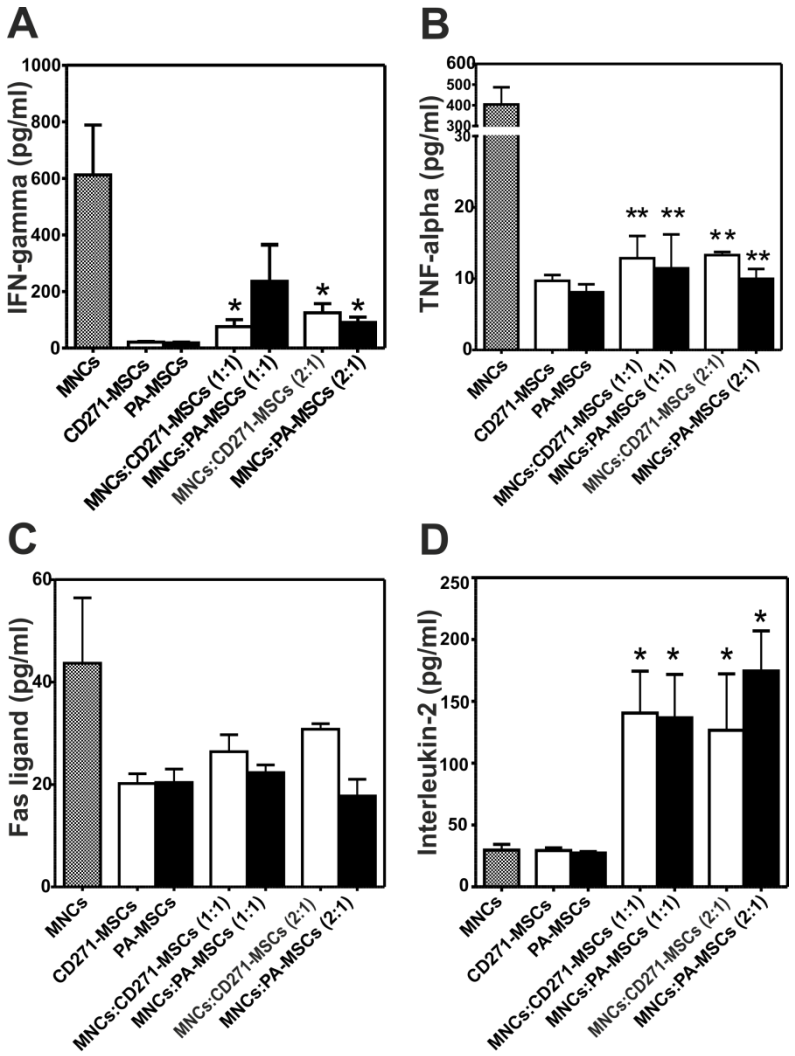

Figure 19. ***Estimation of cytokine levels in the supernatants of MLR.***
Supernatants of MLR were collected on day 6 and were frozen until use. After thawing, they were appropriately diluted and used to estimate the levels of a series of cytokines e.g. IFN-gamma (A), TNF-alpha (B), Fas-L (C) and IL-2 (D) by BD FACSArray. Results are shown as mean ± SEM of 4 independent experiments.

4.1.6. T regulatory cells (T regs)

$CD4^+CD25^+$ T cells are potent regulators of alloimmune responses. In order to assess their role in MSC-mediating immunosuppression of allogeneic reaction the proportion of these cells at day 0 and 6 in mixed lymphocyte reaction was estimated. Flow cytometric analysis demonstrated that the percentage of T regs in the mixture of MNCs of 2 HLA-mismatched donors was 3±2.2% (Figure 20A) whereas proportion of naïve T regs ($CD4^+CD25^{high}CD45RA^+$) was 34.5± 6.4%. By the time in culture (day 6) number of T regs as a consequence of allogeneic reaction significantly increased from 3±2.2% to 21.6±5.3% ($P<0.02$) (Figure 20A). In contrast, in presence of CD271-MSC the number of T regs at day 6 significantly decreased to 8.5±1.9% compared to the percentage of these cells in the absence of MSCs (21.6±5.3%) ($P<0.05$) (Figure 20B). Remarkably, despite the decrease of number of T regs in the presence of CD271-MSCs the percentage of naïve T regs ($CD4^+CD25^{high}CD45RA^+$) increased significantly from 37.1± 5.9% (day 6, MNCs without MSCs) to 66.5± 4.7% ($P<0.02$) (Fig. 20C). All these cells (98±1.4%) expressed CD62L, an important T-cell homing receptor. PA-MSCs showed a similar effect on T regs and their subpopulations.

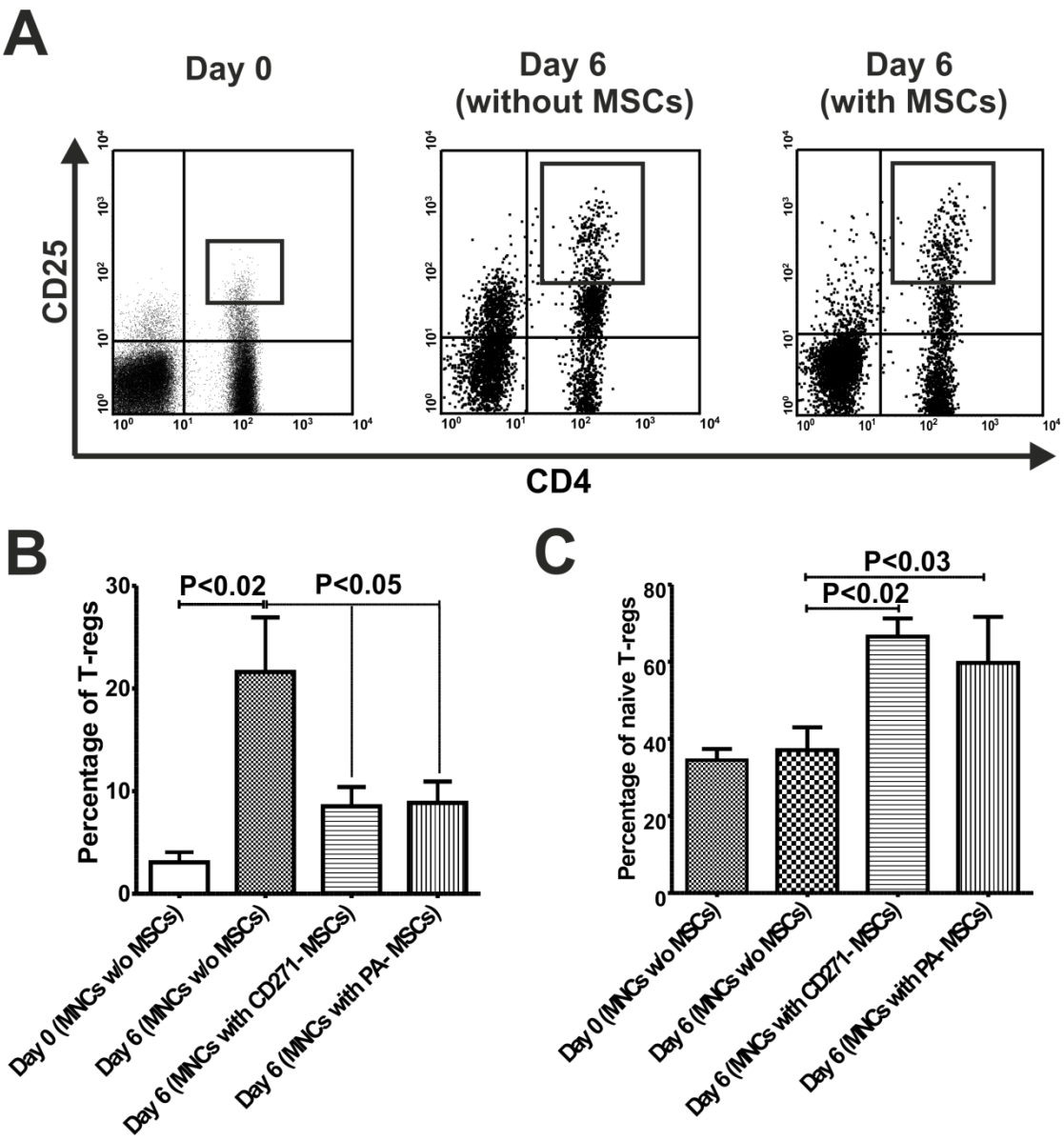

Figure 20. ***The effect of CD271-MSCs on T-regulatory cells in MLR.***
(A) A representative dot plot of T-regulatory cells on day 0 of MLR and day 6 (in absence or presence of CD271-MSCs). CD271-MSCs like PA-MSCs decreased the overall number of $CD4^{+}CD25^{high}$ *T-regs on day 6 of MLR (B). In contrast, they increased significantly the percentage of naïve T-regulatory cells (*$CD4^{+}CD25^{high}CD45RA^{+}CD62L^{+}$*) within population of T-regs (C). Results are presented as mean ± SEM of 6 independent experiments.*

4.2. *In vivo* studies

4.2.1. Multilineage engraftment of hematopoietic CD133$^+$ stem cells after co-transplantation with CD271-mesenchymal stromal cells

Several lines of evidence suggest that PA-MSC induce improved hematopoietic engraftment. However, thus far there is no evidence regarding the capacity of CD271-MSC on engraftment of hematopoietic stem cells or their multilineage differentiation potential *in vivo*. Flow cytometric analysis using an anti-human CD45 antibody demonstrated significantly improved engraftment of hematopoietic CD133$^+$ cells in the bone marrow of NOD/SCID mice co-transplanted with either CD271- MSC (2.9±0.9%, P<0.01) or PA-MSC (2.0±0.5%, P<0.02) at a ratio of 1:1 in comparison to that in a control group of mice transplanted with CD133$^+$ cells only (0.3±0.02%) (Figure 21).

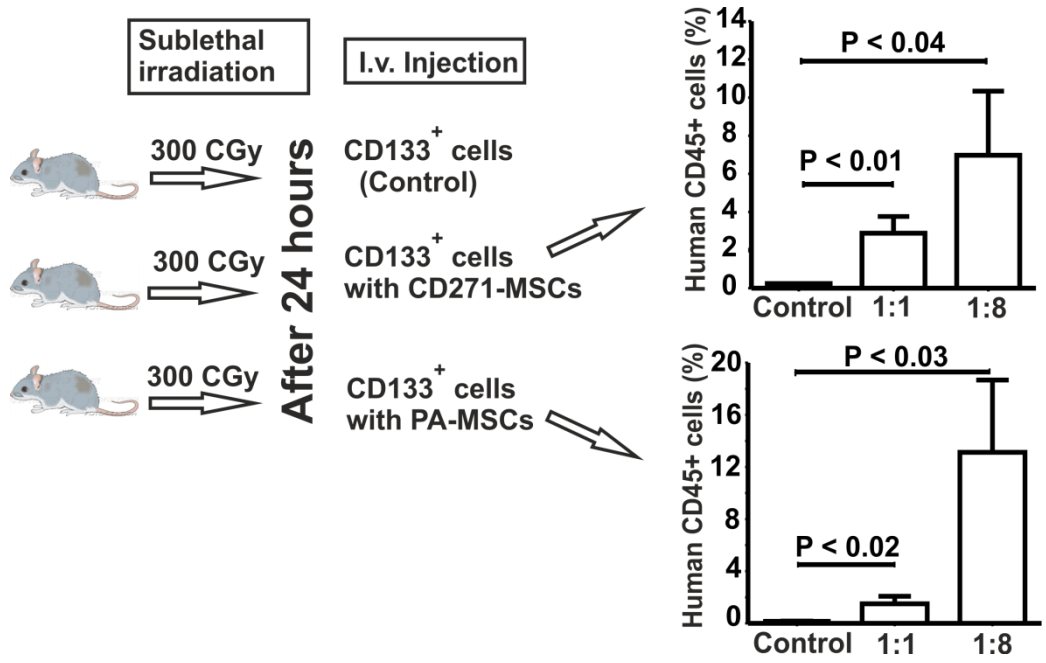

Figure 21. ***Hematopoietic engraftment of human CD133$^+$ cells in bone marrow of NOD/SCID IL-2Rγ^{null} mice.*** *Experimental design of the in vivo studies: Five groups of NOD/SCID IL-2Rγ^{null} mice (5 mice each) were sublethaly irradiated and on the next day transplanted with 1x10^5 human CD133$^+$ cells only (control group), 1x10^5 CD133$^+$ cells and 1x10^5 human GFP-transduced CD271-MSC (ratio 1:1) and the other group with 1x10^5 CD133$^+$ cells and 7x10^5 human GFP-transfected CD271-MSC (ratio 1:8). At the same ratios 1x10^5 CD133$^+$ cells were transplanted with GFP-transduced PA-MSC. The overall human cell engraftment in the bone marrow (as measured by anti-human CD45 immunostaining) 14 weeks post-transplantation is shown in the right panel. The top right panel shows the graph for co-transplantation of CD133$^+$ cells with CD271-MSC; the bottom right panel shows co-transplantation of CD133$^+$ cells with PA-MSC.*

Both types of MSC at this ratio showed similar effects; the number of myeloid ($CD33^+$) cells increased between 2- and 3-fold, whereas the number of megakaryocytes ($CD41a^+$) remained at levels comparable to those present in the control group. It is noteworthy that, at this ratio, both types of co-transplanted MSC increased the number of cells with a B-cell phenotype ($CD19^+$) about 8- to 9-fold (15.4±8.1% when CD271-MSC were co-transplanted and 13.3±4.2% when PA-MSC were co-transplanted) compared with the number in the control group (1.7±0.7%). Furthermore, neither type of MSC at this ratio showed an effect on the development of cells with a T-cell ($CD3^+$), NK-cell ($CD56^+$), or NKT-cell ($CD3^+CD56^+$) phenotype from engrafted $CD133^+$ cells (data not shown).

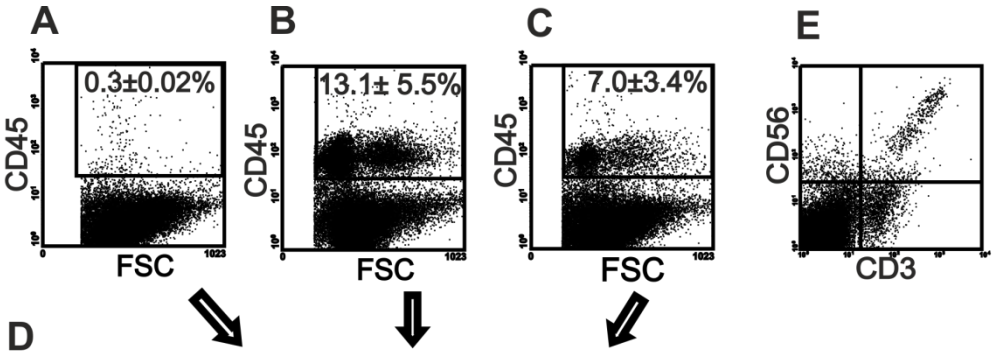

Multilineage engraftment	$CD133^+$ cells (Group A)	$CD133^+$ cells and PA-MSCs (1:8) (Group B)	$CD133^+$ cells and CD271-MSCs (1:8) (Group C)	Significant differences	
				Group C versus group A	Group C versus group B
$CD3^+$	0.8 ± 0.09	0.5 ± 0.2	5.2 ± 1.5	P < 0.01	P < 0.02
$CD56^+$	38.3 ± 5.7	1.9 ± 0.5	4.8 ± 2.1	P < 0.005	P < 0.007
$CD3^+CD56^+$	0.7 ± 0.2	0.9 ± 0.2	4.9 ± 3.8	P < 0.03	P < 0.04
$CD19^+$	1.7 ± 0.7	1.6 ± 0.3	5.7 ± 1.7	P < 0.04	P < 0.03
$CD41a^+$	11.8 ± 9.1	20.5 ± 2.8	24.5 ± 2.3	P < 0.03	--
$CD33^+$	12.4 ± 8.2	27.3 ± 3.4	28.2 ± 2.4	P < 0.04	--

Figure 22. ***Multilineage differentiation of $CD133^+$ hematopoietic stem cells after co-transplantation with mesenchymal stromal cells.*** *(A) A representative dot plot of the group transplanted with $1x10^5$ mobilized peripheral blood $CD133^+$ cells only, the group co-transplantated with PA-MSC at the ratio 1:8 (B) and the group co-transplanted with CD271-MSC at the ratio 1:8 (C). (D) Multilineage differentiation of $CD133^+$ without or with co-transplantation of CD271-MSC or PA-MSC, respectively. The percentage of positive cells for each lineage marker was determined by gating on human $CD45^+$ cells as shown in panels A, B and C. Differences in the engraftment level of each cell population between the groups were tested by Student's t-test. A P value of less than 0.05 was considered to be statistically significant. (E) Representative flow cytometric data on the engraftment of human T, NK and NKT cells in the group transplanted with 10^5 $CD133^+$ cells and $7x10^5$ CD271-MSC (1:8 ratio).*

In contrast, co-transplantation of $CD133^+$ cells with PA-MSC at a ratio of 1:8 (Figure 22B) induced greater overall engraftment of the hematopoietic cells in the bone marrow compared to CD271-MSC (Figure 22C) and to the control group (Figure 22A). Both types of MSC transplanted at this ratio doubled the number of myeloid cells ($CD33^+$) and megakaryocytes ($CD41a^+$) in comparison to the group transplanted with $CD133^+$ cells alone. However, co-transplantation of $CD133^+$ hematopoietic cells with CD271-MSC at a ratio of 1:8 induced their multilineage differentiation by giving rise to cells with a lymphoid lineage phenotype.
The numbers of cells with a T-cell and B-cell phenotype were roughly 7-fold ($P<0.01$) and 4-fold higher than those in the control group (Figure 22D). The number of NK cells decreased significantly (Figure 22E) to the normal levels compared to the control group, thereby demonstrating a declined expansion ($P<0.0005$) and suggesting that CD271-MSC may control the in vivo proliferation of these cells. In contrast, PA-MSC failed to give rise to the lymphoid lineage to the same extent as CD271-MSC, indicating a major qualitative difference between these two MSC populations.

4.2.2. Distribution of human cells in the organs of co-transplanted NOD/SCID mice

Real-time polymerase chain reaction analysis of organs from the mice co-transplanted with $CD133^+$ hematopoietic stem cells and CD271-MSC or PA-MSC demonstrated a detectable presence of human DNA in all organs (Figure 23A–C). When both types of MSC were transplanted with hematopoietic stem cells at a ratio of 1:1, most of the human DNA was detected in the brain and, to a lesser extent, in the lungs, liver, heart, and skeletal muscle. Approximately 2% of the human DNA in immunodeficient mice was detected in the brain. In contrast to this finding, co-transplantation of $CD133^+$ hematopoietic stem cells with MSCs at a ratio of 1:8 was associated with an increase in human DNA in the lungs, suggesting the possible entrapment of human cells in this organ. When hematopoietic stem cells were co-transplanted with CD271-MSC or PA-MSC at a ratio of 1:8, the amount of human DNA in the lungs represented about 0.7±0.16% or 1.4±0.25%, respectively. In addition to the lungs, the second organ in which human DNA was detected at significant quantities was the liver; very low amounts of human DNA were detected in the brain, heart, and skeletal muscle (Figure 23C). In contrast, real-time polymerase chain reaction analysis of mouse organs transplanted with different doses of CD271-MSC or PA-MSC separately revealed consistently higher amounts of human DNA in the lungs, and very low levels in the liver, heart, and skeletal muscle. No human DNA was detected in the brain of the mice indicating a typical migration pattern of MSC with lung entrapment of these cells (data not shown).

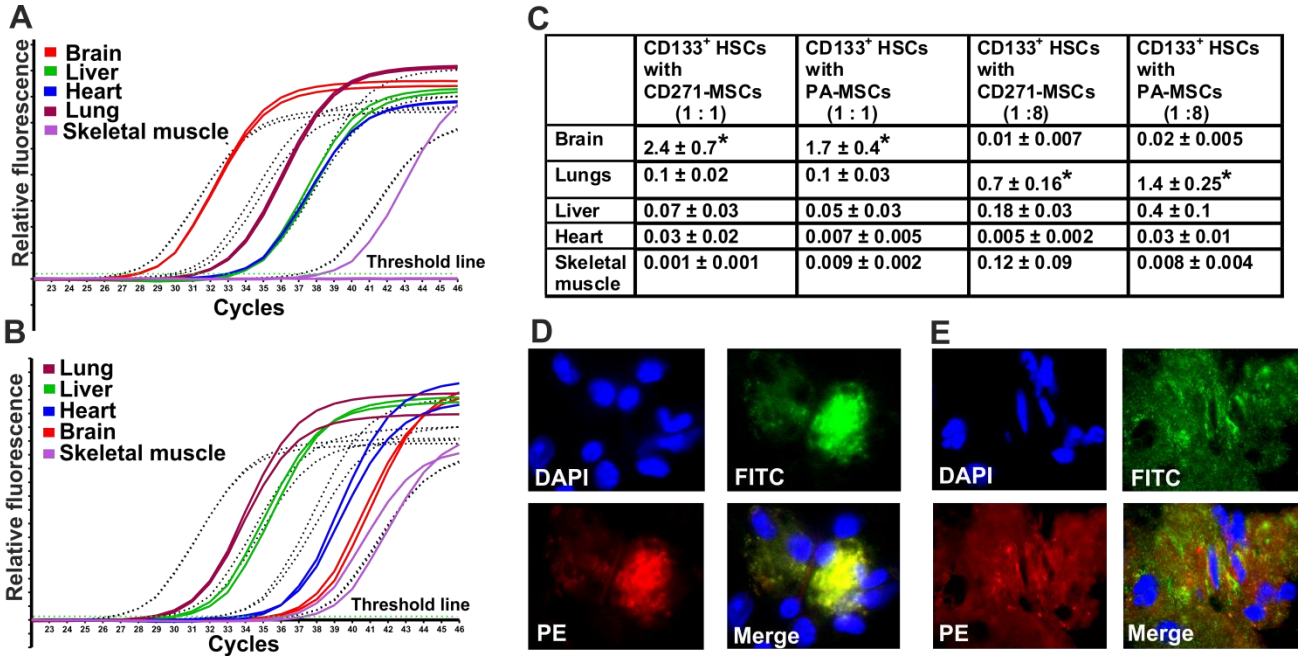

	CD133⁺ HSCs with CD271-MSCs (1 : 1)	CD133⁺ HSCs with PA-MSCs (1 : 1)	CD133⁺ HSCs with CD271-MSCs (1 :8)	CD133⁺ HSCs with PA-MSCs (1 :8)
Brain	2.4 ± 0.7*	1.7 ± 0.4*	0.01 ± 0.007	0.02 ± 0.005
Lungs	0.1 ± 0.02	0.1 ± 0.03	0.7 ± 0.16*	1.4 ± 0.25*
Liver	0.07 ± 0.03	0.05 ± 0.03	0.18 ± 0.03	0.4 ± 0.1
Heart	0.03 ± 0.02	0.007 ± 0.005	0.005 ± 0.002	0.03 ± 0.01
Skeletal muscle	0.001 ± 0.001	0.009 ± 0.002	0.12 ± 0.09	0.008 ± 0.004

Figure 23. ***Distribution of human cells in the tissues of NOD/SCID mice 14 weeks after transplantation.*** *(A) Real-time PCR amplification of human albumin gene in tissue samples of mice co-transplanted with human CD133$^+$ cells and CD271-MSC at a ratio of 1:1. (B) Real-time PCR amplification of human albumin gene in tissue samples of mice co-transplanted with human CD133$^+$ cells and CD271-MSC at a ratio 1:8. Standard curve achieved from serial dilutions of human DNA in mouse DNA (10^{-1} to 10^{-4}) is depicted with dashed lines. (C) Organ distribution of human cells in mouse tissues. Fourteen weeks after transplantation genomic DNA was extracted and the presence of human-specific DNA in the organs of transplanted mice was confirmed by real-time PCR for human albumin gene. The values represent calculated mean percentages of human DNA ± SD of four measurements. Significant differences were observed in the brain of groups co-transplanted with HSC and MSC at the 1:1 ratio as compared with the content of human DNA in the brain of groups co-transplanted with HSC and MSC at a 1:8 ratio (*P<0.04 when HSC were co-transplanted with CD271-MSC and *P<0.01 when HSC were co-transplanted with PA-MSC). In contrast, when HSC were co-transplanted with MSC at a 1:8 ratio a significantly higher amount of human DNA was observed in the lungs as compared to the content of human DNA in the same organ of mice co-transplanted with HSC and MSC at a 1:1 ratio (*P<0.01 when HSC were co-transplanted with CD271-MSC and *P<0.04 when HSC were co-transplanted with PA-MSC) (D) and (E) A representative immunostaining of GFP-transduced CD271-MSC in the tissue sections with phycoerythrin (PE)-conjugated mouse anti-human HLA-class I and Alexa 488-conjugated anti-GFP antibody. Localization of MSC-derived cells in the lungs (D) of mice co-transplanted with 7x10^5 CD271-MSC and 10^5 CD133$^+$ HSC and brain (E) when CD271-MSC were co-transplanted with CD133$^+$ HSC at a ratio of 1:1 (magnification 600x).*

5. DISCUSSION

5.1. The need for novel markers for prospective isolation of progenitor cells for MSCs

Most of the researchers agree that one of the drawbacks of generating MSC through plastic adherence is the unknown MSC progenitor cell and the derivation of a very heterogeneous cell population with regard to proliferative and differentiation potentials. Since the origin of MSC still remains elusive, there is an increasing need for novel markers and methods of detection, enumeration, and isolation of MSC progenitor cells from the bone marrow and other tissues as a prerequisite for establishing stringent protocols for the clinical-scale generation of MSC without any hematopoietic contamination (17;93;99;100).

5.2. Clonogenic, proliferative and differentiation potential of CD271-MSCs

5.2.1. Clonogenic potential

The frequency of $CD271^+$ cells in our sample as assessed by flow cytometry was 0.6±0.1% (range, 0.2% to 1.2%; median 0.5%), demonstrating similar values as described by Poloni et al. (102). However, it was lower than the frequency of $CD271^+$ cells reported by Quirici et al. (17). The frequency of $CD271^+$ BM-MNCs in our study varied from donor to donor and no correlation between this parameter and donor age has been observed which is in agreement with the results of Jones et al. (108). In addition, the number of colonies generated with the enriched $CD271^+$ BM-MNCs in our study (2043 colonies, range 480-4540) was similar to the findings of Qurici et al. (17) who described an average of 2700 colonies per $1x10^6$ of positively selected $CD271^+$ BM-MNCs (range 200-8700) and Poloni et al. (102) (1760±1130 CFU-Fs). On the other hand, Jarocha et al. (104) obtained a three-fold lesser number of CFU-Fs with the enriched $CD271^+$ BM-MNCs compared to our data. Also, we did not observe a correlation between the number of CFU-Fs generated by positively selected $CD271^+$BM-MNCs and the percentage of $CD271^+$ BM-MNCs of the same donor. Using flow cytometry, we also found that CFU-Fs generated with highly enriched $CD271^+$ BM-MNCs contained a very low contamination with hematopoietic cells (<1%) compared to the CFU-Cs generated from unseparated BM-MNCs which contained in average 13% hematopoietic cells (range: 3 to 21.6%) (data not shown). Therefore, the enrichment of $CD271^+$ cells enables a positive selection of MSC-progenitors from bone marrow and consequently prevents contamination of these progenitors with undesired hematopoietic cells. In contrast, the number of CFU-Fs generated from 1 $x10^6$ of unseparated BM-MNCs differed largely between different groups

working with MSCs, starting from 2.5 (104), 13.6 (10) and increasing to 26-30 colonies (60;102;177), 44 colonies (17) or 80 colonies (108). The average number of CFU-Fs generated from 1 x 10^6 unseparated BM-MNCs in our study was 77 colonies (range 12- 154), which was similar to the findings of Jones et al. (108).

These differences may be explained by different culture conditions used by each group e.g. Quirici et al. (17) used 20% FBS to generate CFU-Fs and scored their number on day 9 as did Jarocha et al. (104). Another important point is that most of the groups use ficoll gradient 1.077 g/cm^3 to isolate BM-MNCs from bone marrow samples, which usually results in contamination of mononuclear cell fraction with a large number of granulocytes. We observed the same phenomenon in 2 out of 10 bone marrow samples in which this contamination diminished the number of colonies generated from unseparated BM-MNCs. Use of the ficoll gradient with a lower density 1.073 g/cm^3 resulted in a 3-4 fold higher number of CFU-Fs, that was also demonstrated by another group (178). Several lines of evidence showed that there is negative correlation between the number of CFU-Fs and the age of bone marrow donors (60;61). In this study, we did not observe such a negative correlation most probably due to the small difference in the age of bone marrow donors (20-40 years old).

5.2.2. Proliferative potential

Several reports demonstrated that MSCs generated from $CD271^+$ BM-MNCs possess a significantly higher proliferative potential than the MSCs derived from unseparated BM-MNCs. Quirici et al. (17) found a 100-fold higher proliferation rate of CD271-MSCs compared to the PA-MSCs by using a medium supplemented with 20% FBS and bFGF. In this study, we used culture medium supplemented with 10% FBS only and that may be the reason that we were not able to observe any difference in the growth rate of both MSC-populations. Consequently, estimation of population doublings (PD) over a period of 30 days in culture revealed a similar growth kinetics of both types of MSCs cultured either with FBS (CD271-MSCs: 19.5 ± 1.3 PD; PA-MSCs: 19.3 ± 1.0 PD) or with platelet lysate (CD271-MSCs: 17.0 ± 1.2; PA-MSCs: 14.7 ± 2.6). Determination of doubling time demonstrated that CD271-MSCs need a shorter time to duplicate themselves when cultured in serum-free medium. In addition, the doubling time was prolongated by the time in culture, e.g. while at passage 1 and 2 the doubling time of these MSCs was in average 1.6 days (38.4 hours), by passage 4 the doubling time became significantly longer (2.3 days or 55.2 hours). PA-MSCs at passage 4 cultured under the same conditions needed in average 2.96 days (71 hours) to

duplicate themselves. However, the differences were not statistically significant and the doubling times were comparable to the doubling times of CD271-MSCs and PA-MSCs cultured in presence of animal serum (10% FBS), suggesting that platelet lysate has equal stimulatory properties for proliferation of both types of MSCs as FBS. Our data therefore suggest that platelet lysate can be used as effectively as FBS in generating bulk quantities of MSCs under serum-free conditions for a clinical application.

Jones et al. (108) demonstrated an inverse correlation between the age of bone marrow donors (10-85 years) and the number of population doublings. In our sample we did not observe such a correlation most probably because of small differences in the age of bone marrow donors (20-40 years old donors). However, we observed large variations in proliferative potential of MSCs in the first passage between donors of bone marrow in agreement with the data reported by Phinney et al. (67).

5.2.3. Differentiation potential

Most of the authors agree that the differentiation potential of MSCs may be dependent on the age of the donor (66;69). Based on several investigations, the osteogenic differentiation of MSCs declined progressively with age (60;70;71). Evaluation of the levels of specific ALP activity showed that the osteogenic potential of MSCs declined progressively in donors older than 40 years, compared to "young" MSCs (donors 7-18 years old) and "adult" MSCs (18 -40 years old), whereas chondrogenic differentiation also declined in ''aged'' MSCs but this did not reach significance. In addition, adipogenic differentiation did not change significantly with age (60). In contrast, other authors did not observe any differences (64). On the other hand it has been reported that adipogenic differentiation of MSCs did not change significantly with age (60), in contrast to Moerman et al. (70) who found that aging activates adipogenic differentiation. There are also reports which demonstrated changes in dhe the differentiation potential of MSCs in the same donor depending on the time of donation (67). In our study we observed no correlation between differentiation potential of CD271-MSCs and the age of donors. The reason for that may be the pretty homogeneous age of donors (20-40 years old). However, differentiation potential of CD271-MSCs was donor-dependent i.e. CD271-MSCs of some donors differentiated better than the CD271-MSCs of the other donors. In addition, we did not observe any differences in the differentiation potential between CD271-MSCs and PA-MSCs from the same donor.

5.3. The immunosuppressive properties of CD271-MSCs

Mesenchymal stromal cells have been shown to exert a pleiotropic immunosuppressive effect. There are, however, no data so far on whether CD271-MSC share at least the same *in vitro* and *in vivo* immunosuppressive and engraftment-promoting properties with PA-MSC (74;159;163;179;180). Our *in vitro* data demonstrated that CD271-MSC strongly inhibited the mitogenic-induced proliferation of PB-MNC after stimulation with concanavalin-A (65.7±8.2% inhibition), phytohemagglutinin (58.7%±2.9%), or pokeweed mitogen (51.9±9.1%) and are in agreement with the findings of Aggarwal et al. (74). On the other hand, CD271-MSCs as well as PA-MSCs in our experiments effectively suppressed the allogeneic reaction ranging from 40-80% of the maximal proliferation. Le Blanc et al.(72) demonstrated this immunosuppressive effect by PA-MSCs.

In the present study we also attempted to identify possible molecular mechanisms underlying the immunosuppressive effect of CD271-MSC on the allogeneic reaction *in vitro*. In contrast to Krampera et al. (181) who demonstrated that MSC- T cell contact is indispensable for their immunosuppressive effect, a number of studies showed that the suppression is variably sustained in transwell experiments, suggesting that a series of soluble factors is involved.

Several reports showed that PGE2 is one of the most important molecules which mediate the immunossuppressive effect of PA-MSCs (74;182;183). Aggarwal and Pittenger (74) have shown that human MSCs can secrete PGE2 in quantities that may be sufficient to be involved in MSC-mediated immunomodulation. Yanez et al. (182) claimed that PGE2 has a major role in the inhibitory effects of MSCs on the proliferative response of T lymphocytes to mitogenic or allogeneic stimulation. In contrast to these data, Rasmusson et al. (75) concluded that addition of indomethacin, an inhibitor of prostaglandin synthesis, restored part of the inhibition by MSCs in PHA cultures, but did not affect MSC-induced inhibition of allogenic proliferation in MLR. In addition, Tse et al. (76) also reported low levels of PGE2 secretion by MSCs, but they did not see significant reversal in T cell proliferation when using PGE2 synthesis inhibitors.

In our study, we asked therefore whether PGE2 is involved in the suppression of allogeneic reaction *in vitro* by CD271-MSCs in different MSC:MNC ratios. Consistent with the data of Aggarwal and Pittenger (74) and Yanez et al. (182) we found a significant increase of PGE2 concentration when CD271-MSCs were co-incubated with MNCs at the ratio 1:1 or 1:2 (about 4.5-fold) compared to baseline levels of PGE2 produced by CD271-MSCs. This correlated very well with the inhibitory effect of CD271-MSCs on allogeneic reaction in

MLR at these ratios. Indomethacin, an inhibitor of cyclooxygenase-1 and -2 necessary for the biosynthesis of PGE2, mitigated the overall MSC suppressive effects only when CD271-MSCs were co-incubated with MNCs at the ratio 1:1. However, this effect was not observed when CD271-MSCs were co-incubated with MNCs at ratio 1:2, suggesting that although present at high levels in the culture, PGE2 does not play an exclusive major role in the inhibitory effects of MSCs when allogeneic MNCs are in excess. In contrast, PGE2 concentration remained at baseline levels when CD271-MSCs were co-incubated with MNCs at the ratio 1:10. Remarkably, only CD271-MSCs were able to elicit a potent allosuppression at this ratio. To our knowledge, this is the first time to demonstrate that CD271-MSC are more effective in suppression of alloantigen-induced response at lower concentrations and that they use PGE2 as a mediator of this effect only when they are present in equal numbers with MNCs (1:1 ratio) but not when the MNCs are in excess (1:2 and 1:10 ratio).

Recently, Selmani et al. (184;185) reported that the nonclassic human leukocyte antigen (HLA) class I molecule HLA-G is responsible for the immunomodulatory properties of MSCs. They showed that MSCs secrete the soluble isoform HLA-G5 and that such secretion is interleukin-10-dependent. Moreover, cell contact between MSCs and allostimulated T cells is required to obtain a full HLA-G5 secretion and, as consequence, a full immunomodulation from MSCs. In addition, Sato et al. (174) found in mice that Stat5 phosphorylation in T cells is suppressed in the presence of MSCs and that nitric oxide (NO) is involved in the suppression of Stat5 phosphorylation and T-cell proliferation. In the present study we assessed whether PGE2 acted alone or in concert with soluble HLA-G isoforms (HLA-G1 and HLA-G5) and nitric oxide in order to suppress the allogeneic reaction in MLR. In co-culture conditions at all CD271-MSC:MNC ratios used in our experiments we did not find any significant increase of soluble HLA-G molecules. Their levels (3.0±0.08 ng/ml) did not significantly differ from baseline levels (2.6±0.3 ng/ml) produced by MNCs only. This disagreement with the results reported by Selmani et al. (185) may be explained by the fact that the authors stimulated secretion of sHLA-G by exogeneous addition of IL-10. Low levels of this cytokine as measured in the MLR supernatants of our samples (data not shown) were apparently not sufficient to initiate secretion of HLA-G molecules by CD271-MSC. To the question of whether nitric oxide is produced by CD271-MSC in co-culture with allogeneic MNCs, we detected comparable amounts of this molecule which were not different from amounts produced by MNCs only. Moreover, L-NAME (a specific NO-synthase inhibitor) was not able to restore MNC proliferation in MLR (data not shown), indicating that this molecule does not contribute to the MSC-mediated immunosuppression in humans, either.

The immune behavior of MSCs can be influenced not only by neighboring cells but also environmental factors like systemic or local inflammation as in case of graft versus host disease (GVHD). An emerging body of evidence indicates that pro-inflammatory cytokines IFN-gamma and TNF-alpha are key mediating inflammatory events during several injury and pathological situations. IFN-gamma has been reported to enhance the immune-suppressive behavior of MSCs by upregulation of inhibitory molecule B7-H1 (186) or by IDO production as a key player in immuno-suppression of T cells (167). On the other hand, experiments *in vitro* showed that the addition of TNF-alpha to MLR (187) was sufficient to reverse the immunosuppressive effect of MSCs on T cell proliferation, and this observation was associated with an increase in interleukin-6 secretion. In our experimental MLR setting we observed high levels of IFN-gamma and TNF-alpha as a result of allogeneic reaction between two HLA-mismatched donors of MNCs. CD271-MSCs themselves produced low levels of these two cytokines. However, CD271-MSCs in co-culture with allogeneic MNCs, were able to significantly decrease concentration of IFN-gamma (about 80%) and TNF-alpha (about 90%) at both 1:1 and 1:2 ratio, indicating their strong anti-inflammatory effect. Aggarwal et al. (74) reported a decrease of IFN-gamma for about 50% in the presence of PA-MSCs. In addition, CD271-MSCs revealed also a considerable anti-apoptotic effect in the MLR by reducing levels of Fas ligand, as a member of tumor necrosis factor family. A similar effect has been observed for PA-MSCs, either. Rasmusson et al. (75) have found that MSCs increased the production of IL-2 and IL-2R in MLRs, on both the transcriptional and translational level. Furthermore, they also demonstrated that MSCs do not produce IL-2, IL-2R, or IL-10 as culture supernatants were negative. Remarkably, our data show that the allogeneic reaction by itself does not result in an increase of IL-2 production. However, co-culture with either CD271-MSCs or PA-MNCs induced a significant elevation of IL-2 levels in the MLR-supernatants. Despite this increase, MSCs were able to significantly suppress proliferation of MNCs, indicating that MSCs inhibit T cells even when more IL-2 is secreted, probably by activating a point of inhibition downstream of IL-2 activation.

Most of human MSC-mediated immunosuppressive function on alloantigen-activated T-lymphocyte proliferation was related to the secretion of anti-proliferative soluble factors (72;74;75;77;167). Recently, there is increasing evidence that the immunosuppressive effect of MSCs is not mediated by soluble immunosuppressive molecules only, but also may be mediated through cellular components of MLR e.g. subsets of T regulatory cells. However, the role of naturally occurring $CD4^+CD25^+$ T-regs in MSC-mediated immunosuppressive effect is still controversial. Krampera et al. (188) reported that MSCs induce a strong anti-

proliferative effect not associated with any effect on enhancement of T regulatory activity. On the other hand, Maccario et al. (189) showed that lymphocyte populations containing variable proportions of putative $CD4^+CD25^+$ T-regs were obtained when MSCs were added to MLR, as a third party, at ratios of 1:1 and 1:2 MSC:MNC. Furthermore, Prevosto et al. (190) reported that powerful regulatory $CD4^+$ or $CD8^+$ lymphocytes are generated in co-cultures of MNCs with MSCs which may amplify the reported MSC-mediated immunosuppressive effect. In light of these controversial data we asked whether CD271-MSC cells use this additional mechanism to suppress alloantigen driven proliferation of MNCs in MLR. In contrast to the data of Maccario et al. (189) we found an increase in the percentage of $CD4^+CD25^{high}$ T regs as a result of allogeneic reaction on day 6 of MLR (from 3±2.2% on day 0 to 21.6±5.3% on day 6). In presence of CD271-MSCs the total number of $CD4^+CD25^{high}$ T regs on day 6 of MLR decreased significantly (8.5±1.9%) compared to the number of T regs in the wells where MNCs were cultured without MSCs (21.6±5.3%). Remarkably, flow cytometric analysis of these co-cultured MNCs with MSCs for 6 days revealed a significant increase of naïve $CD4^+CD25^{high}CD45RA^+CD62L^+$ T regs (66.5±4.7%, $P<0.02$) compared to the percentage of T regs in allogeneic MNCs cultured without MSCs (37.1±5.9%). Having in mind the evidence that only naïve T regs with this phenotype show a profound suppressive activity (191) and represent the only subset of T regs that protect mice from lethal acute GvHD (192), we presume that interactions between CD271-MSCs and alloantigen-activated lymphocytes promote a selective expansion of this subset of T regs, which may further propagate and extend the immunosuppressive effect of these MSCs.

Taken together, we conclude that, unlike PA-MSCs, CD271-MSCs elicit a potent allosuppression even at lower concentrations and that the majority of immunossuppressive effect of CD271-MSCs is mediated via PGE2, but not via HLA-G, NO or IL-10 molecules. In addition, selective expansion of a subset of naïve T regulatory cells in presence of CD271-MSC may further contribute to the suppression of alloantigen-activated lymphocytes. Based on the evidence that CD271-MSCs exert potent allosuppressive properties *in vitro* we suggest that these MSCs represent an unequivocal alternative to PA-MSCs for the treatment of patients with GvHD and other inflammatory disorders.

5.4. The engraftment-promoting properties of CD271-MSCs

An emerging body of evidence indicates that co-transplantation of PA-MSC with human $CD34^+$ cells facilitates their engraftment and induces a shift in their differentiation from

predominantly B lymphocytes to predominantly enhanced myelopoiesis ($CD13^{+,}$ $CD14^{+}$, and $CD33^{+}$ cells) and megakaryocytopoiesis (193). We asked whether CD271-MSC share the same properties with PA-MSC or may be more efficient in modulating hematopoietic engraftment. Our *in vivo* data revealed that co-transplantation of $CD133^{+}$ cells with CD271-MSC significantly improved their multilineage engraftment in the bone marrow of immunodeficient NOD/SCID mice at both 1:1 (about 10-fold) and 1:8 (about 23-fold) ratios in comparison to transplantation of $CD133^{+}$ cells alone. We found an approximately 2- to 3-fold increase in the number of myeloid cells ($CD33^{+}$) and enhanced megakaryopoiesis ($CD41a^{+}$), especially at the 1:8 ratio (about 2-fold more megakaryocytes); these findings indicate the differentiation of $CD133^{+}$ cells towards more primitive $CD45^{+}CD41a^{+}$ megakaryocytes (194). In contrast to the above studies, however, co-transplantation of $CD133^{+}$ hematopoietic stem cells with CD271-MSC at a ratio of 1:8 promoted their differentiation towards the lymphoid lineage, in addition to megakaryopoiesis and myelopoiesis. Remarkably, the number of $CD3^{+}$ cells increased 10.4-fold ($P<0.02$), the number of NK cells increased 2.5-fold ($P<0.0007$) and the number of B cells increased 3.6-fold ($P<0.03$), compared to the group transplanted with $CD133^{+}$ hematopoietic stem cells and PA-MSC at the same ratio. In addition, CD271-MSC decreased the number of $CD56^{+}$ cells to approximately normal levels, whereas in the control group an expansion of these cells was observed. This finding is in agreement with data demonstrating that MSC may alter the phenotype of NK cells and suppress proliferation, cytokine secretion, and cytotoxicity against HLA class I-expressing targets (195). Taken together, our data demonstrate that, in contrast to PA-MSC, CD271-MSC are able not only to improve the engraftment of hematopoietic stem cells, but also to promote their differentiation into myeloid and lymphoid lineages. After co-transplantation with human $CD34^{+}$ hematopoietic cells in children with hematologic malignancies, PA-MSC induced a sustained engraftment that, nonetheless, did not promote any significant T- or NK-cell recovery relative to the control group transplanted with hematopoietic stem cells alone (196). Based on our findings, we assume that CD271-MSC offer a better alternative to PA-MSC for post-transplant T-cell reconstitution, which substantially contributes to the successful outcome of hematopoietic stem cell transplantation.

5.5. Migratory potential of CD271-MSCs.

Systemic delivery of MSC has been reported by several groups, who found that the majority of cells were entrapped in the lungs and a small amount engrafted in the heart, liver, and spleen (197;198). Data obtained from experiments in which CD271-MSCs or PA-MSCs were individually transplanted into NOD/SCID mice via an intravenous route revealed a similar organ distribution, with the majority of the cells being entrapped in the lungs. When expanded CD271-MSC or PA-MSC were co-transplanted with hematopoietic stem cells at a ratio of 1:1, however, quantitative polymerase chain reaction analysis for the human albumin gene demonstrated that the cells migrated more efficiently to brain than to the lungs, liver, heart, or skeletal muscle. In contrast, when co-transplanted with hematopoietic stem cells at a ratio of 8:1, CD271-MSC or PA-MSC migrated mainly to the lungs and, to a much lesser extent, to the liver, brain, heart, and skeletal muscle. Our data, therefore, suggest that not only can MSC influence hematopoietic stem cell engraftment but also that hematopoietic stem cells may affect the migration and homing pattern of MSC *in vivo*.

6. CONCLUSIONS

Based on the data obtained from this study we conclude that:

1. The frequency of $CD271^+$ bone marrow mononuclear cells (BM-MNCs) in our sample as assessed by flow cytometry was 0.6±0.1% (range, 0.2% to 1.2%; median 0.5%).

2. The frequency of $CD271^+$ BM-MNCs in our study varied from donor to donor and no correlation between this parameter and donor age was observed.

3. Enriched $CD271^+$ BM-MNCs generated a 26-fold higher number of CFU-Fs than compared to unselected BM-MNCs.

4. In contrast to the CD271 negative cell fraction, only positively selected $CD271^+$ BM-MNCs gave rise to the CFU-Fs, suggesting that this cell fraction contains all progenitor cells for mesenchymal stromal cells (MSCs).

5. No correlation between the number of CFU-Fs and the age of donors has been observed, most probably due to the small difference in the age of bone marrow donors included in this study (20-40 years old).

6. Estimation of population doublings (PD) over a period of 30 days in culture revealed similar growth kinetics of both types of MSCs cultured either with FBS or with platelet lysate.

7. Platelet lysate demonstrated equal stimulatory properties for proliferation of both CD271-MSCs and PA-MSCs as FBS. Our data therefore suggest that platelet lysate can be used as effectively as FBS in generating bulk quantities of MSCs under serum-free conditions for a clinical application.

8. CD271-MSC inhibited the mitogenic-induced proliferation of peripheral blood mononuclear cells (PB-MNCs) after stimulation with concanavalin-A, phytohemagglutinin, or pokeweed mitogen at comparable levels with PA-MSCs.

9. CD271-MSCs as well as PA-MSCs significantly suppressed the allogeneic reaction *in vitro* ranging from 40-80% of the maximal proliferation, as estimated by BrdU assay.

10. The significant increase of prostaglandin E2 (PGE2) levels at co-incubation of CD271-MSCs with PB-MNCs at the ratio 1:1 or 1:2 (about 4.5-fold) correlated very well with the inhibitory effect of CD271-MSCs on allogeneic reaction in MLR at these ratios.

11. Indomethacin, an inhibitor of cyclooxygenase-1 necessary for the biosynthesis of PGE2, mitigated the overall suppressive effect of CD271-MSCs on proliferation of PB-MNCs when co-cultured at ratio 1:1, suggesting that PGE2 represents one of the major mediators of this effect.

12. On the other hand, indomethacin was not able to reverse the inhibitory effect of CD271-MSCs when these MSCs were co-incubated with MNCs at 1:2 or 1:10 ratio, suggesting that PGE2 does not affect the MSCs-mediated immunosuppression when allogeneic MNCs are in excess.

13. Estimation of the levels of soluble HLA-G or nitric oxide in the supernatants of MLR demonstrated that none of these molecules is responsible for the MSC-mediating immunosuppression *in vitro*.

14. CD271-MSCs in co-culture with allogeneic MNCs, were able to significantly decrease concentration of IFN-gamma (about 80%) and TNF-alpha (about 90%) in MLR at both 1:1 and 1:2 ratio, indicating their strong anti-inflammatory effect. However, no increase of IL-10 levels was observed.

15. In presence of CD271-MSCs the total number of $CD4^{+}CD25^{high}$ T regulatory cells on day 6 of MLR decreased significantly (about 2.5-fold) compared to the number of T regs in the wells where MNCs were cultured without MSCs.

16. Flow cytometric analysis of co-cultured CD271-MSCs with MNCs for 6 days revealed a significant increase (about 2-fold) of naïve $CD4^{+}CD25^{high}CD45RA^{+}CD62L^{+}$ T regs, indicating that this subset of T regs may extend the immunosuppressive acitivity of CD271-MSCs.

17. Our *in vivo* data revealed that co-transplantation of $CD133^{+}$ hematopoietic stem cells with CD271-MSC significantly improved the overall engraftment in the bone marrow of immunodeficient NOD/SCID mice at both 1:1 (about 10-fold) and 1:8 (about 23-fold) ratios in comparison to transplantation of $CD133^{+}$ cells alone.

18. After co-transplantation with CD271-MSCs at 1:1 ratio, $CD133^{+}$ hematopoietic stem cells gave rise to approximately 2- to 3-fold more myeloid cells ($CD33^{+}$) and more primitive $CD45^{+}CD41a^{+}$ megakaryocytes.

19. Remarkably, co-transplantation of $CD133^{+}$ hematopoietic stem cells with CD271-MSC at a ratio of 1:8 promoted their differentiation not only towards myelopoiesis, but also to the lymphoid lineage. This represents a substantial qualitative difference between CD271-MSCs and PA-MSCs.

20. Migration studies as evaluated by the quantitative polymerase chain reaction analysis for the human albumin gene demonstrated a characteristic distribution of MSCs in transplanted mouse organs. When CD271-MSCs were co-transplanted with $CD133^{+}$ cells at ratio 1:1 most of the MSCs were found in the brain, in contrast to the MSC:$CD133^{+}$ ratio 8:1, whereby most of these MSCs were entrapped in the lungs.

21. Taken together, our results indicate that CD271 antigen provides a versatile marker for prospective isolation and expansion of multipotent mesenchymal stromal cells with immunosuppressive and lymphohematopoietic engraftment-promoting properties. The co-transplantation of such cells together with hematopoietic stem cells in patients with hematologic malignancies may prove valuable in the prevention of impaired/delayed T-cell recovery and graft-*versus*-host disease.

7. SUMMARY

OBJECTIVE. *In vitro* proliferative and differentiation potential of mesenchymal stromal cells (MSCs) generated from $CD271^+$ bone marrow mononuclear cells (CD271-MSCs) has been demonstrated in several earlier and recent reports. In the present study we focused, in addition to proliferative and differentiation potential, on *in vitro* and *in vivo* immunosuppressive and lymphohematopoietic engraftment-promoting potential of these mesenchymal stromal cells compared to bone marrow-derived mesenchymal stromal cells generated by plastic adherence (PA-MSCs).

MATERIALS AND METHODS. We set up a series of experimental protocols in order to determine the phenotype of bone marrow-derived CD271-MSCs, their clonogenic, proliferative, differentiation and immunosuppressive potential. The potential of CD271-MSCs to improve the engraftment of $CD133^+$ hematopoietic stem cells at co-transplantation was evaluated in immunodeficient NOD/SCID-IL2Rγ^{null} mice.

RESULTS. *In vitro* studies demonstrated that CD271-mesenchymal stromal cells differentiate along adipogenic, osteogenic and chondrogenic lineages (trilineage potential), and significantly inhibit the proliferation of allogeneic T-lymphocytes in mixed lymphocyte reaction assays. Elevated levels of prostaglandin E_2, but not nitric monoxide, IL-10 or soluble HLA-G, mediated the majority of this immunosuppressive effect. *In vivo* studies showed that CD271-mesenchymal stromal cells promoted significantly greater lymphoid engraftment than did PA-MSCs when co-transplanted with $CD133^+$ hematopoietic stem cells at a ratio of 8:1 in immunodeficient NOD/SCID-IL2Rγ^{null} mice. They induced a 10.4-fold increase in the number of T cells, a 2.5-fold increase in the number of NK cells, and a 3.6-fold increase in the number of B cells, indicating a major qualitative difference between these two mesenchymal stromal cell populations.

CONCLUSIONS. Our results indicate that CD271 antigen provides a versatile marker for prospective isolation and expansion of MSCs with immunosuppressive and lymphohematopoietic engraftment-promoting properties. The co-transplantation of such cells together with hematopoietic stem cells in patients with hematologic malignancies may prove valuable in the prevention of impaired/delayed T-cell recovery and graft-*versus*-host disease.

8. SAŽETAK

SVRHA I CILJ RADA. In vitro proliferacijski i diferencijacijski potencijal mezenhimskih stromalnih stanica podrijetlom od $CD271^+$ mononuklearnih stanica koštane srži (CD271-MSS) pokazan je u nekoliko nedavno objavljenih radova i izvješća. U ovom smo se radu, pored proliferacijskog i diferencijacijskog potencijala tih mezenhimalnih stromalnih stanica fokusirali na njihov *in vitro* i *in vivo* imunosupresijski potencijal i potencijal za promociju prihvaćanja limfohematopoetskog presatka u odnosu na mezenhimske stromalne stanica podrijetlom iz koštane srži koje su proizvedene adherencijom na plastiku (PA-MSS).

MATERIJAL I METODE. U radu smo postavili niz eksperimentalnih protokola u cilju određivanja fenotipa CD271-MSS podrijetlom iz koštane srži, kao i njihov klonogeni, proliferacijski, diferencijacijski i imunosupresijski potencijal. Potencijal CD271-MSS za promociju prihvaćanja $CD133^+$ krvotvornih matičnih stanica nakon njihove kotransplantacije ispitan je u modelu imunodeficijentnih miševa NOD/SCID-IL2Rγ^{null}.

REZULTATI. *In vitro* pokusi pokazali su da se CD271-mezenhimske stromalne stanice diferenciraju u adipogenu, osteogenu i hondrogenu liniju (trilinijski potencijal) te značajno inhibiraju proliferaciju alogeničnih limfocita T u reakciji pomiješanih limfocita. Glavnina imunosupresijskog učinka posredovana je povećanom razinom prostaglandina E2, a ne dušičnim monoksidom (NO), interleukinom-10 (IL-10) ili topljivim molekulama HLA-G. Pokusi *in vivo* pokazali su da CD271-mezenhimske stromalne stanice značajno bolje promoviraju prihvaćanje limfoidnih stanica nego li PA-MSS nakon kotransplantacije s CD133+ krvotvornim matičnim stanicama u odnosu 8:1 u imunodeficijentne miševe NOD/SCID-IL2Rγ^{null}. Pri tome CD271-MSS uzrokuju povećanje broja limfocita T za 10,4x, povećanje broja NK-stanica za 2,5x, kao i povećanje broja B-stanica za 3,6x, što ujedno i predstavlja glavnu kvalitativnu razliku između te dvije populacije mezenhimskih stromalnih stanica.

ZAKLJUČCI. Naši rezultati pokazuju da antigen CD271 predstavlja pogodan biljeg za prospektivno izdvajanje i ekspanziju mezenhimskih stromalnih stanica koje posjeduju imunosupresijski potencijal i promoviraju prihvaćanje limfohematopoetskog presatka. Kotransplantacija CD271-MSS zajedno s krvotvornim matičnim stanicama u bolesnika s malignim hematološkim bolestima može se pokazati korisnim za sprečavanje poremećaja ili odgođenog oporavka limfocita T, kao i za sprečavanje bolesti zbog reakcije presatka na domaćina (graft-*versus*-host disease).

9. LITERATURE

1. Ringden O, le BK. Allogeneic hematopoietic stem cell transplantation: state of the art and new perspectives. APMIS 2005;113:813-30.

2. Cohnheim J. Über Entzündung und Eiterung. J Arch Path Anat Physiol Klin Med 1867;40:1-79.

3. Friedenstein AJ, Piatetzky-Shapiro II, Petrakova KV. Osteogenesis in transplants of bone marrow cells. J Embryol Exp Morphol 1966;16:381-90.

4. Friedenstein AJ, Chailakhjan RK, Lalykina KS. The development of fibroblast colonies in monolayer cultures of guinea-pig bone marrow and spleen cells. Cell Tissue Kinet 1970;3:393-403.

5. Friedenstein AJ, Deriglasova UF, Kulagina NN et al. Precursors for fibroblasts in different populations of hematopoietic cells as detected by the in vitro colony assay method. Exp Hematol 1974;2:83-92.

6. Friedenstein AJ. Precursor cells of mechanocytes. Int Rev Cytol 1976;47:327-59.

7. Friedenstein AJ, Chailakhyan RK, Latsinik NV, Panasyuk AF, Keiliss-Borok IV. Stromal cells responsible for transferring the microenvironment of the hemopoietic tissues. Cloning in vitro and retransplantation in vivo. Transplantation 1974;17:331-40.

8. Friedenstein AJ, Gorskaja JF, Kulagina NN. Fibroblast precursors in normal and irradiated mouse hematopoietic organs. Exp Hematol 1976;4:267-74.

9. Mackay AM, Beck SC, Murphy JM, Barry FP, Chichester CO, Pittenger MF. Chondrogenic differentiation of cultured human mesenchymal stem cells from marrow. Tissue Eng 1998;4:415-28.

10. Castro-Malaspina H, Gay RE, Resnick G et al. Characterization of human bone marrow fibroblast colony-forming cells (CFU-F) and their progeny. Blood 1980;56:289-301.

11. Owen M. Marrow stromal stem cells. J Cell Sci Suppl 1988;10:63-76.

12. Owen M, Friedenstein AJ. Stromal stem cells: marrow-derived osteogenic precursors. Ciba Found Symp 1988;136:42-60.

13. Caplan AI. Mesenchymal stem cells. J Orthop Res 1991;9:641-50.

14. Horwitz EM, le BK, Dominici M et al. Clarification of the nomenclature for MSC: The International Society for Cellular Therapy position statement. Cytotherapy 2005;7:393-5.

15. Pittenger MF, Mackay AM, Beck SC et al. Multilineage potential of adult human mesenchymal stem cells. Science 1999;284:143-7.

16. Caplan AI. Adult mesenchymal stem cells for tissue engineering versus regenerative medicine. J Cell Physiol 2007;213:341-7.

17. Quirici N, Soligo D, Bossolasco P, Servida F, Lumini C, Deliliers GL. Isolation of bone marrow mesenchymal stem cells by anti-nerve growth factor receptor antibodies. Exp Hematol 2002;30:783-91.

18. Tondreau T, Lagneaux L, Dejeneffe M et al. Isolation of BM mesenchymal stem cells by plastic adhesion or negative selection: phenotype, proliferation kinetics and differentiation potential. Cytotherapy 2004;6:372-9.

19. Izadpanah R, Trygg C, Patel B et al. Biologic properties of mesenchymal stem cells derived from bone marrow and adipose tissue. J Cell Biochem 2006;99:1285-97.

20. Rodriguez AM, Elabd C, Amri EZ, Ailhaud G, Dani C. The human adipose tissue is a source of multipotent stem cells. Biochimie 2005;87:125-8.

21. Oedayrajsingh-Varma MJ, van Ham SM, Knippenberg M et al. Adipose tissue-derived mesenchymal stem cell yield and growth characteristics are affected by the tissue-harvesting procedure. Cytotherapy 2006;8:166-77.

22. Lee OK, Kuo TK, Chen WM, Lee KD, Hsieh SL, Chen TH. Isolation of multipotent mesenchymal stem cells from umbilical cord blood. Blood 2004;103:1669-75.

23. Erices A, Conget P, Minguell JJ. Mesenchymal progenitor cells in human umbilical cord blood. Br J Haematol 2000;109:235-42.

24. De CP, Bartsch G, Jr., Siddiqui MM et al. Isolation of amniotic stem cell lines with potential for therapy. Nat Biotechnol 2007;25:100-6.

25. Delo DM, De CP, Bartsch G, Jr., Atala A. Amniotic fluid and placental stem cells. Methods Enzymol 2006;419:426-38.

26. Soncini M, Vertua E, Gibelli L et al. Isolation and characterization of mesenchymal cells from human fetal membranes. J Tissue Eng Regen Med 2007;1:296-305.

27. Miao Z, Jin J, Chen L et al. Isolation of mesenchymal stem cells from human placenta: comparison with human bone marrow mesenchymal stem cells. Cell Biol Int 2006;30:681-7.

28. In 't Anker PS, Noort WA, Kruisselbrink AB et al. Nonexpanded primary lung and bone marrow-derived mesenchymal cells promote the engraftment of umbilical cord blood-derived CD34(+) cells in NOD/SCID mice. Exp Hematol 2003;31:881-9.

29. Lai RC, Arslan F, Tan SS et al. Derivation and characterization of human fetal MSCs: an alternative cell source for large-scale production of cardioprotective microparticles. J Mol Cell Cardiol 2010;48:1215-24.

30. Campagnoli C, Roberts IA, Kumar S, Bennett PR, Bellantuono I, Fisk NM. Identification of mesenchymal stem/progenitor cells in human first-trimester fetal blood, liver, and bone marrow. Blood 2001;98:2396-402.

31. Covas DT, Panepucci RA, Fontes AM et al. Multipotent mesenchymal stromal cells obtained from diverse human tissues share functional properties and gene-expression profile with CD146+ perivascular cells and fibroblasts. Exp Hematol 2008;36:642-54.

32. Kim JH, Lee MC, Seong SC, Park KH, Lee S. Enhanced proliferation and chondrogenic differentiation of human synovium-derived stem cells expanded with basic fibroblastic growth factor. Tissue Eng Part A 2010.

33. Zvaifler NJ, Marinova-Mutafchieva L, Adams G et al. Mesenchymal precursor cells in the blood of normal individuals. Arthritis Res 2000;2:477-88.

34. Villaron EM, Almeida J, Lopez-Holgado N et al. Mesenchymal stem cells are present in peripheral blood and can engraft after allogeneic hematopoietic stem cell transplantation. Haematologica 2004;89:1421-7.

35. Caballero M, Reed CR, Madan G, van Aalst JA. Osteoinduction in umbilical cord- and palate periosteum-derived mesenchymal stem cells. Ann Plast Surg 2010;64:605-9.

36. Djouad F, Delorme B, Maurice M et al. Microenvironmental changes during differentiation of mesenchymal stem cells towards chondrocytes. Arthritis Res Ther 2007;9:R33.

37. Jones EA, Crawford A, English A et al. Synovial fluid mesenchymal stem cells in health and early osteoarthritis: detection and functional evaluation at the single-cell level. Arthritis Rheum 2008;58:1731-40.

38. Mouiseddine M, Mathieu N, Stefani J, Demarquay C, Bertho JM. Characterization and histological localization of multipotent mesenchymal stromal cells in the human postnatal thymus. Stem Cells Dev 2008;17:1165-74.

39. Sellheyer K, Krahl D. [Cutaneous mesenchymal stem cells. Current status of research and potential clinical applications]. Hautarzt 2010;61:429-34.

40. Lushaj EB, Anstadt E, Haworth R et al. Mesenchymal stromal cells are present in the heart and promote growth of adult stem cells in vitro. Cytotherapy 2010.

41. Kraft DC, Bindslev DA, Melsen B, Klein-Nulend J. Human dental pulp cells exhibit bone cell-like responsiveness to fluid shear stress. Cytotherapy 2010.

42. Gronthos S, Brahim J, Li W et al. Stem cell properties of human dental pulp stem cells. J Dent Res 2002;81:531-5.

43. Hegyi B, Sagi B, Kovacs J et al. Identical, similar or different? Learning about immunomodulatory function of mesenchymal stem cells isolated from various mouse tissues: bone marrow, spleen, thymus and aorta wall. Int Immunol 2010;22:551-9.

44. Dominici M, le BK, Mueller I et al. Minimal criteria for defining multipotent mesenchymal stromal cells. The International Society for Cellular Therapy position statement. Cytotherapy 2006;8:315-7.

45. Prockop DJ, Sekiya I, Colter DC. Isolation and characterization of rapidly self-renewing stem cells from cultures of human marrow stromal cells. Cytotherapy 2001;3:393-6.

46. Sekiya I, Larson BL, Smith JR, Pochampally R, Cui JG, Prockop DJ. Expansion of human adult stem cells from bone marrow stroma: conditions that maximize the yields of early progenitors and evaluate their quality. Stem Cells 2002;20:530-41.

47. Pereira RF, Halford KW, O'Hara MD et al. Cultured adherent cells from marrow can serve as long-lasting precursor cells for bone, cartilage, and lung in irradiated mice. Proc Natl Acad Sci U S A 1995;92:4857-61.

48. Colter DC, Class R, DiGirolamo CM, Prockop DJ. Rapid expansion of recycling stem cells in cultures of plastic-adherent cells from human bone marrow. Proc Natl Acad Sci U S A 2000;97:3213-8.

49. Gregory CA, Singh H, Perry AS, Prockop DJ. The Wnt signaling inhibitor dickkopf-1 is required for reentry into the cell cycle of human adult stem cells from bone marrow. J Biol Chem 2003;278:28067-78.

50. Heiskanen A, Satomaa T, Tiitinen S et al. N-glycolylneuraminic acid xenoantigen contamination of human embryonic and mesenchymal stem cells is substantially reversible. Stem Cells 2007;25:197-202.

51. Sundin M, Ringden O, Sundberg B, Nava S, Gotherstrom C, le BK. No alloantibodies against mesenchymal stromal cells, but presence of anti-fetal calf serum antibodies, after transplantation in allogeneic hematopoietic stem cell recipients. Haematologica 2007;92:1208-15.

52. Doucet C, Ernou I, Zhang Y et al. Platelet lysates promote mesenchymal stem cell expansion: a safety substitute for animal serum in cell-based therapy applications. J Cell Physiol 2005;205:228-36.

53. Castro-Malaspina H, Ebell W, Wang S. Human bone marrow fibroblast colony-forming units (CFU-F). Prog Clin Biol Res 1984;154:209-36.

54. Zohar R, Sodek J, McCulloch CA. Characterization of stromal progenitor cells enriched by flow cytometry. Blood 1997;90:3471-81.

55. Bianco P, Riminucci M, Gronthos S, Robey PG. Bone marrow stromal stem cells: nature, biology, and potential applications. Stem Cells 2001;19:180-92.

56. D'Ippolito G, Schiller PC, Ricordi C, Roos BA, Howard GA. Age-related osteogenic potential of mesenchymal stromal stem cells from human vertebral bone marrow. J Bone Miner Res 1999;14:1115-22.

57. Egrise D, Martin D, Vienne A, Neve P, Schoutens A. The number of fibroblastic colonies formed from bone marrow is decreased and the in vitro proliferation rate of trabecular bone cells increased in aged rats. Bone 1992;13:355-61.

58. Baxter MA, Wynn RF, Jowitt SN, Wraith JE, Fairbairn LJ, Bellantuono I. Study of telomere length reveals rapid aging of human marrow stromal cells following in vitro expansion. Stem Cells 2004;22:675-82.

59. Tokalov SV, Gruener S, Schindler S, Iagunov AS, Baumann M, Abolmaali ND. A number of bone marrow mesenchymal stem cells but neither phenotype nor differentiation capacities changes with age of rats. Mol Cells 2007;24:255-60.

60. Stolzing A, Jones E, McGonagle D, Scutt A. Age-related changes in human bone marrow-derived mesenchymal stem cells: consequences for cell therapies. Mech Ageing Dev 2008;129:163-73.

61. Choumerianou DM, Martimianaki G, Stiakaki E, Kalmanti L, Kalmanti M, Dimitriou H. Comparative study of stemness characteristics of mesenchymal cells from bone marrow of children and adults. Cytotherapy 2010;12:881-7.

62. Mets T, Verdonk G. Variations in the stromal cell population of human bone marrow during aging. Mech Ageing Dev 1981;15:41-9.

63. Katsara O, Mahaira LG, Iliopoulou EG et al. Effects of Donor Age, Gender, and In Vitro Cellular Aging on the Phenotypic, Functional, and Molecular Characteristics of Mouse Bone Marrow-Derived Mesenchymal Stem Cells. Stem Cells Dev 2011.

64. Stenderup K, Justesen J, Eriksen EF, Rattan SI, Kassem M. Number and proliferative capacity of osteogenic stem cells are maintained during aging and in patients with osteoporosis. J Bone Miner Res 2001;16:1120-9.

65. Stenderup K, Justesen J, Clausen C, Kassem M. Aging is associated with decreased maximal life span and accelerated senescence of bone marrow stromal cells. Bone 2003;33:919-26.

66. Mareschi K, Ferrero I, Rustichelli D et al. Expansion of mesenchymal stem cells isolated from pediatric and adult donor bone marrow. J Cell Biochem 2006;97:744-54.

67. Phinney DG, Kopen G, Righter W, Webster S, Tremain N, Prockop DJ. Donor variation in the growth properties and osteogenic potential of human marrow stromal cells. J Cell Biochem 1999;75:424-36.

68. Lund TC, Kobs A, Blazar BR, Tolar J. Mesenchymal stromal cells from donors varying widely in age are of equal cellular fitness after in vitro expansion under hypoxic conditions. Cytotherapy 2010;12:971-81.

69. D'Ippolito G, Howard GA, Roos BA, Schiller PC. Sustained stromal stem cell self-renewal and osteoblastic differentiation during aging. Rejuvenation Res 2006;9:10-9.

70. Moerman EJ, Teng K, Lipschitz DA, Lecka-Czernik B. Aging activates adipogenic and suppresses osteogenic programs in mesenchymal marrow stroma/stem cells: the role of PPAR-gamma2 transcription factor and TGF-beta/BMP signaling pathways. Aging Cell 2004;3:379-89.

71. Sethe S, Scutt A, Stolzing A. Aging of mesenchymal stem cells. Ageing Res Rev 2006;5:91-116.

72. le BK, Tammik L, Sundberg B, Haynesworth SE, Ringden O. Mesenchymal stem cells inhibit and stimulate mixed lymphocyte cultures and mitogenic responses independently of the major histocompatibility complex. Scand J Immunol 2003;57:11-20.

73. le BK, Tammik C, Rosendahl K, Zetterberg E, Ringden O. HLA expression and immunologic properties of differentiated and undifferentiated mesenchymal stem cells. Exp Hematol 2003;31:890-6.

74. Aggarwal S, Pittenger MF. Human mesenchymal stem cells modulate allogeneic immune cell responses. Blood 2005;105:1815-22.

75. Rasmusson I, Ringden O, Sundberg B, le BK. Mesenchymal stem cells inhibit lymphocyte proliferation by mitogens and alloantigens by different mechanisms. Exp Cell Res 2005;305:33-41.

76. Tse WT, Pendleton JD, Beyer WM, Egalka MC, Guinan EC. Suppression of allogeneic T-cell proliferation by human marrow stromal cells: implications in transplantation. Transplantation 2003;75:389-97.

77. Di NM, Carlo-Stella C, Magni M et al. Human bone marrow stromal cells suppress T-lymphocyte proliferation induced by cellular or nonspecific mitogenic stimuli. Blood 2002;99:3838-43.

78. le BK, Frassoni F, Ball L et al. Mesenchymal stem cells for treatment of steroid-resistant, severe, acute graft-versus-host disease: a phase II study. Lancet 2008;371:1579-86.

79. Muller I, Kordowich S, Holzwarth C et al. Application of multipotent mesenchymal stromal cells in pediatric patients following allogeneic stem cell transplantation. Blood Cells Mol Dis 2008;40:25-32.

80. Sarugaser R, Hanoun L, Keating A, Stanford WL, Davies JE. Human mesenchymal stem cells self-renew and differentiate according to a deterministic hierarchy. PLoS One 2009;4:e6498.

81. Muraglia A, Cancedda R, Quarto R. Clonal mesenchymal progenitors from human bone marrow differentiate in vitro according to a hierarchical model. J Cell Sci 2000;113 (Pt 7):1161-6.

82. Russell KC, Lacey MR, Gilliam JK, Tucker HA, Phinney DG, O'Connor KC. Clonal analysis of the proliferation potential of human bone marrow mesenchymal stem cells as a function of potency. Biotechnol Bioeng 2011;108:2716-26.

83. Xu G, Zhang L, Ren G et al. Immunosuppressive properties of cloned bone marrow mesenchymal stem cells. Cell Res 2007;17:240-8.

84. Simmons PJ, Torok-Storb B. Identification of stromal cell precursors in human bone marrow by a novel monoclonal antibody, STRO-1. Blood 1991;78:55-62.

85. Gronthos S, Graves SE, Ohta S, Simmons PJ. The STRO-1+ fraction of adult human bone marrow contains the osteogenic precursors. Blood 1994;84:4164-73.

86. Gronthos S, Simmons PJ. The growth factor requirements of STRO-1-positive human bone marrow stromal precursors under serum-deprived conditions in vitro. Blood 1995;85:929-40.

87. Zannettino AC, Paton S, Kortesidis A, Khor F, Itescu S, Gronthos S. Human mulipotential mesenchymal/stromal stem cells are derived from a discrete subpopulation of STRO-1bright/CD34 /CD45(-)/glycophorin-A-bone marrow cells. Haematologica 2007;92:1707-8.

88. Lin G, Liu G, Banie L et al. Tissue distribution of mesenchymal stem cell marker Stro-1. Stem Cells Dev 2011.

89. Gronthos S, Fitter S, Diamond P, Simmons PJ, Itescu S, Zannettino AC. A novel monoclonal antibody (STRO-3) identifies an isoform of tissue nonspecific alkaline phosphatase expressed by multipotent bone marrow stromal stem cells. Stem Cells Dev 2007;16:953-63.

90. Gronthos S, McCarty R, Mrozik K et al. Heat shock protein-90 beta is expressed at the surface of multipotential mesenchymal precursor cells: generation of a novel monoclonal antibody, STRO-4, with specificity for mesenchymal precursor cells from human and ovine tissues. Stem Cells Dev 2009;18:1253-62.

91. Haynesworth SE, Baber MA, Caplan AI. Cell surface antigens on human marrow-derived mesenchymal cells are detected by monoclonal antibodies. Bone 1992;13:69-80.

92. Barry FP, Boynton RE, Haynesworth S, Murphy JM, Zaia J. The monoclonal antibody SH-2, raised against human mesenchymal stem cells, recognizes an epitope on endoglin (CD105). Biochem Biophys Res Commun 1999;265:134-9.

93. Jones EA, Kinsey SE, English A et al. Isolation and characterization of bone marrow multipotential mesenchymal progenitor cells. Arthritis Rheum 2002;46:3349-60.

94. Aslan H, Zilberman Y, Kandel L et al. Osteogenic differentiation of noncultured immunoisolated bone marrow-derived CD105+ cells. Stem Cells 2006;24:1728-37.

95. Cheifetz S, Bellon T, Cales C et al. Endoglin is a component of the transforming growth factor-beta receptor system in human endothelial cells. J Biol Chem 1992;267:19027-30.

96. Rokhlin OW, Cohen MB, Kubagawa H, Letarte M, Cooper MD. Differential expression of endoglin on fetal and adult hematopoietic cells in human bone marrow. J Immunol 1995;154:4456-65.

97. Barry F, Boynton R, Murphy M, Haynesworth S, Zaia J. The SH-3 and SH-4 antibodies recognize distinct epitopes on CD73 from human mesenchymal stem cells. Biochem Biophys Res Commun 2001;289:519-24.

98. njos-Afonso F, Bonnet D. Nonhematopoietic/endothelial SSEA-1+ cells define the most primitive progenitors in the adult murine bone marrow mesenchymal compartment. Blood 2007;109:1298-306.

99. Gang EJ, Bosnakovski D, Figueiredo CA, Visser JW, Perlingeiro RC. SSEA-4 identifies mesenchymal stem cells from bone marrow. Blood 2007;109:1743-51.

100. Martinez C, Hofmann TJ, Marino R, Dominici M, Horwitz EM. Human bone marrow mesenchymal stromal cells express the neural ganglioside GD2: a novel surface marker for the identification of MSCs. Blood 2007;109:4245-8.

101. Jones EA, English A, Kinsey SE et al. Optimization of a flow cytometry-based protocol for detection and phenotypic characterization of multipotent mesenchymal stromal cells from human bone marrow. Cytometry B Clin Cytom 2006;70:391-9.

102. Poloni A, Maurizi G, Rosini V et al. Selection of CD271(+) cells and human AB serum allows a large expansion of mesenchymal stromal cells from human bone marrow. Cytotherapy 2009;11:153-62.

103. Hermida-Gomez T, Fuentes-Boquete I, Gimeno-Longas MJ et al. Bone Marrow Cells Immunomagnetically Selected For CD271+ Antigen Promote In Vitro the Repair of Articular Cartilage Defects. Tissue Eng Part A 2011.

104. Jarocha D, Lukasiewicz E, Majka M. Adventage of mesenchymal stem cells (MSC) expansion directly from purified bone marrow CD105+ and CD271+ cells. Folia Histochem Cytobiol 2008;46:307-14.

105. Kuci S, Kuci Z, Kreyenberg H et al. CD271 antigen defines a subset of multipotent stromal cells with immunosuppressive and lymphohematopoietic engraftment-promoting properties. Haematologica 2010;95:651-9.

106. Quirici N, Scavullo C, de GL et al. Anti-L-NGFR and -CD34 monoclonal antibodies identify multipotent mesenchymal stem cells in human adipose tissue. Stem Cells Dev 2010;19:915-25.

107. Yamada T, Akamatsu H, Hasegawa S et al. Age-related changes of p75 neurotrophin receptor-positive adipose-derived stem cells. J Dermatol Sci 2010;58:36-42.

108. Jones E, English A, Churchman SM et al. Large-scale extraction and characterization of CD271+ multipotential stromal cells from trabecular bone in health and osteoarthritis: implications for bone regeneration strategies based on uncultured or minimally cultured multipotential stromal cells. Arthritis Rheum 2010;62:1944-54.

109. Lu B, Pang PT, Woo NH. The yin and yang of neurotrophin action. Nat Rev Neurosci 2005;6:603-14.

110. Nykjaer A, Willnow TE, Petersen CM. p75NTR--live or let die. Curr Opin Neurobiol 2005;15:49-57.

111. Rogers ML, Beare A, Zola H, Rush RA. CD 271 (P75 neurotrophin receptor). J Biol Regul Homeost Agents 2008;22:1-6.

112. Huebner K, Isobe M, Chao M et al. The nerve growth factor receptor gene is at human chromosome region 17q12-17q22, distal to the chromosome 17 breakpoint in acute leukemias. Proc Natl Acad Sci U S A 1986;83:1403-7.

113. Levi-Montalcini R, Angeletti PU. Essential role of the nerve growth factor in the survival and maintenance of dissociated sensory and sympathetic embryonic nerve cells in vitro. Dev Biol 1963;7:653-9.

114. Levi-Montalcini R, Angeletti PU. Nerve growth factor. Physiol Rev 1968;48:534-69.

115. Roux PP, Barker PA. Neurotrophin signaling through the p75 neurotrophin receptor. Prog Neurobiol 2002;67:203-33.

116. Chesa PG, Rettig WJ, Thomson TM, Old LJ, Melamed MR. Immunohistochemical analysis of nerve growth factor receptor expression in normal and malignant human tissues. J Histochem Cytochem 1988;36:383-9.

117. Schor NF. The p75 neurotrophin receptor in human development and disease. Prog Neurobiol 2005;77:201-14.

118. Richardson PM, Issa VM, Riopelle RJ. Distribution of neuronal receptors for nerve growth factor in the rat. J Neurosci 1986;6:2312-21.

119. Cattoretti G, Schiro R, Orazi A, Soligo D, Colombo MP. Bone marrow stroma in humans: anti-nerve growth factor receptor antibodies selectively stain reticular cells in vivo and in vitro. Blood 1993;81:1726-38.

120. Caneva L, Soligo D, Cattoretti G, De HE, Deliliers GL. Immuno-electron microscopy characterization of human bone marrow stromal cells with anti-NGFR antibodies. Blood Cells Mol Dis 1995;21:73-85.

121. Wheeler EF, Bothwell M. Spatiotemporal patterns of expression of NGF and the low-affinity NGF receptor in rat embryos suggest functional roles in tissue morphogenesis and myogenesis. J Neurosci 1992;12:930-45.

122. Thompson SJ, Schatteman GC, Gown AM, Bothwell M. A monoclonal antibody against nerve growth factor receptor. Immunohistochemical analysis of normal and neoplastic human tissue. Am J Clin Pathol 1989;92:415-23.

123. Fabricant RN, De Larco JE, Todaro GJ. Nerve growth factor receptors on human melanoma cells in culture. Proc Natl Acad Sci U S A 1977;74:565-9.

124. Rettig WJ, Spengler BA, Chesa PG, Old LJ, Biedler JL. Coordinate changes in neuronal phenotype and surface antigen expression in human neuroblastoma cell variants. Cancer Res 1987;47:1383-9.

125. Thomson TM, Rettig WJ, Chesa PG, Green SH, Mena AC, Old LJ. Expression of human nerve growth factor receptor on cells derived from all three germ layers. Exp Cell Res 1988;174:533-9.

126. Deans RJ, Moseley AB. Mesenchymal stem cells: biology and potential clinical uses. Exp Hematol 2000;28:875-84.

127. Zhang J, Niu C, Ye L et al. Identification of the haematopoietic stem cell niche and control of the niche size. Nature 2003;425:836-41.

128. Wilson A, Trumpp A. Bone-marrow haematopoietic-stem-cell niches. Nat Rev Immunol 2006;6:93-106.

129. Majumdar MK, Thiede MA, Mosca JD, Moorman M, Gerson SL. Phenotypic and functional comparison of cultures of marrow-derived mesenchymal stem cells (MSCs) and stromal cells. J Cell Physiol 1998;176:57-66.

130. Devine SM, Hoffman R. Role of mesenchymal stem cells in hematopoietic stem cell transplantation. Curr Opin Hematol 2000;7:358-63.

131. Masuda S, Ageyama N, Shibata H et al. Cotransplantation with MSCs improves engraftment of HSCs after autologous intra-bone marrow transplantation in nonhuman primates. Exp Hematol 2009;37:1250-7.

132. Kim DH, Yoo KH, Yim YS et al. Cotransplanted bone marrow derived mesenchymal stem cells (MSC) enhanced engraftment of hematopoietic stem cells in a MSC-dose dependent manner in NOD/SCID mice. J Korean Med Sci 2006;21:1000-4.

133. Koc ON, Gerson SL, Cooper BW et al. Rapid hematopoietic recovery after coinfusion of autologous-blood stem cells and culture-expanded marrow mesenchymal stem cells in advanced breast cancer patients receiving high-dose chemotherapy. J Clin Oncol 2000;18:307-16.

134. Lee ST, Jang JH, Cheong JW et al. Treatment of high-risk acute myelogenous leukaemia by myeloablative chemoradiotherapy followed by co-infusion of T cell-depleted haematopoietic stem cells and culture-expanded marrow mesenchymal stem cells from a related donor with one fully mismatched human leucocyte antigen haplotype. Br J Haematol 2002;118:1128-31.

135. Lazarus HM, Koc ON, Devine SM et al. Cotransplantation of HLA-identical sibling culture-expanded mesenchymal stem cells and hematopoietic stem cells in hematologic malignancy patients. Biol Blood Marrow Transplant 2005;11:389-98.

136. Wang H, Wang Z, Xue M, Liu J, Yan H, Guo Z. Co-transfusion of haplo-identical hematopoietic and mesenchymal stromal cells to treat a patient with severe aplastic. Cytotherapy 2010;12:563-5.

137. Bernardo ME, Ball LM, Cometa AM et al. Co-infusion of ex vivo-expanded, parental MSCs prevents life-threatening acute GVHD, but does not reduce the risk of graft failure in pediatric patients undergoing allogeneic umbilical cord blood transplantation. Bone Marrow Transplant 2011;46:200-7.

138. Mahmood A, Lu D, Lu M, Chopp M. Treatment of traumatic brain injury in adult rats with intravenous administration of human bone marrow stromal cells. Neurosurgery 2003;53:697-702.

139. Murphy JM, Fink DJ, Hunziker EB, Barry FP. Stem cell therapy in a caprine model of osteoarthritis. Arthritis Rheum 2003;48:3464-74.

140. Kasper G, Dankert N, Tuischer J et al. Mesenchymal stem cells regulate angiogenesis according to their mechanical environment. Stem Cells 2007;25:903-10.

141. Caplan AI, Dennis JE. Mesenchymal stem cells as trophic mediators. J Cell Biochem 2006;98:1076-84.

142. Prockop DJ. Repair of tissues by adult stem/progenitor cells (MSCs): controversies, myths, and changing paradigms. Mol Ther 2009;17:939-46.

143. Rojas M, Xu J, Woods CR et al. Bone marrow-derived mesenchymal stem cells in repair of the injured lung. Am J Respir Cell Mol Biol 2005;33:145-52.

144. Ferrari G, Cusella-De AG, Coletta M et al. Muscle regeneration by bone marrow-derived myogenic progenitors. Science 1998;279:1528-30.

145. Schuleri KH, Feigenbaum GS, Centola M et al. Autologous mesenchymal stem cells produce reverse remodelling in chronic ischaemic cardiomyopathy. Eur Heart J 2009;30:2722-32.

146. Dormady SP, Bashayan O, Dougherty R, Zhang XM, Basch RS. Immortalized multipotential mesenchymal cells and the hematopoietic microenvironment. J Hematother Stem Cell Res 2001;10:125-40.

147. Block GJ, Ohkouchi S, Fung F et al. Multipotent stromal cells are activated to reduce apoptosis in part by upregulation and secretion of stanniocalcin-1. Stem Cells 2009;27:670-81.

148. Karp JM, Leng Teo GS. Mesenchymal stem cell homing: the devil is in the details. Cell Stem Cell 2009;4:206-16.

149. Chen L, Tredget EE, Wu PY, Wu Y. Paracrine factors of mesenchymal stem cells recruit macrophages and endothelial lineage cells and enhance wound healing. PLoS One 2008;3:e1886.

150. Horwitz EM, Prockop DJ, Gordon PL et al. Clinical responses to bone marrow transplantation in children with severe osteogenesis imperfecta. Blood 2001;97:1227-31.

151. Quarto R, Mastrogiacomo M, Cancedda R et al. Repair of large bone defects with the use of autologous bone marrow stromal cells. N Engl J Med 2001;344:385-6.

152. Lemischka I. A few thoughts about the plasticity of stem cells. Exp Hematol 2002;30:848-52.

153. Kopen GC, Prockop DJ, Phinney DG. Marrow stromal cells migrate throughout forebrain and cerebellum, and they differentiate into astrocytes after injection into neonatal mouse brains. Proc Natl Acad Sci U S A 1999;96:10711-6.

154. Azizi SA, Stokes D, Augelli BJ, Digirolamo C, Prockop DJ. Engraftment and migration of human bone marrow stromal cells implanted in the brains of albino rats--similarities to astrocyte grafts. Proc Natl Acad Sci U S A 1998;95:3908-13.

155. Schwartz RE, Reyes M, Koodie L et al. Multipotent adult progenitor cells from bone marrow differentiate into functional hepatocyte-like cells. J Clin Invest 2002;109:1291-302.

156. Wakitani S, Saito T, Caplan AI. Myogenic cells derived from rat bone marrow mesenchymal stem cells exposed to 5-azacytidine. Muscle Nerve 1995;18:1417-26.

157. Prockop DJ, Kota DJ, Bazhanov N, Reger RL. Evolving paradigms for repair of tissues by adult stem/progenitor cells (MSCs). J Cell Mol Med 2010;14:2190-9.

158. Nauta AJ, Fibbe WE. Immunomodulatory properties of mesenchymal stromal cells. Blood 2007;110:3499-506.

159. Bartholomew A, Sturgeon C, Siatskas M et al. Mesenchymal stem cells suppress lymphocyte proliferation in vitro and prolong skin graft survival in vivo. Exp Hematol 2002;30:42-8.

160. Tyndall A, Walker UA, Cope A et al. Immunomodulatory properties of mesenchymal stem cells: a review based on an interdisciplinary meeting held at the Kennedy Institute of Rheumatology Division, London, UK, 31 October 2005. Arthritis Res Ther 2007;9:301.

161. Gotherstrom C, Ringden O, Tammik C, Zetterberg E, Westgren M, le BK. Immunologic properties of human fetal mesenchymal stem cells. Am J Obstet Gynecol 2004;190:239-45.

162. Nauta AJ, Westerhuis G, Kruisselbrink AB, Lurvink EG, Willemze R, Fibbe WE. Donor-derived mesenchymal stem cells are immunogenic in an allogeneic host and stimulate donor graft rejection in a nonmyeloablative setting. Blood 2006;108:2114-20.

163. Fibbe WE, Nauta AJ, Roelofs H. Modulation of immune responses by mesenchymal stem cells. Ann N Y Acad Sci 2007;1106:272-8.

164. Rasmusson I, Ringden O, Sundberg B, le BK. Mesenchymal stem cells inhibit the formation of cytotoxic T lymphocytes, but not activated cytotoxic T lymphocytes or natural killer cells. Transplantation 2003;76:1208-13.

165. Nasef A, Mathieu N, Chapel A et al. Immunosuppressive effects of mesenchymal stem cells: involvement of HLA-G. Transplantation 2007;84:231-7.

166. Glennie S, Soeiro I, Dyson PJ, Lam EW, Dazzi F. Bone marrow mesenchymal stem cells induce division arrest anergy of activated T cells. Blood 2005;105:2821-7.

167. Meisel R, Zibert A, Laryea M, Gobel U, Daubener W, Dilloo D. Human bone marrow stromal cells inhibit allogeneic T-cell responses by indoleamine 2,3-dioxygenase-mediated tryptophan degradation. Blood 2004;103:4619-21.

168. Spaggiari GM, Capobianco A, Abdelrazik H, Becchetti F, Mingari MC, Moretta L. Mesenchymal stem cells inhibit natural killer-cell proliferation, cytotoxicity, and cytokine production: role of indoleamine 2,3-dioxygenase and prostaglandin E2. Blood 2008;111:1327-33.

169. Zhang W, Ge W, Li C et al. Effects of mesenchymal stem cells on differentiation, maturation, and function of human monocyte-derived dendritic cells. Stem Cells Dev 2004;13:263-71.

170. Jiang XX, Zhang Y, Liu B et al. Human mesenchymal stem cells inhibit differentiation and function of monocyte-derived dendritic cells. Blood 2005;105:4120-6.

171. Zhang B, Liu R, Shi D et al. Mesenchymal stem cells induce mature dendritic cells into a novel Jagged-2-dependent regulatory dendritic cell population. Blood 2009;113:46-57.

172. Spaggiari GM, Abdelrazik H, Becchetti F, Moretta L. MSCs inhibit monocyte-derived DC maturation and function by selectively interfering with the generation of immature DCs: central role of MSC-derived prostaglandin E2. Blood 2009;113:6576-83.

173. Spaggiari GM, Capobianco A, Becchetti S, Mingari MC, Moretta L. Mesenchymal stem cell-natural killer cell interactions: evidence that activated NK cells are capable of killing MSCs, whereas MSCs can inhibit IL-2-induced NK-cell proliferation. Blood 2006;107:1484-90.

174. Sato K, Ozaki K, Oh I et al. Nitric oxide plays a critical role in suppression of T-cell proliferation by mesenchymal stem cells. Blood 2007;109:228-34.

175. Cristofalo VJ, Allen RG, Pignolo RJ, Martin BG, Beck JC. Relationship between donor age and the replicative lifespan of human cells in culture: a reevaluation. Proc Natl Acad Sci U S A 1998;95:10614-9.

176. Pongers-Willemse MJ, Verhagen OJ, Tibbe GJ et al. Real-time quantitative PCR for the detection of minimal residual disease in acute lymphoblastic leukemia using junctional region specific TaqMan probes. Leukemia 1998;12:2006-14.

177. Pieri L, Urbani S, Mazzanti B et al. Human mesenchymal stromal cells preserve their stem features better when cultured in the Dulbecco's modified Eagle medium. Cytotherapy 2011;13:539-48.

178. Grisendi G, Anneren C, Cafarelli L et al. GMP-manufactured density gradient media for optimized mesenchymal stromal/stem cell isolation and expansion. Cytotherapy 2010;12:466-77.

179. Jones S, Horwood N, Cope A, Dazzi F. The antiproliferative effect of mesenchymal stem cells is a fundamental property shared by all stromal cells. J Immunol 2007;179:2824-31.

180. le BK. Immunomodulatory effects of fetal and adult mesenchymal stem cells. Cytotherapy 2003;5:485-9.

181. Krampera M, Glennie S, Dyson J et al. Bone marrow mesenchymal stem cells inhibit the response of naive and memory antigen-specific T cells to their cognate peptide. Blood 2003;101:3722-9.

182. Yanez R, Oviedo A, Aldea M, Bueren JA, Lamana ML. Prostaglandin E2 plays a key role in the immunosuppressive properties of adipose and bone marrow tissue-derived mesenchymal stromal cells. Exp Cell Res 2010;316:3109-23.

183. Najar M, Raicevic G, Boufker HI et al. Mesenchymal stromal cells use PGE2 to modulate activation and proliferation of lymphocyte subsets: Combined comparison of adipose tissue, Wharton's Jelly and bone marrow sources. Cell Immunol 2010;264:171-9.

184. Selmani Z, Naji A, Gaiffe E et al. HLA-G is a crucial immunosuppressive molecule secreted by adult human mesenchymal stem cells. Transplantation 2009;87:S62-S66.

185. Selmani Z, Naji A, Zidi I et al. Human leukocyte antigen-G5 secretion by human mesenchymal stem cells is required to suppress T lymphocyte and natural killer function and to induce CD4+CD25highFOXP3+ regulatory T cells. Stem Cells 2008;26:212-22.

186. Sheng H, Wang Y, Jin Y et al. A critical role of IFNgamma in priming MSC-mediated suppression of T cell proliferation through up-regulation of B7-H1. Cell Res 2008;18:846-57.

187. Djouad F, Fritz V, Apparailly F et al. Reversal of the immunosuppressive properties of mesenchymal stem cells by tumor necrosis factor alpha in collagen-induced arthritis. Arthritis Rheum 2005;52:1595-603.

188. Krampera M, Cosmi L, Angeli R et al. Role for interferon-gamma in the immunomodulatory activity of human bone marrow mesenchymal stem cells. Stem Cells 2006;24:386-98.

189. Maccario R, Podesta M, Moretta A et al. Interaction of human mesenchymal stem cells with cells involved in alloantigen-specific immune response favors the differentiation of CD4+ T-cell subsets expressing a regulatory/suppressive phenotype. Haematologica 2005;90:516-25.

190. Prevosto C, Zancolli M, Canevali P, Zocchi MR, Poggi A. Generation of CD4+ or CD8+ regulatory T cells upon mesenchymal stem cell-lymphocyte interaction. Haematologica 2007;92:881-8.

191. Hoffmann P, Eder R, Boeld TJ et al. Only the CD45RA+ subpopulation of CD4+CD25high T cells gives rise to homogeneous regulatory T-cell lines upon in vitro expansion. Blood 2006;108:4260-7.

192. Ermann J, Hoffmann P, Edinger M et al. Only the CD62L+ subpopulation of CD4+CD25+ regulatory T cells protects from lethal acute GVHD. Blood 2005;105:2220-6.

193. Angelopoulou M, Novelli E, Grove JE et al. Cotransplantation of human mesenchymal stem cells enhances human myelopoiesis and megakaryocytopoiesis in NOD/SCID mice. Exp Hematol 2003;31:413-20.

194. Qiao X, Loudovaris M, Unverzagt K et al. Immunocytochemistry and flow cytometry evaluation of human megakaryocytes in fresh samples and cultures of CD34+ cells. Cytometry 1996;23:250-9.

195. Sotiropoulou PA, Perez SA, Gritzapis AD, Baxevanis CN, Papamichail M. Interactions between human mesenchymal stem cells and natural killer cells. Stem Cells 2006;24:74-85.

196. Ball LM, Bernardo ME, Roelofs H et al. Cotransplantation of ex vivo expanded mesenchymal stem cells accelerates lymphocyte recovery and may reduce the risk of graft failure in haploidentical hematopoietic stem-cell transplantation. Blood 2007;110:2764-7.

197. Barbash IM, Chouraqui P, Baron J et al. Systemic delivery of bone marrow-derived mesenchymal stem cells to the infarcted myocardium: feasibility, cell migration, and body distribution. Circulation 2003;108:863-8.

198. Gao J, Dennis JE, Muzic RF, Lundberg M, Caplan AI. The dynamic in vivo distribution of bone marrow-derived mesenchymal stem cells after infusion. Cells Tissues Organs 2001;169:12-20.

10. CURRICULUM VITAE

Name:	Zyrafete Kuçi
Date of birth:	21st April, 1958
Place of birth:	Gjilan, Kosovo
Nationality:	Kosovo
Affiliation:	University Children's Hospital, Dept. of Hematology/Oncology, Laboratory for Stem Cell Research and Cell therapy, Frankfurt am Main, Germany

Education:

1976 – 1982	Graduate studies at the Medical School in Prishtina (Kosovo). Achievement of the title: MD
1982 – 1983	Practical year in the clinics of Medical School in Prishtina, Kosovo
1984 – 1985	Postgraduate studies in Clinical Pharmacology at the School of Medicine,University of Zagreb, Croatia
1991	Defense of the Master work and achievement of the title „Master of medical sciences" (Mentor: Prof. dr. Z. Lacković)

Working experience:

July 2007-	Scientific co-worker at University Children's Hospital, Dept. of Hematology/Oncology, Frankfurt am Main, Germany. Coordinator of the project: "Generation and expansion of mesenchymal stromal cells derived from $CD271^+$ bone marrow cells and their application in haploidentically transplanted children" (Leader: Prof. dr. P. Bader)
1998 – 2006	Scientific co-worker at University Children's Hospital, Dept. of Hematology/Oncology, Tübingen, Germany. Coordinator of 5 scientific projects. (Leader: Prof. dr. Gernot Bruchelt)
1983 – 1990	Assistent at the Institute of Pharmacology of the Medical School in Prishtina.
Publications:	13 scientific publications (in 5 of them as the first author and in 8 as a co-author)